UNIVERSITÉ DU QUÉBEC

MÉMOIRE PRÉSENTÉ À
L'UNIVERSITÉ DU QUÉBEC À TROIS-RIVIÈRES

COMME EXIGENCE PARTIELLE
DE LA MAÎTRISE EN SCIENCES DE L'ENVIRONNEMENT

PAR
NAÏM PERREAULT

IMPACT DE LA FORMATION DE RAVINS DE THERMO-EROSION SUR LES MILIEUX HUMIDES, ÎLE BYLOT, NUNAVUT, CANADA

SEPTEMBRE 2012

REMERCIEMENTS

La réalisation de ce mémoire a été possible grâce à la collaboration de plusieurs personnes. Je tiens d'abord à adresser mes remerciements à ma directrice, Dre Esther Lévesque, pour son inspiration, son enthousiasme et son dynamisme irréprochable. Mes remerciements s'adressent également à mon codirecteur, Dr Daniel Fortier, pour son encouragement et son soutien. Merci à vous deux d'avoir partagé, chacun à votre façon, votre passion pour le Grand Nord canadien et de m'avoir confié ce formidable projet. Je tiens également à remercier mon comité d'orientation composé de Drs Esther Lévesque, Daniel Fortier, Denis Gratton et Gilles Gauthier pour leurs suggestions fort constructives tout au long de mon cheminement. Merci à Dr Marco A. Rodriguez de m'avoir initié aux analyses statistiques.

Je remercie Alexandre Guertin-Pasquier et Étienne Godin pour leur contribution lors des campagnes terrain ainsi qu'Alexandre Moreau, Stéphane Ouellet et Noémie Boulanger-Lapointe pour leur participation aux analyses statistiques. Merci également aux équipes Bylot 2009 et 2010 et à l'équipe du laboratoire d'écologie végétale pour avoir été des sources constantes d'énergie et d'inspiration. Merci à la Communauté de Pond Inlet (Mittimatalik) pour son accueil en début et en fin de chacune des campagnes de terrain.

Merci à Parcs Canada - Parc national Sirmilik, au Centre d'études nordiques (CEN) et à Dr Gilles Gauthier pour l'accès au camp de recherche durant les étés 2009-2010. Ce projet a été possible grâce à la contribution logistique de Polar Continental Shelf Program (PCSP) ainsi que grâce à la contribution financière des organismes subventionnaires suivants: le Programme du gouvernement du Canada pour l'Année polaire internationale (API) , le Conseil de recherches en sciences naturelles et en génie du Canada (CRSNG), le Fonds québécois de la recherche sur la nature et les technologies (FQRNT), le réseau des centres d'excellence du Canada ArcticNet, le Programme de formation scientifique dans le Nord (PFSN) géré par le ministère des

Affaires indiennes et du Nord canadien, le Programme de formation FONCER du CRSNG en sciences environnementales nordiques (EnviroNord) et le Groupe de recherche en biologie végétale (GRBV) de l'Université du Québec à Trois-Rivières.

AVANT-PROPOS

Ce mémoire de maîtrise a été réalisé sous la direction de Dre Esther Lévesque de l'Université du Québec à Trois-Rivières et la codirection de Dr Daniel Fortier de l'Université de Montréal. Il comprend trois sections principales, soit une mise en contexte générale en français suivi de deux articles scientifiques en anglais : 1) *Impact of permafrost gullying on wetland habitat, Bylot Island, Nunavut, Canada*; 2) *Remote sensing estimate of wetland degradation surrounding thermo-erosion gullies, Bylot Island, Nunavut, Canada*. Ce mémoire est complété par sept annexes présentant des informations complémentaires non intégrées aux deux articles précédents : évaluation du couvert végétal à l'aide de photographies verticales (annexe A); liste complète des espèces végétales inventoriées lors des campagnes terrain 2009 et 2010 (annexe B); couvert et fréquence de l'ensemble des taxa pour chacune des catégories d'environnement (annexe C); calibrations radiométriques apportées à l'image satellite GeoEye-1 (annexe D); classification hiérarchique des 212 sites d'échantillonnage selon la méthode TWINSPAN (annexe E); description des quatre stations d'enregistrement d'humidité installées durant la saison 2010 (annexe F), dates des mesures ponctuelles d'humidité prises au cours de l'été 2010 (annexe G).

Je suis premier auteur des deux articles (chapitres II et III), qui seront éventuellement soumis à la revue *Permafrost and Periglacial Processes*. Drs Esther Lévesque et Daniel Fortier sont coauteurs pour les deux articles et Dr Denis Gratton est coauteur pour le second article.

TABLE DES MATIÈRES

LISTE DES FIGURES

LISTE DES TABLEAUX

Tableau **Page**

RÉSUMÉ

Le développement de ravins de thermo-érosion perturbe les milieux humides en drainant les polygones à centre concave adjacents aux zones d'effondrement. Les conséquences de ce bouleversement sur la végétation des milieux humides, essentielle à la croissance rapide de la Grande Oie des neiges (*Chen caerulescens atlanticus*), sont actuellement méconnues.

La caractérisation de 212 sites d'échantillonnage lors de campagnes terrains menées en 2009 et 2010 a été réalisée à proximité de trois ravins de thermo-érosion de la vallée Qarlikturvik (73°N, 80°N, Nunavut, Canada). Ces ravins mesurent respectivement 835 m, 717 m et 180 m de long et sont localisés dans le complexe de polygones à centre concave. Dans le but de représenter l'ensemble des environnements présents à la marge de ces ravins, les sites d'échantillonnage ont été choisis de manière stratifiée aléatoire selon six catégories établies en fonction des communautés végétales, du niveau d'humidité du sol et de l'intégrité des bourrelets périphériques (*i.e.* présence de fissures, de brèches et d'effondrements complets/partiels). Les trois premières catégories illustrent le changement progressif que subissent les polygones à centre concave situés en marge du ravinement : 1) Polygones humides : polygones non perturbés par le ravinement; 2) Polygones drainés : polygones présentant une dégradation récente (moins de 5 ans) des bourrelets périphériques; et 3) Polygones asséchés : polygones affectés par une dégradation plus ancienne (entre 5 et 10 ans) des bourrelets périphériques. Les deux catégories de milieux mésiques (Zones mésiques et Bourrelets de polygones) sont utilisées à titre comparatif et représentent les secteurs non perturbés dominés par des plantes de milieux mésiques, c'est-à-dire mieux drainés. Finalement, les Zones de sédimentation correspondent aux zones recouvertes de sédiments déposés lors du processus actif de ravinement.

Dans le but de quantifier l'influence du ravinement sur les communautés végétales adjacentes, les communautés végétales, l'épaisseur de la couche active et l'humidité du

sol ont été étudiées pour l'ensemble des sites d'échantillonnage. Le recouvrement des différentes espèces végétales a été évalué de la mi-juillet à la première semaine d'août aux étés 2009 et 2010 grâce à l'utilisation de photographies verticales (parcelles de 0,7 m * 0,7 m) en plus d'une évaluation conventionnelle réalisée sur le terrain. L'épaisseur de la couche active a été mesurée au centre de chacun des sites d'échantillonnage à la fin du mois de juillet de 2009 et de 2010. Finalement, l'humidité du sol a été évaluée au cours de l'été 2010 grâce à des mesures ponctuelles enregistrées tout au long de la période estivale. Des mesures en continu ont également été enregistrées durant la période du 25 juin au 31 juillet 2010 pour 14 sites d'échantillonnages. Concernant l'analyse des données, une analyse de correspondance détendancée (DCA) et une analyse canonique des correspondances (CCA) ont d'abord permis de valider l'utilisation des six catégories d'environnements déterminés lors des campagnes terrains. Les résultats indiquent que le développement de ravins de thermo-érosion favorise la baisse du taux d'humidité et l'amincissement de la couche active chez les polygones à centre concave. Ces modifications environnementales permettent l'installation d'espèces caractéristiques des environnements mésiques au détriment d'espèces de milieux humides, qui caractérisent habituellement le centre des polygones.

Vingt quadrats de biomasse ont été réalisés dans 14 sites d'échantillonnages afin de permettre une évaluation de l'impact du ravinement sur la biomasse disponible pour la Grande Oie des neiges. L'installation d'exclos en début d'été a permis de limiter l'effet des oies dans ces secteurs d'intérêts. En fin de saison, le tri, le séchage et le pesage des plantes graminoïdes ont été réalisés selon un protocole standard. Les résultats indiquent que la biomasse totale des plantes graminoïdes est pratiquement deux fois plus importante chez les polygones humides que chez les polygones asséchés, soit 33 g/m^2 et 17 g/m^2 respectivement. Chez les bourrelets de polygones, le résultat obtenu est de 19 g/m^2. Ces résultats indiquent que la nourriture favorite de la Grande Oie des neiges chez les polygones perturbés par le drainage est comparable à la nourriture disponible en environnement mésique.

Une image satellite GeoEye-1 datant du 2 septembre 2010 a été utilisée afin de déterminer la superficie directement affectée par le ravinement. Grâce à cette image, les valeurs de NDVI (Normalized Difference Vegetation Index) couvrant l'ensemble de la vallée ont été calculées et les zones adjacentes aux ravins possédant un faible NDVI ont pu être extraites. Pour ce faire, une classification non supervisée des valeurs de NDVI a permis de distinguer les secteurs perturbés des secteurs non perturbés à proximité des ravins de thermo-érosion. Les résultats obtenus ont été validés à l'aide des nombreux sites d'échantillonnage localisé à la marge des ravins. Les résultats indiquent que les superficies perturbées pour les trois ravins étudiés se limitent aux polygones adjacents aux zones d'effondrement et représentent respectivement 60 344 m^2, 30 480 m^2 et 4 012 m^2. En moyenne, pour chaque mètre linéaire de ravin, il s'agit d'une superficie de 55 m^2 qui est affectée. L'utilisation d'une image satellite a également permis de déterminer qu'actuellement, aucun autre ravin n'a de conséquences aussi importantes sur les milieux humides que les deux ravins majeurs dans la vallée Qarlikturvik.

Ainsi, les résultats de cette étude permettent de démontrer que les ravins de thermo-érosion entraînent une transformation de la couverture végétale à la marge des zones d'effondrement, ce qui engendre une diminution de la biomasse des plantes graminoïdes utilisées par la Grande Oie des neiges. Cette étude permet ainsi de mieux comprendre les conséquences à court terme du développement de ravins de thermo-érosion sur la végétation des milieux humides de l'Arctique.

CHAPITRE I

CONTEXTE GÉNÉRAL DE L'ÉTUDE

1.1 Les milieux humides de l'Arctique

La présence du pergélisol constitue le principal élément expliquant l'existence de milieux humides en hautes latitudes (Woo & Young 2006). Ce sol, dont la température est inférieure à 0 °C durant un minimum de deux années consécutives (French 2007), restreint de façon significative l'infiltration de l'eau en profondeur (Rovansek *et al.* 1996). Durant la période estivale, une mince couche en surface est soumise au dégel annuel : il s'agit de la couche active (van Everdingen 1998). Son épaisseur est principalement influencée par la température moyenne et la durée de la période de dégel, mais plusieurs autres facteurs tels la couverture végétale, les propriétés thermiques du substrat et l'humidité du sol sont également à considérer (Jorgenson *et al.* 2001; Kane *et al.* 2001; Walker *et al.* 2003). Grâce à cette couche superficielle, l'eau provenant majoritairement de la fonte des neiges et du dégel de la couche active y est emmagasinée (Roulet & Woo 1986; Rovansek *et al.* 1996). Les précipitations estivales contribuent de façon plus négligeable à cet approvisionnement (Roulet & Woo 1986).

Minke *et al.* (2007) évaluent qu'à l'intérieur du cercle arctique polaire, les milieux humides existant grâce à la présence de complexes polygonaux occupent une superficie totale de 250 000 km^2. La formation de fissures de retraits thermiques causés par les baisses de température au cours de l'hiver rend possible la création des polygones à coins de glace (Mackay 2000). Durant la période estivale, de l'eau s'infiltre dans ces fentes de gel et forme, au fil des années, de véritables veines de glaces (French 2007). La croissance syngénétique des coins de glace permet le développement de polygones à centre concave en favorisant l'expansion de crêtes qui délimitent chacun des polygones (Mackay & Burn 2002; Plug & Werner 2008). Ces crêtes restreignent l'écoulement de l'eau en surface durant le court été Arctique. Les polygones à centre concave peuvent

être de formes rectangulaires, pentagonales, hexagonales ou presque circulaires (Minke *et al.* 2007) et posséder une taille variant entre 5 à 40 mètres de diamètre (Allard 1996).

La saturation estivale au niveau de la dépression centrale des polygones à centre concave favorise la présence de conditions anaérobiques qui, en limitant le taux de décomposition, facilitent l'accumulation de tourbe (Woo & Young 2006). La présence de cyanobactéries permet la fixation de l'azote et favorise l'existence de milieux propices à la croissance des plantes (Woo & Young 2003). En raison de leurs situations géographiques et de leurs caractéristiques écologiques, les polygones à centre concave de l'Arctique canadien s'apparentent aux tourbières minérotrophes à structure polygonale du Nord québécois (Payette & Rochefort 2001).

En Arctique, les milieux humides constituent un habitat ainsi qu'un site d'alimentation important pour la Grande Oie des neiges (*Chen caerulescens atlanticus*; Gauthier *et al.* 1996). Les plantes graminoïdes (*i.e. Poaceae* et *Cyperaceae*) dominent et constituent l'alimentation préférée de l'oie (Gauthier *et al.*1995; 1996). Ces plantes sont faciles à digérer et possèdent une forte valeur nutritive de par leur faible concentration en fibres et en composés phénoliques ainsi qu'une concentration élevée en azote, en eau et en minéraux (Laing & Raveling 1993; Manseau & Gauthier 1993). L'Île Bylot est d'ailleurs le plus important site de nidification de cette espèce, avec une population estimée à 20 000 couples nicheurs (Reed *et al.* 2002). Selon Massé *et al.* (2001), les milieux humides de la plaine sud de l'Île Bylot seraient utilisés à 46 ± 10 % de leur capacité de support. Une part de l'alimentation se déroule également dans les habitats mésiques (Duclos 2002). Malgré une composition floristique plus diversifiée qu'en milieux humides, les graminoïdes y représentent moins de 11 % du couvert végétal mais restent les espèces préférentiellement sélectionnées par l'oie (Audet *et al.* 2007a; 2007b). La baisse saisonnière de la qualité alimentaire et l'épuisement des plantes favorites dans les milieux humides ainsi que les déplacements nécessaires entre les milieux humides sont des facteurs qui poussent les oies à s'y alimenter (Hughes *et al.* 1994; Duclos 2002).

Les études de Lecompte *et al.* (2008; 2009) démontrent que la disponibilité des milieux humides a également des effets bénéfiques sur la réussite de la nidification de la Grande Oie des neiges. La présence de sources d'eau permanentes, telle que les mares et les lacs, à proximité des nids permet d'améliorer la qualité de l'habitat des oies, en particulier durant les étés secs, en limitant la prédation des nids pendant la période d'incubation (Laing & Raveling 1993).

1.2 Les ravins de thermo-érosion

Le réchauffement climatique actuel de l'Arctique (ACIA 2005) peut aboutir à l'altération du pergélisol (Yochikawa & Hinzman 2003; Hinzman *et al.* 2005; Couture & Pollard 2007). Selon les recherches de Jorgenson *et al.* (2006), une dégradation des coins de glace est en cours dans le nord de l'Alaska. La dégradation de ces structures, qui nécessitent des siècles pour se développer (Fortier & Allard 2004), conduit à des modifications géomorphologiques à l'échelle locale en formant des dépressions à la surface du sol (Jorgenson & Osterkamp 2005; Toniolo *et al.* 2009). Il s'en suit une redistribution des eaux de surface adjacentes au réseau d'affaissement thermokarstique (Fortier *et al.* 2007). Ces changements hydrologiques génèrent des modifications au niveau des communautés végétales présentes, de la biodiversité locale et de l'utilisation du milieu par la faune (Jorgenson *et al.* 2006).

En périphérie de la zone de dégradation du pergélisol, des changements sont apportés à la composition végétale étant donné la baisse de la nappe phréatique (Woo & Young 2006). Ces zones sont rapidement drainées, augmentant le taux de mortalité de la mousse et perturbant les communautés végétales (Osterkamp *et al*, 2009). L'abaissement de la nappe phréatique permet l'apparition d'une couche ayant des propriétés isolantes supérieures, ce qui limite la progression du front de dégel lors de la période estivale (Billings & Peterson 1980). De nouvelles plantes typiques des milieux mésiques s'y installent, les plus communes étant: *Alopecurus alpinus, Arctagrostis latifolia, Cerastium* spp., *Cochlearia officinalis, Draba* spp., *Papaver* spp., *Potentilla hypartica, Saxifraga cernua, Luzula arctica, Luzula confusa* et *Poa arctica* (Billings &

Peterson 1980). Leur recouvrement demeure cependant faible et clairsemé. L'apparition de lichens et de nouvelles espèces de mousses (*Psilopilum cavifolium* et *Dicranum* spp.) marque également la transition vers un environnement mésique (Billings & Peterson 1980).

Le processus de ravinement par thermo-érosion est actuellement étudié à l'Île Bylot. Ces ravins se développent principalement au printemps, lorsque la fonte de la neige génère une importante quantité d'eau. Le ruissellement de surface est d'autant plus important étant donné que la couche active n'est pas formée à cette période (Roulet & Woo 1986; Thompson & Woo 2009). L'eau de ruissellement parvient alors à s'infiltrer dans les fissures de gel et à circuler plus en profondeur. Après quelques jours seulement, la circulation de l'eau a suffisamment élargi les fissures pour former de véritables tunnels (Godin & Fortier 2010; Godin & Fortier en révision). Ceux-ci suivent la structure des coins de glaces compte tenu de leur sensibilité élevée à l'érosion thermique (Fortier *et al.* 2007). Comme les centres des polygones sont constitués d'une concentration plus élevée en sédiments, ils demeurent peu affectés par ce type d'érosion. La convergence de l'eau de surface dans le réseau de canaux contribue par la suite au développement du ravin en érodant les parois et en retirant les accumulations de sédiments grâce à l'érosion mécanique jusqu'à ce qu'il y ait stabilisation du système (Fortier *et al.* 2007).

1.3 L'utilisation de la télédétection

L'utilisation de la télédétection constitue une source importante d'information pour l'étude de la végétation au sein des différents écosystèmes de la planète à l'échelle régionale, continentale ou globale (Campbell 2007). Malgré la végétation clairsemée et le niveau d'hétérogénéité élevé de la toundra Arctique, la disponibilité croissante de capteurs à haute résolution spatiale et l'évolution des techniques d'analyse d'images font de la télédétection un outil qui permet d'obtenir des résultats de plus en plus intéressants (Laidler & Treitz 2003). Plusieurs projets traitant de l'étude de la végétation ont jusqu'à

maintenant été menées en Arctique (*e.g.* Stow *et al.* 1993; Gould 2000; Walker *et al.* 2005; Laidler *et al.* 2008).

L'utilisation des indices de végétation permet d'améliorer le signal de la végétation en combinant les données de plusieurs bandes spectrales (Ray 1994; Treitz & Howarth 1999). Cette transformation permet entre autres de minimiser les variations d'éclairement solaire, d'atténuer l'irrégularité du relief et de limiter l'effet des conditions climatiques (Jackson & Huete 1991). Le NDVI (Normalized Difference Vegetation Index; Rouse *et al.* 1973) est l'indice de végétation le plus utilisé afin d'étudier les propriétés de réflectance de la végétation en Arctique (Laidler & Treitz 2003). Ce dernier permet de normaliser la différence entre l'absorption maximale des pigments chlorophylliens dans la bande rouge et la réflectance maximale des cellules végétales dans le proche infrarouge (Stow *et al.* 1998). La relation fournit d'importantes informations concernant les propriétés de la végétation (*e.g.* la santé, le niveau de stress, la quantité de biomasses verte et la teneur en chlorophylle; Laidler & Treitz 2003). L'indice de NDVI est présenté par un rapport dont les valeurs théoriques varient entre -1 et 1 (Ray 1994). Toutefois, la présence de végétation est indiquée par un NDVI supérieur à 0 (Jackson & Huete 1991).

1.4 Objectifs

À l'Île Bylot, au Nunavut, on observe depuis quelques années la formation de ravins de thermo-érosion au sein des milieux humides de la vallée Qarlikturvik. Ces formations modifient le régime hydrologique de surface en favorisant le drainage rapide des polygones humides adjacents. Déjà, des changements sont perceptibles dans la composition végétale de ces milieux essentiels à la croissance de la Grande Oie des neiges (*Chen caerulescens atlantica*).

Ainsi, mes objectifs de recherche sont : 1) Quantifier l'influence du ravinement sur les communautés végétales adjacentes; 2) Évaluer l'impact du ravinement sur la biomasse disponible pour la Grande Oie des neiges; 3) Déterminer la superficie

directement affectée par le ravinement. Les hypothèses étudiées sont : A) Suite au ravinement, les espèces végétales hydrophiles sont remplacées par des espèces évoluant en milieux mésiques; B) Le drainage diminue la biomasse des plantes favorites des oies, affectant la capacité de support du milieu; C) La superficie directement affectée se limite aux polygones adjacents au ravinement. Les deux premiers objectifs de recherche sont traités dans le chapitre II, tandis que le troisième objectif de recherche est traité dans le chapitre III.

1.5 Site à l'étude

La présente étude se déroule à l'Île Bylot, Nunavut, Canada. Localisée au nord de la Terre de Baffin, cette île se situe au 73^{e} parallèle et fait partie du Haut-Arctique canadien. Sur une superficie totale de 10 750 km^2, quelques 5 000 km^2 sont couverts par une calotte glacière (Zoltai *et al.* 1983). Dans le secteur sud-ouest de la plaine sud de l'île, la vallée Qarlikturvik occupe une superficie de 70 km^2 (Hughes *et al.* 1994). Cette vallée glaciaire a été formée par le retrait de deux glaciers et est actuellement traversée par une rivière proglaciaire. De part et d'autre de cette rivière, l'accumulation de dépôts éoliens constituée de sable et de limon (Fortier & Allard 2004) ainsi que l'accumulation de dépôts organiques ont permis le développement de terrasses (Allard, 1996). Cette déposition a permis d'accroître le coefficient de contraction thermique du sol, responsable de la configuration actuelle des complexes de polygones à coins de glace qui ont amorcé leur formation il y a 6 000 BP (Fortier & Allard 2004). La température annuelle moyenne était de -14,5 °C et la température estivale moyenne (juin à août) de 4,5 °C pour la période de 1994 à 2007 à l'Île Bylot (Cadieux *et al.* 2008). Des données climatiques enregistrées à Pond Inlet entre 1971 et 2000 par Environnement Canada (2002) indiquent que les précipitations annuelles moyennes sont de l'ordre de 191 mm, dont près de 75 % sous forme solide.

Selon Hughes *et al.* (1994), 16.1 km^2 de la vallée sur une superficie totale de 70 km^2 correspondent à un environnement humide. Toutefois, d'après Massé (1998), ce serait plutôt 19 km^2 sur une superficie totale évaluée à 56 km^2. La vallée Qarlikturvik est

un des principaux sites d'élevage des oisons pendant l'été. Certaines familles marchent jusqu'à 30 km pour avoir accès à ce site (Mainguy *et al.* 2006a; Mainguy *et al.* 2006b). L'abondance de milieux humides dominés par des communautés végétales à dominance de cypéracées (*Carex aquatilis, Eriophorum scheuchzeri, Eriophorum angustifolium*) et de graminées (*Dupontia fisheri, Arctagrostis latifolia, Pleuropogon sabinei*) caractérise cette vallée (Zoltai *et al.* 1983; Gauthier *et al.* 1996).

Des dizaines de ravins de thermo-érosion ont été répertoriés à l'échelle de la vallée Qarlikturvik (Godin & Fortier 2012). Certains d'entre eux se sont développés dans les dépôts organiques et affectent directement les milieux humides avoisinants. Leur évolution spatio-temporelle est actuellement étudiée. En dix ans par exemple, une section de coins de glace s'est transformée en un ravin de thermo-érosion faisant au total 835 m de long sur l'axe principal et couvrant une superficie de 27 762 m^2 (Godin & Fortier 2012). Un deuxième cas d'importance présente quant à lui une longueur de 717 m et une superficie de 14 825 m^2 (Godin & Fortier 2012).

1.6 Références

ACIA (2005) *Arctic Climate Impact Assessment*. Cambridge University Press: New York, 1042 pp.

Allard M (1996) Geomorphological changes and permafrost dynamics: key factors in changing arctic ecosystems. An example from Bylot Island, Nunavut, Canada. *Geoscience Canada*, **23**, 205–212.

Audet B, Gauthier G, Levesque E (2007a) Feeding ecology of greater snow goose goslings in mesic tundra on Bylot Island, Nunavut, Canada. *The Condor*, **109**, 361–376.

Audet B, Levesque E, Gauthier G (2007b) Seasonal variation in plant nutritive quality for greater snow goose goslings in mesic tundra. *Canadian Journal of Botany*, **85**, 457–462.

Billings WD, Peterson KM (1980) Vegetational change and ice-wedge polygons through the thaw-lake cycle in Arctic Alaska. *Arctic and Alpine Research*, **12**, 413–432.

Cadieux M-C, Gauthier G, Gagnon C, *et al.* (2008) *Monitoring the environmental and ecological impacts of climate change on Bylot Island, Sirmilik National Park: 2004–2008 final report.* Centre d'études nordiques, Université Laval, Québec, 113 pp.

Campbell JB (2007) *Introduction to remote sensing, 4th. ed.* The gilford press, 626 pp.

Couture NJ, Pollard WH (2007) Modelling geomorphic response to climatic change. *Climatic Change*, **85**, 407–431.

Duclos I (2002) Milieux mésiques et secs de l'Île Bylot, Nunavut (Canada): caractérisation et utilisation par la Grande Oie des Neiges. Mémoire de maîtrise, Université du Québec à Trois-Rivières, Trois Rivières, 113 pp.

Environment Canada (2002) *Archives nationales de données climatiques et météorologiques pour le Canada*. Disponible à: www.climat.meteo.gc.ca (Consulté en janvier 2012).

Fortier D, Allard M (2004) Late Holocene syngenetic ice-wedge polygons development, Bylot Island, Canadian Arctic Archipelago. *Canadian Journal of Earth Sciences*, **41**, 997–1012.

Fortier D, Allard M, Shur Y (2007) Observation of rapid drainage system development by thermal erosion of ice wedges on Bylot Island, Canadian Arctic Archipelago. *Permafrost and Periglacial Processes*, **18**, 229–243.

French HM (2007) *The Periglacial Environment, Third Edition*. John Wiley & Sons Ltd, 458 pp.

Gauthier G, Hughes RJ, Reed R, *et al.* (1995) Effect of grazing by greater snow geese on the production of graminoids at an arctic site (Bylot Island, NWT, Canada). *Journal of Ecology*, **83**, 653–664.

Gauthier G, Rocheford L, Reed A (1996) The exploitation of wetland ecosystems by herbivores on Bylot Island. *Geoscience Canada*, **23**, 253–259.

Godin E, Fortier D (2010) Geomorphology of thermo-erosion gullies – case study from Bylot Island, Nunavut, Canada. *Dans: Proceedings 6th Canadian Permafrost Conference and 63rd Canadian Geotechnical Conference, Calgary.*

Godin E, Fortier D (2012) Fine scale spatio-temporal monitoring of multiple thermo-erosion gullies development on Bylot Island, eastern canadian archipelago. *In: Proceedings Tenth International Conference on Permafrost (TICOP), Salekhard, Russia.*

Godin E, Fortier D (en révision) Geomorphology and spatio-temporal characterization of a thermo-erosion gully in the valley of glacier C-79, Bylot Island, Nunavut, Canada. *Canadian Journal of Earth Sciences*.

Gould W (2000) Remote sensing of vegetation, plant species richness, and regional biodiversity hotspots. *Ecological Applications*, **10**, 1861–1870.

Hinzman LD, Bettez ND, Bolton WR, *et al.* (2005) Evidence and implications of recent climate change in northern Alaska and other arctic regions. *Climatic Change*, **72**, 251–298.

Hughes RJ, Reed A, Gauthier G (1994) Space and habitat use by greater snow goose broods on Bylot Island, Northwest Territories. *Journal of Wildlife Management*, **58**, 536–545.

Jackson RD, Huete AR (1991) Interpreting vegetation indices. *Preventive Veterinary Medicine*, **11**, 185–200.

Jorgenson MT, Osterkamp TE (2005) Response of boreal ecosystems to varying modes of permafrost degradation. *Canadian Journal of Forest Research*, **35**, 2100–2111.

Jorgenson MT, Racine CH, Walters JC, *et al.* (2001) Permafrost degradation and ecological changes associated with a warming climate in central Alaska. *Climatic Change*, **48**, 551–579.

Jorgenson MT, Shur YL, Pullman ER (2006) Abrupt increase in permafrost degradation in Arctic Alaska. *Geophysical Research Letters*, **33**, L02503, doi: 02510.01029/02005GL024960.

Kane DL, Hinkel KM, Goering DJ, *et al.* (2001) Non-conductive heat transfer associated with frozen soils. *Global and Planetary Change*, **29**, 275–292.

Laidler GJ, Treitz P (2003) Biophysical remote sensing of arctic environments. *Progress in Physical Geography*, **27**, 44–68.

Laidler GJ, Treitz P, Atkinson D (2008) Remote sensing of Arctic vegetation: relations between the NDVI, spatial resolution and vegetation cover on Boothia Peninsula, Nunavut. *Arctic*, **61**, 1–13.

Laing KK, Raveling DG (1993) Habitat and food selection by emperor goose goslings. *The Condor*, **95**, 879–888.

Lecomte N, Gauthier G, Giroux J-F (2008) Breeding dispersal in a heterogeneous landscape: the influence of habitat and nesting success in greater snow geese. *Oecologia*, **155**, 33–41.

Lecomte N, Gauthier G, Giroux J-F (2009) A link between water availability and nesting success mediated by predator-prey interactions in the Arctic. *Ecology*, **90**, 465–475.

Mackay JR (2000) Thermally induced movements in ice-wedge polygons, western arctic coast: a long-term study. *Geographie physique et Quaternaire*, **54**, 41–68.

Mackay JR, Burn CR (2002) The first 20 years (1978-1979 to 1998-1999) of ice-wedge growth at the Illisarvik experimental drained lake site, western Arctic coast, Canada. *Canadian Journal of Earth Sciences*, **39**, 95–111.

Mainguy J, Gauthier G, Giroux J-F, *et al.* (2006a) Gosling growth and survival in relation to brood movements in greater snow geese (*Chen caerulescens atlantica*). *The Auk*, **123**, 1077–1089.

Mainguy J, Gauthier G, Giroux J-F, *et al.* (2006b) Habitat use and behaviour of greater snow geese during movements from nesting to brood-rearing areas. *Canadian Journal of Zoology*, **84**, 1096–1103.

Manseau M, Gauthier G (1993) Interactions between greater snow geese and their rearing habitat. *Ecology*, **74**, 2045–2055.

Masse H (1998) *Estimation de la capacité de support des différents écosystèmes humides utilisés par la grande oie des neiges nichant à l'Île Bylot (Nunavut, Canada).* Mémoire de maîtrise, Université Laval, Québec, 98 pp.

Masse H, Rochefort L, Gauthier G (2001) Carrying capacity of wetland habitats used by breeding greater snow geese. *The Journal of Wildlife Management*, **65**, 271–281.

Minke M, Donner D, Karpov NS, *et al.* (2007) Distribution, diversity, development and dynamics of polygon mires: examples from Northeast Yakutia (Siberia). *Peatlands International*, **1**, 36–40.

Osterkamp TE, Jorgenson MT, Schuur EAG, *et al.* (2009) Physical and ecological changes associated with warming permafrost and thermokarst in interior Alaska. *Permafrost and Periglacial Processes*, **20**, 235–256.

Payette S, Rocheford L (2001) *Écologie des tourbières du Québec-Labrador*. Les Presses de l'Université Laval, 621 pp.

Plug LJ, Werner BT (2008) Modelling of ice-wedge networks. *Permafrost and Periglacial Processes*, **19**, 63–69.

Ray (1994) *A FAQ on vegetation in remote sensing*. California Institute of Technology. Pasadena, California, USA, 18 pp.

Reed A, Hughes RJ, Boyd H (2002) Patterns of distribution and abundance of Greater Snow Geese on Bylot Island, Nunavut, Canada 1983-1998. *Wildfowl*, **53**, 53–65.

Roulet NT, Woo M-K (1986) Hydrology of a wetland in the continuous permafrost region. *Journal of Hydrology*, **89**, 73–91.

Rouse JW, Haas RH, Schell JA, *et al.* (1973) Monitoring vegetation systems in the Great Plains with ERTS. *Third ERTS Symposium*, NASA SP-351 **1**, 309–317.

Rovansek RJ, Hinzman LD, Kane DL (1996) Hydrology of a tundra wetland complex on the Alaskan Arctic Coastal Plain, U.S.A. *Arctic and Alpine Research*, **28**, 311–317.

Stow DA, Burn BH, Hope AS (1993) Spectral, spatial, and temporal characteristics on Arctic tundra reflectance. *International Journal of Remote Sensing*, **14**, 2445–2462.

Stow D, Hope A, Boynton W, *et al.* (1998) Satellite-derived vegetation index and cover type maps for estimating carbon dioxide flux for arctic tundra regions. *Geomorphology*, **21**, 313–327.

Thompson DK, Woo M-K (2009) Seasonal hydrochemistry of a high Arctic wetland complex. *Hydrological Processes*, **23**, 1397–1407.

Toniolo H, Kodial P, Hinzman LD, *et al.* (2009) Spatio-temporal evolution of a thermokarst in Interior Alaska. *Cold Regions Science and Technology*, **56**, 39–49.

Treitz PM, Howarth PJ (1999) Hyperspectral remote sensing for estimating biophysical parameters of forest ecosystems. *Progress in Physical Geography*, **23**, 359–390.

van Everdingen R (1998) *Multi-Language Glossary of Permafrost and Related Ground-Ice Terms, revised May 2005.* National Snow and Ice Data Center/World Data Center for Glaciology, Boulder, Colorado. Disponible à: http://nsidc.org/fgdc/glossary/ (Consulté en janvier 2012).

Walker DA, Jia GJ, Epstein HE, *et al.* (2003) Vegetation-soil-thaw-depth relationships along a Low-Arctic bioclimate gradient, Alaska: synthesis of information from the ATLAS studies. *Permafrost and Periglacial Processes*, **14**, 103–123.

Walker DA, Raynolds MK, Daniëls FJA, *et al.* (2005) The circumpolar Arctic vegetation map. *Journal of Vegetation Science*, **16**, 267–282.

Woo M-K, Young KL (2003) Hydrogeomorphology of patchy wetlands in the High Arctic, polar desert environment. *Wetlands*, **23**, 291–309.

Woo M-K, Young KL (2006) High Arctic wetlands: their occurrence, hydrological characteristics and sustainability. *Journal of Hydrology*, **320**, 432–450.

Yoshikawa K, Hinzman LD (2003) Shrinking thermokarst ponds and groundwater dynamics in discontinuous permafrost near Council, Alaska. *Permafrost and Periglacial Processes*, **14**, 151–160.

Zoltai SC, McCormick KJ, Scotter GW (1983) *A natural resource survey of Bylot Island and adjacent Baffin Island, Northwest Territories*. Parks Canada, Ottawa, Canada, 176 pp.

CHAPITRE II

IMPACT OF PERMAFROST GULLYING ON WETLAND HABITAT, BYLOT ISLAND, NUNAVUT, CANADA

En attente de soumission

Authors:

Naïm Perreault[1,2], Esther Lévesque[1,2], Daniel Fortier[2,3]

[1] Département de Chimie-Biologie, Université du Québec à Trois-Rivières, Trois-Rivières, QC, G9A 5H7, Canada

[2] Centre d'études nordiques, Université Laval, Québec, QC, G1V 0A6, Canada
[3] Département de géographie, Université de Montréal, Montréal, QC, H2V 2B8, Canada

Corresponding author: Esther Lévesque, tel. +1-819-376-5011 ext.3351, fax +1-819-376-5210, e-mail: esther.levesque@uqtr.ca

Keywords: Arctic wetlands, thermo-erosion gullying, drainage, wetland vegetation, ice-wedge polygons, carrying capacity, geese.

2.1 Abstract

Arctic wetlands provide essential summer feeding, nesting and breeding sites for many migratory bird species, particularly the Greater Snow Goose. A rapid melting of permafrost currently induces the development of thermo-erosion gullying in wetlands heavily used by the largest goose colony at Bylot Island, Nunavut. These new disturbances drain the center of adjacent low-centered polygon wetlands by the collapse the ice-wedges. The aims of this paper are to: 1) Determine how thermo-erosion gullying affects soil moisture content and thawing front depth of low-centered polygon; 2) Measure changes in plant composition and distribution; 3) Quantify the impact on food resources for snow geese. Low-centered polygons were classified into three eco-terrain units (Wet, Drained and Dried polygons) to better understand and characterize the degradation. Results show that wet polygons remained saturated longer after snowmelt and rainfalls than disturbed polygons. Whereas thaw front depth was approx. 10 cm lower for the low-centered polygons affected by gullying. These environmental changes lead within 10 years to a gradual replacement of vascular vegetation dominated by the species preferred by geese (*Cyperaceae* and *Poaceae*) by vegetation typical of mesic environments (including shrubs). Above-ground graminoid biomass available to herbivores decreased of 15.63 g/m^2 near gullies. This reduction of food in the affected sectors affects herbivores such the Greater Snow Goose.

2.2 Introduction

Arctic wetlands are oases with high productivity (Woo & Young 2006). Locally enhanced water supply and a thin thaw front depth of permafrost allow frequent saturation, causing nutrient enrichment favourable to vegetation development (Woo & Young 2003). The rich plant growth with slow decomposition rate from cold and wet soil conditions promote the accumulation of peat in high latitude (Billings 1987; Vardy *et al.* 2000). Arctic wetlands play important ecological functions for high arctic fauna such as grazing grounds for herbivores (Klein & Bay 1991; Gauthier *et al.* 1996).

Polygon-patterned permafrost is frequently associated to wetlands, particularly the low-centered polygons (Minke *et al.* 2007). This polygon form is characterised by elevated ridges created with the development of ice-wedges that enclose a depression usually flooded by snow meltwater (Woo & Young 2006; French 2007; Minke *et al.* 2007). Saturated center of low-centered polygons are characterized by plant communities dominated by hydrophilic graminoids (*i.e.* sedges and grasses) and fen mosses (Zoltai *et al.* 1983; Gauthier *et al.* 1995; Ellis *et al.* 2008). The ridges of polygons, however, are better drained and support shrubs, forbs and grasses (Zoltai *et al.* 1983). On Bylot Island (Nunavut, Canada), hydrophilic graminoids are consumed intensively and wetlands are the preferred brood-rearing habitat of the Greater Snow Goose (*Chen caerulescens atlanticus*) (Hughes *et al.* 1994; Gauthier *et al.* 1995; Massé *et al.* 2001).

The current climatic warming of the Arctic (ACIA 2005) can lead to alteration of permafrost or deepening of summer thaw front depth. These changes induce rapid geomorphologic modifications (*e.g.* French 1974; Yoshikawa & Hinzman 2003; Hinzman *et al.* 2005, Lantz & Kokelj 2008; Toniolo *et al.* 2009) affecting hydrological regimes and soil moisture contents (Couture & Pollard 2007). Formation and evolution of thermo-erosion gullies have been observed over the last 10 years in the polygon-patterned wetlands on Bylot Island (Fortier *et al.* 2007; Godin & Fortier 2010). This permafrost degradation is caused by the melting of ice-wedges by thermal-erosion and create zig-zag pattern of gullies (Fortier *et al.* 2007). Water running through the gully causes open hollows by eroding the ground (Seppälä 1997). These gullies change the surface hydrology and favour drainage of adjacent wet polygons. The impacts of these new drainage systems on the plant composition and graminoid biomass of wetlands need to be quantified to understand consequences on this high-quality environment used by herbivores like Greater Snow Goose.

The objectives are to present how thermo-erosion gullying affects the soil moisture content and the thawing front (frost table) of low-centered polygon wetlands and how these changes influence plant composition and biomass leading to a decrease of food

resources for geese. Data were collected from three gullies in the polygon-patterned wetlands of Qarlikturvik glacial valley on Bylot Island, Nunavut, Canada. We examine the hypotheses that 1) wetland plant species are rapidly replaced by species living in mesic environments after drainage and 2) these changes reduces the availability of food resources for geese.

2.3 Material and methods

2.3.1 Study area

The study was conducted in the Qarlikturvik valley (73° 09' N, 79° 57' W) on the south-western plain of Bylot Island, Nunavut, Canada (Figure 2.1A) in 2009 and 2010. This glacial valley is bound to the north and south by plateaus ≤ 500 m ASL, to the west by the sea and to the east by two glaciers (Figure 2.1B). The outwash plain is dissected by a proglacial river flowing from the glaciers towards the sea. The accretion of aeolian sands and silts and the concurrent accumulation of peat formed terraces on both sides of the river (Allard 1996). The syngenetic growth of ice-wedges during the Late-Holocene has resulted in the development of polygon-patterned ground (Fortier & Allard 2004). Currently, terraces are characterized by numerous permanent ponds, lakes and wet meadows (Hughes *et al.* 1994). The typical size of polygons is 10 to 20 m in diameter (Gauthier *et al.* 1995) and the thaw front depth is approximately 0.4 m in peaty-silt deposit (Fortier *et al.* 2006).

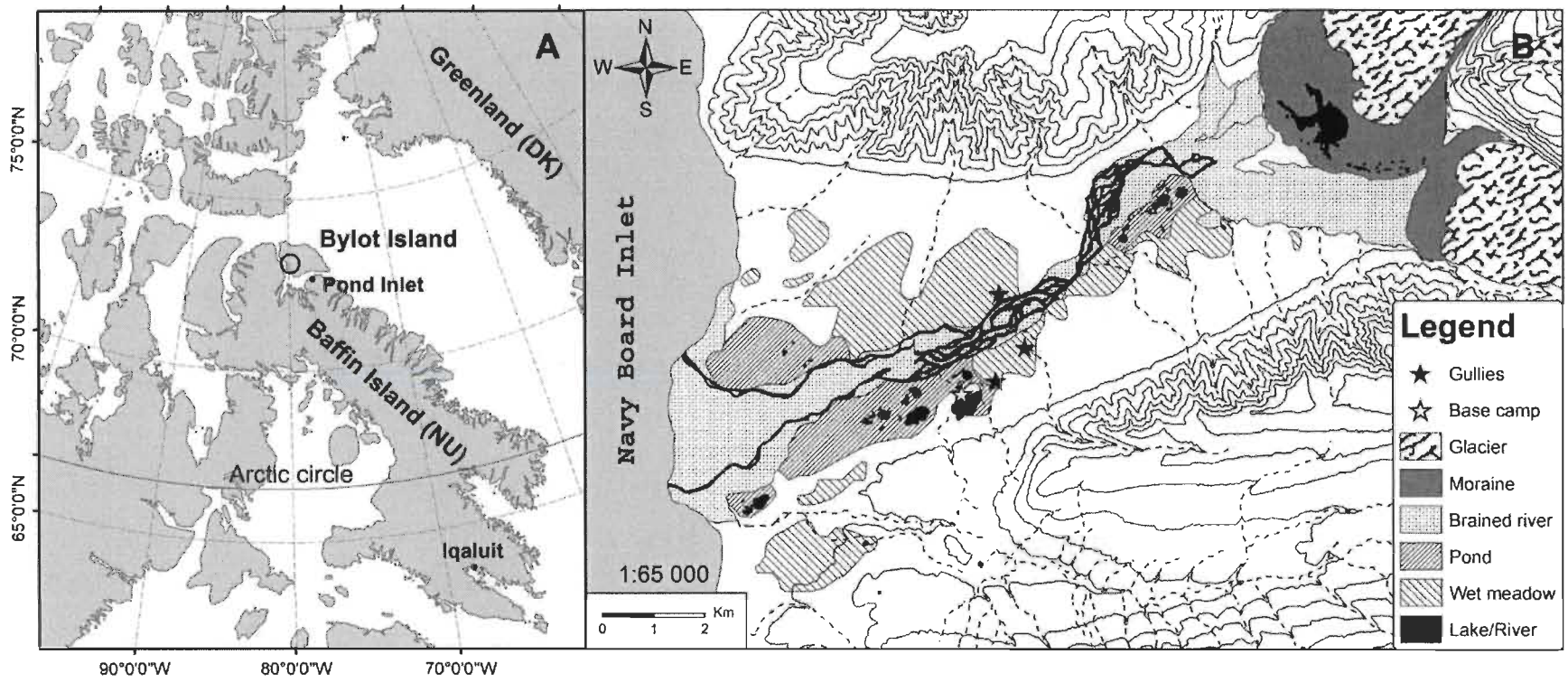

Figure 2.1 : Location of study area. (A) Bylot Island, Nunavut, Canada and the Qarlikturvik valley, south-western plain of Bylot Island (located by circle). (B) Qarlikturvik valley (based on Hughes *et al.* 1994) and the three thermo-erosion gullies studied (located by black stars).

Wetlands concentration in the Qarlikturvik valley is one of the highest on the island and represents approximately 23% of the total area of the valley (*ca* 70 km^2; Hughes *et al.* 1994). Plant communities in low-centered polygons and at the pond margins are relatively homogenous and dominated by sedges (*e.g. Carex aquatilis* Wahlenb. var. *minor* Boott, *Eriophorum scheuchzeri s. lat./russeolum* subsp. *leiocarpum*, *Eriophorum angustifolium* Honck. *cf.* subsp. *angustifolium*), grasses (primarily *Arctagrostis latifolia* R. Br. subsp. *latifolia*, *Dupontia fisheri* R. Br., *Pleuropogon sabinei* R. Br.; Zoltai *et al.* 1983; Gauthier *et al.* 1995) and fen mosses (primarily *Drepanocladus* spp., *Aulocomnium* spp.; Ellis *et al.* 2008). Low-centered polygon rims, sloping terrain and hummocky tundra support mesic species including shrubs (*e.g. Salix* spp., *Vaccinium uliginosum* L.), forbs (*e.g. Cassiope tetragona* (L.) D. Don subsp. *tetragona*, *Oxytropis maydelliana* Trautv. subsp. *melanocephala* (Hook.) Porsild) and grasses (*e.g. Arctagrostis latifolia* R. Br. subsp. *latifolia*, *Alopecurus borealis* Trin., *Poa arctica* R. Br. s. lat., *Luzula confusa* Lindebl.; Zoltai *et al.* 1983). The Greater Snow Goose is the most abundant herbivore from late May to early September on Bylot Island (Gauthier *et al.* 1996). In June, the grazing is light at the Qarlikturvik valley because goose feeding is dispersed spatially and females are incubating (Gauthier *et al.* 1995). The valley is however a major brood rearing site from early July onward and some families walk up to 30 km to access this highly productive site (Mainguy *et al.* 2006a; 2006b).

There are many gullies in the valley (Godin and Fortier, 2012) but we selected three thermo-erosion gullies having similar characteristics and located in the low-centered polygons complex. Gully A is under study since 1999 and it is the largest gully with 835 m long (Figure 2.2; Fortier *et al.* 2007; Godin & Fortier 2012); Gully B is 717 m long and is characterized by a very active erosion process at the head of the gully (Godin & Fortier 2012); Gully C is the smallest one with 180 m long and has not been active in recent years. A total of 212 sampling sites spanning the full length of each gully and representing unaffected and disturbed wet and mesic habitats adjacent to these gullies were chosen during the field seasons 2009 and 2010 (Figure 2.3). Sites included polygons adjacent to the gullies as well as undisturbed ones up to 150 m from the edge

of the gullies. The coordinates of the sampling sites were recorded by GPS (Garmin eTrex Venture HC) with an accuracy of 5 m. Each sampling site was systematically examined to include representative samples from recognized eco-terrain unit. In total, 99, 92 and 21 sampling sites were established surrounding Gully A, B and C respectively.

Figure 2.2 : Oblique aerial view of Gully A in August 2010, Bylot Island, Nunavut and impact on adjacent wetland vegetation.

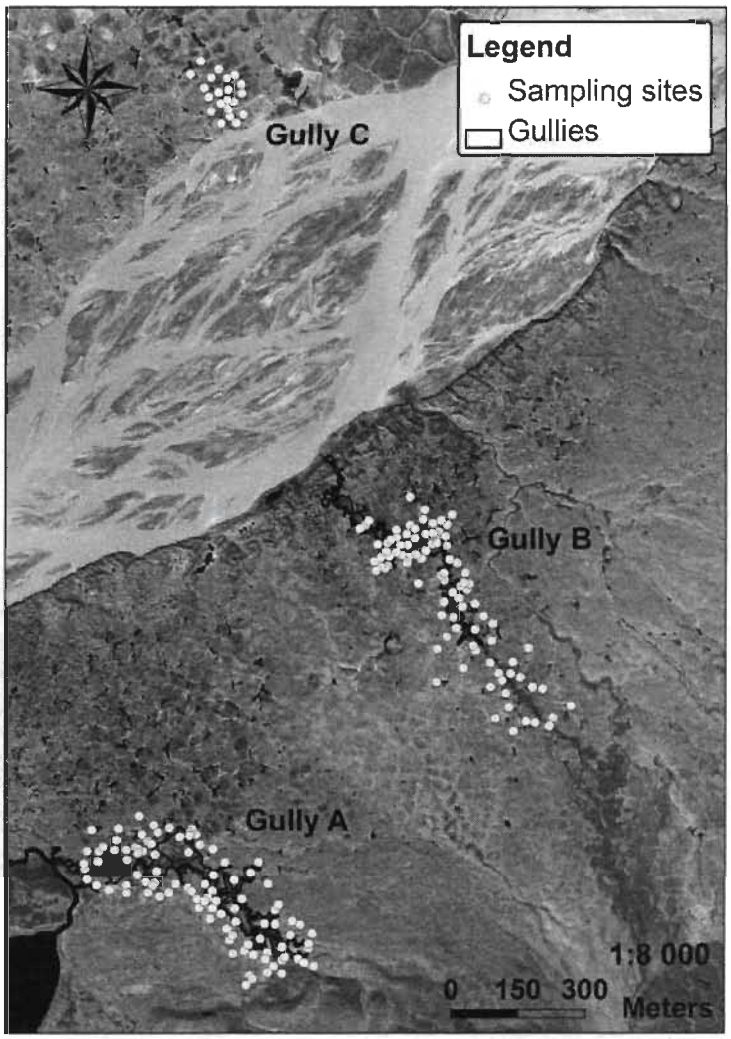

Figure 2.3 : Sampling sites (n = 212) selected during field seasons 2009 and 2010 near three thermo-erosion gullies, Bylot Island, Nunavut.

2.3.2 Field sampling

Six distinct eco-terrain units from intact wet and mesic to disturbed conditions were identified during early reconnaissance visits near the three thermo-erosion gullies (Figure 2.4): Wet polygons (n = 62), Drained polygons (n = 44), Dried polygons (n = 43), Mesic zones (n = 13), Mesic polygon rims (n = 35) and Sediment zones (n = 15).

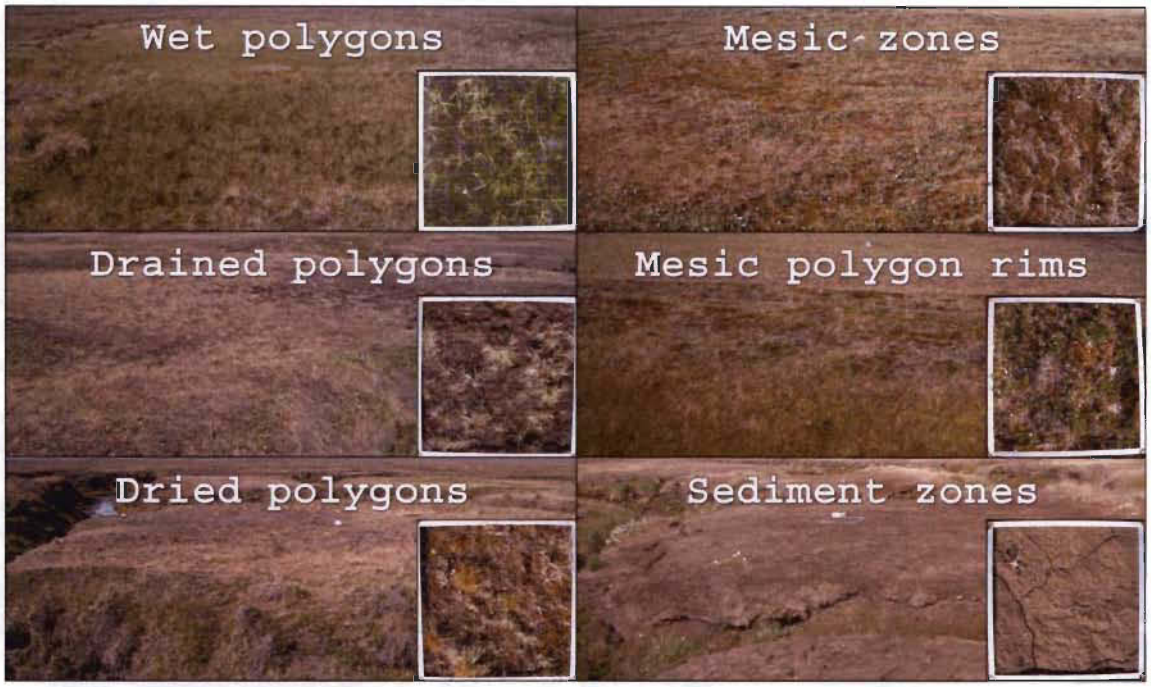

Figure 2.4 : General view and close up of 70 cm * 70 cm quadrat of six eco-terrain units: low-centered polygons (Wet polygons, n = 62; Drained polygons, n = 44; Dried polygons, n = 43), mesic environments (Mesic zones, n = 13; Mesic polygon rims, n = 35) and Sediment zones (n = 15) near three thermo-erosion gullies, Bylot Island, Nunavut.

2.3.2.1 Plant community characterisation

For each site, three random quadrats of 70 cm * 70 cm were photographed vertically in July 2009 or 2010. Pictures were taken from approx. 1.3 m above the quadrats. To reduce distortion, quadrats were positioned in the center of the photograph according to Chen *et al.* (2010) and "Climate Change Impacts on Canadian Arctic Tundra Ecosystems: Interdisciplinary and Multi-scale Assessments (CiCAT)" protocols from International Polar Year (2012). The vascular plant species cover was assessed as a vertical projection onto the ground of all above-ground parts of the individual plants in the lab on digital photographs with a 7 cm superimposed grid integrates to the quadrat frame (annexe A) using a modified scale of Daubenmire's (1959) classification (Table 2.1). Lichens, green mosses (*i.e.* living mosses), dry mosses, cryptogamic crust, nostocs, mushrooms, bare ground, geese feces, grubbing, litter, standing dead and standing water covers were assessed in the same way. Evaluation was combined with a field visual

evaluation of cover in one 70 cm x 70 cm quadrat and an inventory of additional vascular plant species outside the quadrat for species richness of sites and eco-terrain units. These plots were located within areas that were considered ecologically similar, homogeneous and representative of the eco-terrain unit. For statistical analysis, the modified scale of Daubenmire's units (1 to 8) was converted using classes' midpoint and a mean of vegetation cover was calculated for every specific species per sampling site. Species specific mean of vegetation cover were added to provide a cover percentage per family.

Table 2.1 : Cover abundance scale modified from Daubenmire's (1959) and used for estimating the plant abundance (% cover). The midpoint of range (%) was used in calculations and analyses.

Cover Class	Range of cover percentage (%)	Midpoint of Range (%)
0	0	0
1	0 – 1	0.5
2	1 – 5	3
3	5 – 10	7.5
4	10 – 25	17.5
5	25 – 50	37.5
6	50 – 75	62.5
7	75 – 95	85
8	95 – 100	97.5

2.3.2.2 Soil properties and physical characterisation

The thawing front depth (frost table) of sampling sites was recorded at the end of both seasons for Gully A and Gully B (July 31th 2009 and July 30th 2010) and on July 19th 2010 for Gully C. Measurement of the thaw front depth was achieved using a steel rod graduated in centimetre driven into the active layer at the center of polygons. For Mesic zones, Mesic polygon rims and Sediment zones eco-terrain units, three random measurements per site were taken and the mean was used for further analyses. Punctual point measurements of soil moisture (top 10 cm) content were recorded in 2010 (July 30th for Gullies A and Gully B; July 19th for Gully C) at the center of each site using ECH$_2$O EC-5 moisture sensors (Decagon Devices). Twenty sensors connected to four Em5b dataloggers (Decagon Devices) were also disposed in the ground (top 10 cm)

for the summer to document the evolution of soil moisture in the various eco-terrain units : Wet polygons (n = 4); Drained polygons (n = 4); Dried polygons (n = 2); Mesic polygon rims (n = 4). Duplication of some sampling sites was necessary given that the cable length was limited to 5 meters. In the same way, sensors were positioned at a distance of 1-2 meters from the edge of polygons. Daily precipitation was recorded throughout the summer 2010 at the base camp located 700 m west of Gully A (Figure 2.1B) with a manual rain gauge (Gauthier *et al.* 2010) for the interpretation of the soil moisture evolution.

In addition to the thawing front depth and the soil moisture, a physical characterisation of the sampling sites was used to define the eco-terrain units polygon rims integrity. Four categories were used for the description: 1) No water output: low-center polygons non-affected by the gullying process; 2) Gully connection: low-center polygons affected by rim collapse, breaches and/or cracks connecting to the gully; 3) Stream connection: low-center polygons or zones affected by fresh sediment deposition from the stream upstream the gully; 4) Other types: mesic environments where other choices are non-applicable.

2.3.2.3 Biomass

The above-ground biomass in late summer of graminoids in four eco-terrain units: Wet polygons (n = 4), Drained polygons (n = 4), Dried polygons (n = 2) and Mesic polygon rims (n = 4), was measured in 2010 following the protocol of Gauthier *et al.* (1995). Exclosures of 1 m * 1 m were made of chicken wire 30 cm high in late June before the arrival of geese to prevent grazing on the vegetation. Plant biomass was sampled inside the exlosures near peak production in early August (July 31th to August 3rd 2010). The plot size was 25 cm * 25 cm for Wet polygons and Drained polygons and 50 cm * 20 cm for Dried polygons and Mesic polygons rims. Graminoids were first sorted into *Cyperaceae* (*i.e. Carex aquatilis*, *Eriophorum angustifolium*, *Eriophorum scheuchzeri*), *Juncaceae* (*i.e. Luzula arctica*, *Luzula confusa*) and *Poaceae* (*i.e. Anthoxanthum arcticum*, *Arctagrostis latifolia*, *Dupontia fisheri*, *Festuca brachyphylla*). Above-ground live biomass was then oven dried to constant mass and weighed to ± 0.001 g.

2.3.3 Statistical analyses

Variation in plant communities was first summarized using Detrended correspondance analysis (DCA, Hill & Gauch 1980). Plant communities were then related to the environmental conditions with an ordination performed using Canonical correspondence analysis (CCA, ter Braak 1986). CCA is a direct gradient analysis technique that relates community variation (composition and abundance) to environmental variation, enabling the determination of significant relationships between environmental variables and community distribution (Vogiatzakis *et al.* 2003). Data were computed using the program R with the community ecology package "vegan" v2.0-3.

We used an ANOVA type III for unbalanced data to test for significant differences in thaw front depth of eco-terrain units at the end of seasons 2009 and 2010 as well as for above-ground live biomass of eco-terrain units. The program R (Ihaka & Gentleman 1996) v2.15.0 with the package "car" v2.0-12 was used. Normality and homogeneity of data were previously tested using Shapiro-Wilk and Barlett tests respectively. Tukey's Post-hoc test was performed on data using the package "multcomp" v1.2-12.

2.4 Results

Classification of the 212 sampling sites based on plant communities, soil moisture content and integrity of polygon rims (*i.e.* intact, partially degraded, completely collapsed etc.) illustrates the gradual change of the polygons located at the margin of the gully: 1) Wet polygons (n = 62): polygons not affected by gully erosion; 2) Drained polygons (n = 44): polygons with a recent deterioration (within 5 years) of peripheral rims which results in drying of wetlands' mosses and vascular plants; 3) Dried polygons (n = 43): polygons affected by an older deterioration (5-10 years) with a significant number of plant species characteristic of mesic environments. Based on the spatio-temporal evolution of gullying studied by Godin & Fortier (2012) we determined that the transition from Wet polygons to Drained polygons corresponds approximated to five years whereas transition from Wet polygons to Dried polygons corresponds approximated to ten years. Mesic zones (n = 13) and Mesic polygon rims (n = 35)

eco-terrain units represent other environments than low-centered polygons, with a vegetation dominated by plants of mesic environments. Finally, Sediment zones (n = 15) eco-terrain unit corresponds to areas upstream gullies covered with freshly deposited sediment during the process of active gully erosion.

2.4.1 Plant community characteristics

A total of 66 taxa including 59 vascular plant species (annexe B), total lichens cover, total green mosses cover, total dry mosses cover, cryptogamic crust, nostocs and mushrooms were used for the ordinations (annexe C). The first two axes of the DCA biplot explained 28% of the cumulative variation in plant species data (Table 2.2). The eco-terrain units formed distinct groups, except the Mesic zones and the Mesic polygon rims which were undistinguishable (Figure 2.5). The Drained polygons and the Dried polygons formed two dispersed groups, showing a strong variability in the vegetation. For the Wet polygons and the mesic environments, sites were less dispersed suggesting a greater similarity of vegetation among sites of a same eco-terrain unit. Sites of the Sediment zones eco-terrain unit were well dispersed reflecting a wide variation of the plant species cover.

Table 2.2 : Summary of DCA and CCA ordinations on 212 sampling sites containing 66 taxa and four environmental parameters (CCA), Bylot island, Nunavut. Data were computed using the program R v2.15.0 with the community ecology package "vegan" v2.0-3.

	Axis 1	Axis 2	Total inertia
DCA			3.377
Eigenvalue	0.534	0.411	
Cumulative percentage variance			
- of species data	15.2	28	
CCA			3.377
Eigenvalue	0.278	0.188	
Cumulative percentage variance			
- of species data	8.2	13.8	
- of species-environment relation	46.7	78.4	

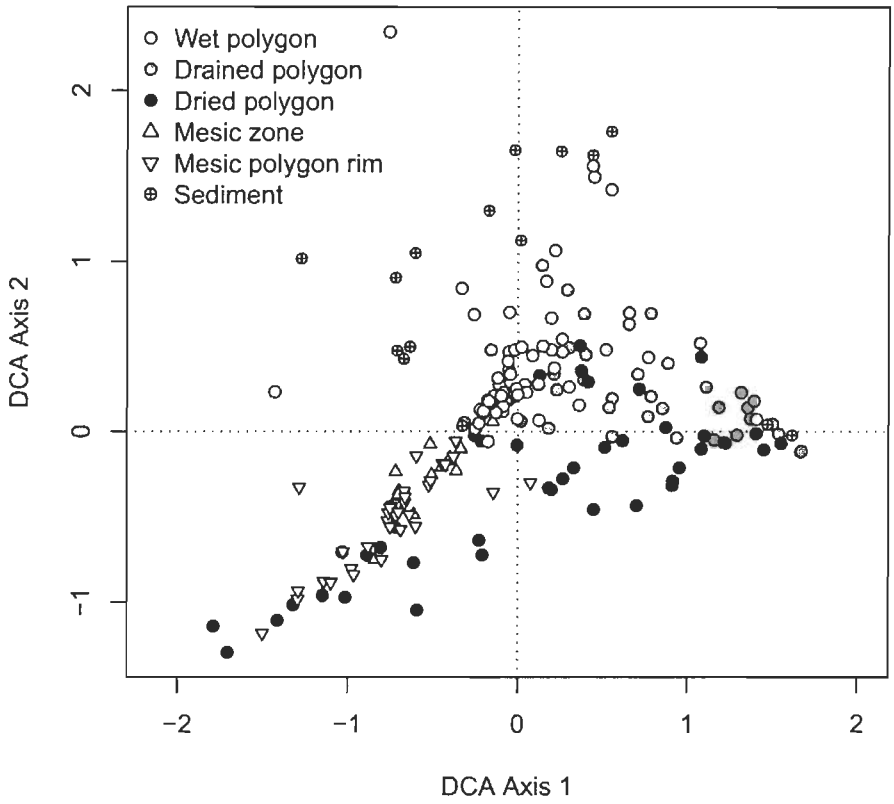

Figure 2.5 : Byplot of first two axes of the detrended correspondence analysis (DCA) for the six eco-terrain units, Bylot Island, Nunavut: 62 Wet polygons, 44 Drained polygons, 43 Dried polygons, 13 Mesic zones, 35 Mesic polygon rims and 15 Sediment zones.

The transition between wetlands and mesic environments through disturbance is highlighted by the general trend of plant family cover change per eco-terrain unit (Table 2.3). *Cyperaceae* and *Poaceae* families, which dominated in Wet polygons (mean cover of 17% and 9% respectively), were slightly affected the first years after gullying (*i.e.* Drained polygons). However, their cover decreased drastically a few years after drainage (*i.e.* Dried polygons) and finally reached 7% and 3% respectively. Plant families such as *Ericaceae*, *Papaveraceae*, *Pyrolaceae*, *Ranunculaceae* and *Rosaceae*, which were absent in Wet polygons, appeared in Dried polygons but had a very low cover. Other families, present throughout the gradient increased in cover with the polygon transition: *Asteraceae*, *Brassicaceae*, *Caryophyllaceae*, *Fabaceae*, *Juncaceae*, *Polygonaceae*, *Salicaceae* and *Saxifragaceae*. The overlap between hydrophilic and mesic species resulted in a greater total species richness in the disturbed polygons, intermediate between the wet and mesic conditions.

Table 2.3 : Mean cover per vascular plant families (%), mean species richness per site and total species richness per eco-terrain units, Bylot Island, Nunavut. Species specific mean vegetation cover were added to provide a cover percentage per family (tr = cover < 0.01%; * = cover < 0.1%; <1 = cover < 1%).

Eco-terrain units		Wet polygons	Drained polygons	Dried polygons	Mesic zones	Mesic polygon rims	Sediment zones
Plant families	**Species richness**	n = 62	n = 44	n = 43	n = 13	n = 35	n = 15
Asteraceae	3	tr	*	*	-	tr	3
Brassicaceae	8	*	*	<1	*	*	*
Caryophyllaceae	5	tr	<1	<1	<1	<1	<1
Cyperaceae	4	17	19	7	3	<1	1
Equisetaceae	1	*	*	*	*	tr	*
Ericaceae	1	-	-	tr	*	tr	-
Fabaceae	2	tr	tr	<1	tr	<1	-
Juncaceae	3	*	<1	3	2	4	tr
Onagraceae	1	tr	-	-	-	-	-
Papaveracea	1	-	-	tr	-	tr	tr
Poaceae	9	9	5	3	3	4	5
Polygonaceae	2	tr	tr	*	-	*	tr
Pyrolaceae	1	-	-	tr	-	-	-
Ranunculaceae	2	-	-	tr	-	tr	<1
Rosaceae	2	-	-	*	*	<1	-
Salicaceae	4	1	<1	3	11	15	<1
Saxifragaceae	8	*	<1	2	*	*	*
Scrophulariaceae	2	<1	<1	*	*	tr	*
Species richness per site		8	11	17	15	15	9
Total species richness	59	36	37	54	36	47	31

2.4.2 Plant community-environment relationships

The same vegetation matrix with 66 taxa was used for the direct gradient analysis (CCA). Selection procedure of environmental variables yielded four variables with a significant contribution ($p = 0.002$) to explain variation in plant communities: litter cover, thaw front depth, soil moisture and polygon rims' integrity (Table 2.4). Variance inflation factors (VIFs) of the environmental factors were below 10, indicating that the canonical coefficients had a low multicollinearity (ter Braak & Smilauer 1998). The first two axes were significant ($p = 0.005$; Table 2.5). They explained 13.8% of the variation in the plant species data and 78.4% for the species-environment relation with a total inertia of 3.377 (Table 2.2).

Table 2.4 : Summary of the nine environmental variables used primarily for the CCA ordination on 212 sampling sites with 66 taxa, Bylot Island, Nunavut. Data were computed using the program R v2.15.0 with the community ecology package "vegan" v2.0-3.

Environmental variables	F	df	p-value
Thaw front depth	14.38	1	0.002
Soil moisture	3.64	1	0.002
polygon rims' integrity	5.29	3	0.002
Litter cover	11.68	1	0.002
Standing dead	4.12	1	0.012
Geese feces	2.56	1	0.022
Bare ground	2.59	1	0.046
Grubbing	1.44	1	0.154
Standing water	0.412	1	0.806

Table 2.5 : Summary of the four first axis of the CCA ordination on 212 sampling sites with 66 taxa, Bylot Island, Nunavut. Data were computed using the program R v2.15.0 with the community ecology package "vegan" v2.0-3.

Environmental variables	F	df	p-value
CCA Axis 1	20.47	1	0.005
CCA Axis 2	13.87	1	0.005
CCA Axis 3	5.98	1	0.005
CCA Axis 4	2.29	1	0.032

The first axis of the biplot was associated to the litter cover wheras the second axis was associated to soil moisture and thaw front depth (Figure 2.6). Eco-terrain units formed coherent groups and the results highlight two main groupings: Wet polygons were associated with high soil moisture content and an important active layer thickness whereas the mesic environments (*i.e.* Mesic zones and Mesic polygon rims) were associated with higher litter cover. Ordination results indicated that soil moisture content and thaw front depths of the Wet polygons were higher than for the Drained polygons and the Dried polygons. Also, the litter cover was more important for the Dried polygons than for the Wet polygons and the Drained polygons. Concerning the centroids of the qualitative environmental factor (No water output, Gully connection, Stream connection, Other types), they had coherent positions: Stream connection centroid was surrounded by Sediment zones sampling sites; No water output centroid was surrounded by Wet polygons sampling sites; Gully connection centroid was surrounded by Drained polygons and Dried polygons sampling sites; and Other types centroid was surrounded by Mesic polygon rims and Mesic zones.

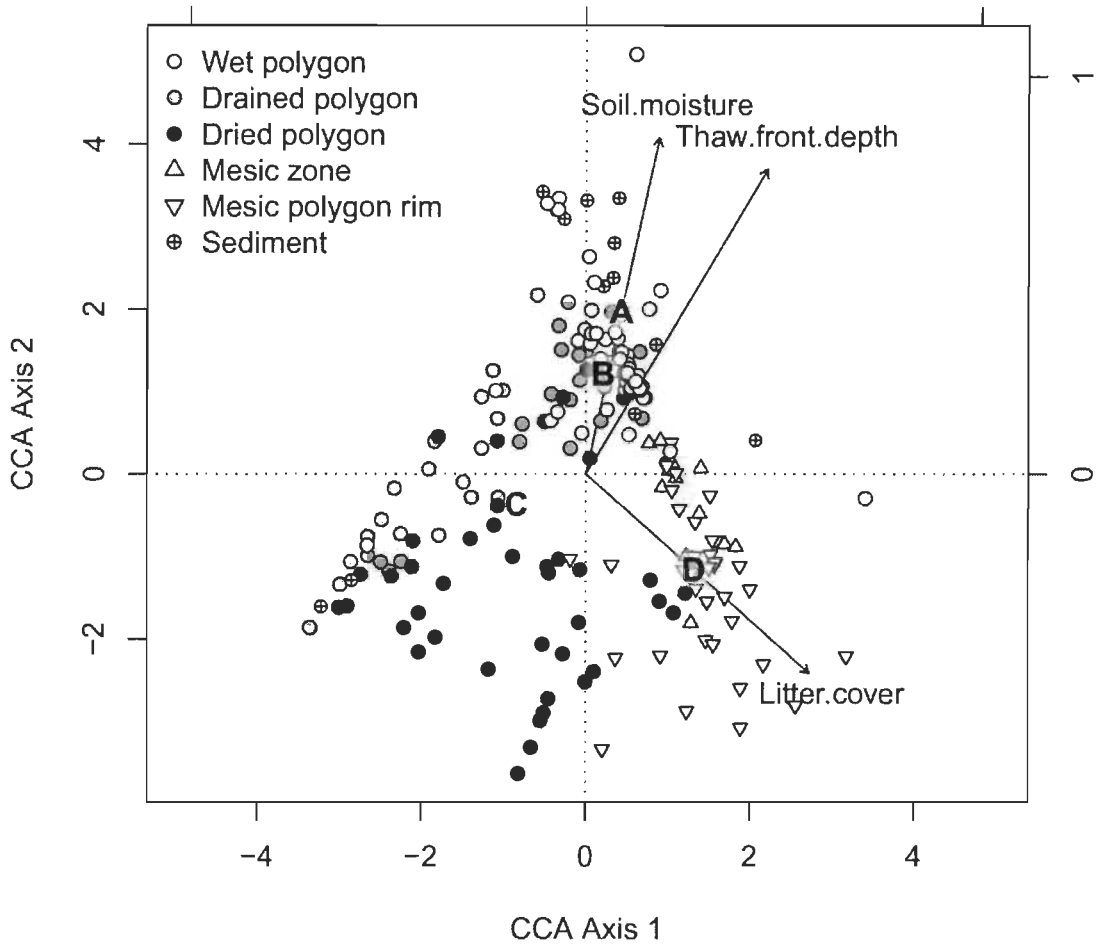

Figure 2.6 : Byplot of first two axes of the canonical correspondence analysis (CCA) for the six eco-terrain units, Bylot Island, Nunavut: 62 Wet polygons, 44 Drained polygons, 43 Dried polygons, 13 Mesic zones, 35 Mesic polygon rims and 15 Sediment zones. The three quantitative environmental variables (Active layer thickness, Soil moisture and Litter cover) are indicated by arrows. The four centroids of the qualitative environmental variable about rims integrity, named Stream connection, No water output, Gully connection and Other types, are labelled "A", "B", "C" and "D" respectively.

2.4.3 Site conditions

The weather conditions on Bylot Island for season 2009 were characterized by a warmer spring than normal. Despite a normal snow pack for the end of winter (snow depth was 26.1 cm on June 1), snowmelt was rapid due to warm conditions (Gauthier *et al.* 2009) of one of the driest summer on record (Gauthier *et al.* 2009). Season 2010 was characterized by a late snowmelt about one week later than normal in the lowland (snow

depth was 41.6 cm on 31 May) due to high snowfall during the winter (Gauthier *et al.* 2010). June and early July was generally warm and sunny while mid-July was characterised by heavy rainfalls (Gauthier *et al.* 2010).

Soil moisture varied greatly through the record period from June 25th to July 31th 2010 for each eco-terrain unit (Figure 2.7). The major trends were based on continuous recording at 10 sampling sites (3 Wet polygons, 3 Drained polygons, 2 Dried polygons and 2 Mesic polygon rims) since four sensors reinserted in soil during the summer had to be excluded. Higher volumetric water content (VWC; %) were observed in Wet polygons at the end of June as well as at the end of July. These sites also had the longer flooding duration after rainfalls. Low-centered polygons affected by gullying (*i.e.* Drained polygons and Dried polygons) had a lower moisture level earlier in the season and even if their volumetric water content reacted to the most important precipitation events their humidity stayed lower than for the Wet polygons. The Mesic polygon rims had the lowest soil moisture content throughout the season and quickly evacuated the water after heavy rainfalls.

As thaw front depth data have failed Shapiro-Wilk normality test ($W = 0.983$, $p = 0.002$), anova was applied on ranked data. Thaw front depth differed significantly among eco-terrain units ($F = 45.82$, $df = 3$, $p < 0.001$) but not between years ($F = 0.20$, $df = 1$, $p = 0.652$) and there were no interaction between eco-terrain units and years ($F = 0.10$, $df = 3$, $p = 0.962$). Wet polygons had deeper active layer (36.0 ± 0.9 cm (2009) and 34.9 ± 0.9 cm (2010)) while Drained polygons, Dried polygons and Mesic zones had a thaw front depth of about 25 cm in 2009 and 2010 (Figure 2.8; Table 2.6). These results show a decrease of about 10 cm for the low-centered polygons affected by gullying (*i.e.* Drained polygons and Dried polygons) compared to the low-centered polygon wetlands not affected by gullying. The thin thaw front depths of the Drained polygons and the Dried polygons were comparable to the thaw front depth of the Mesic zones at the end of July 2009 and 2010.

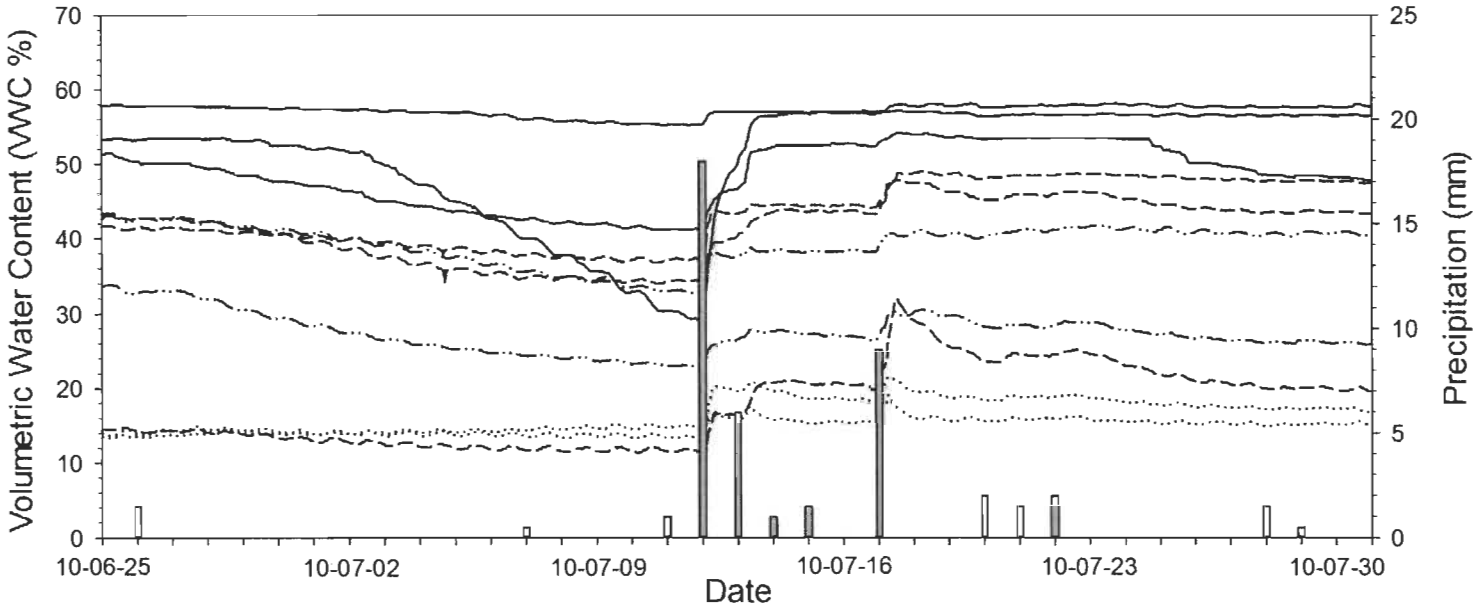

Figure 2.7 : Rainfalls (mm) and temporal variability of top 10 cm volumetric water content (VWC; %) according to eco-terrain units (3 Wet polygons = solid lines; 3 Drained polygons = dash lines; 2 Dried polygons = dash-dot lines; 2 Mesic polygons rims = dotted lines) near thermo-erosion gullies, Bylot Island, Nunavut. Data series started on June 25th 2010 and ended on July 31th 2010 with a resolution of one recording per hour. Rainfalls (mm) are shown as solid vertical bars.

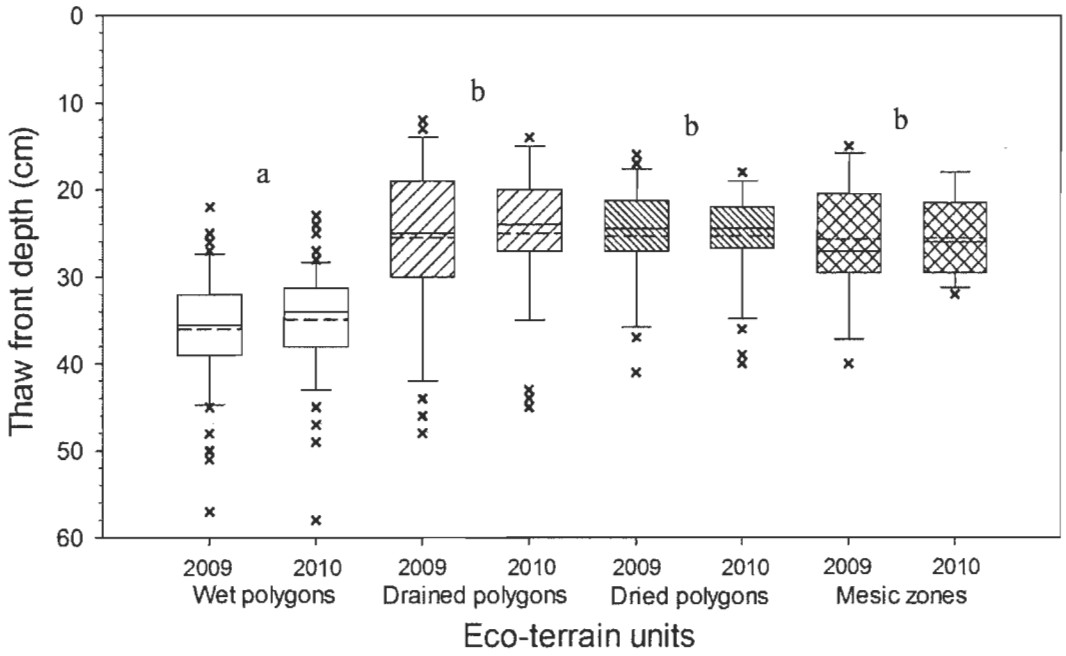

Figure 2.8 : Thaw front depth at the end of seasons (July 31th 2009 and July 30th 2010) according to the eco-terrain units (52 Wet polygons, 39 Drained polygons, 32 Dried polygons and 13 Mesic zones) near thermo-erosion gullies, Bylot Island, Nunavut. 10th percentiles, lower quartile, median, mean (dash), upper quartile and 90th percentiles are shown. Tukey's Post-hoc test results are shown by letters.

Table 2.6 : Summary of the Tukey's Post-hoc test on thaw front depth at the end of seasons 2009 and 2010 for 136 sampling sites, Bylot Island, Nunavut. Data were computed using the program R v2.15.0 with the package "multcomp" v1.2-12.

	Estimate	Std. Error	t value	Pr > t
Drained - Dried	-0.072	1.156	-0.062	1.000
Wet - Dried	10.037	1.089	9.216	< 0.001
Mesic - Dried	0.287	1.594	0.180	1.000
Wet - Drained	10.109	1.027	9.845	< 0.001
Mesic - Drained	0.359	1.552	0.231	0.999
Wet - Mesic	-9.750	1.503	-6.487	< 0.001
Year: 2009 - 2010	-0.428	0.948	-0.451	0.989

2.4.4 Graminoids above-ground live biomass

Above-ground graminoid biomass was normally distributed ($W = 0.889$, $p = 0.077$) and homogenous (K-squared = 5.63, df = 3, $p = 0.131$). There was no significant difference in biomass among eco-terrain units ($F = 1.74$, df = 3, $p = 0.222$). The total above-ground live biomass of graminoids in late summer was highest in Wet polygons (32.7 ± 145 [SE] g/m²) followed Drained polygons (28.7 ± 5.1 g/m²) (Figure 2.9). The general trend observed reflect as general decrease of graminoids biomass with polygon degradation from Wet polygons to mesic habitats. *Poaceae* family and *Carex aquatilis* biomass decreased from Wet polygons to Dried polygons eco-terrain units. *Dupontia fisheri* and *Anthoxanthum arcticum* species found in Wet polygons and Drained polygons were replaced by *Arctagrostis latifolia* and *Festuca brachyphylla* in Dried polygons and Mesic polygon rims. *Eriophorum scheuchzeri*, present only in Wet polygons, was totally replaced by *Eriophorum angustifolium* in Drained polygons and Dried polygons. Our Dried polygons biomass results (17 g/m²) were strongly affected by one quadrat having a very high *Eriophorum angustifolium* biomass (56.5 g/m²). If we exclude this data point, the above ground live biomass of Dried polygons drops to 4.5 g/m² (composed of *Arctagrostis latifolia*, *Festuca brachyphylla*, *Eriophorum angustifolium*, *Carex aquatilis*, *Luzula arctica* and *Luzula confusa*). *Juncaceae* were present in Dried polygons and dominated the graminoids biomass of the Mesic polygon rims.

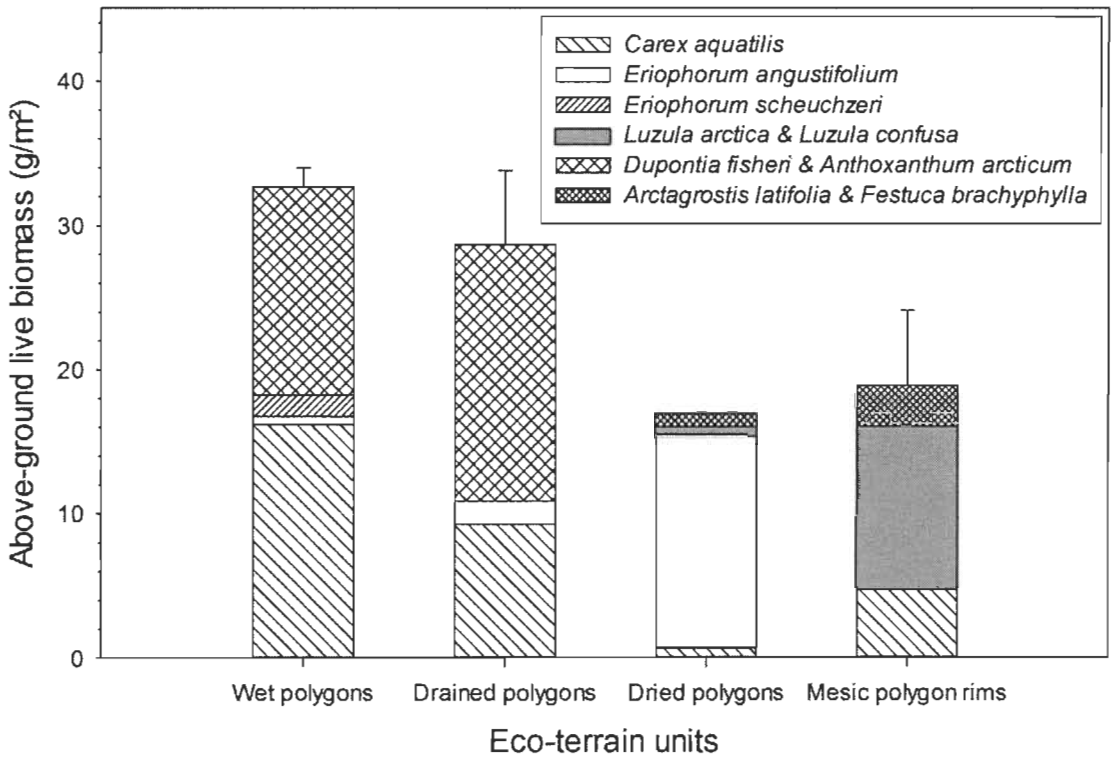

Figure 2.9 : Above-ground live biomass (mean + SE, dry mass) of graminoids at the beginning of August according to the eco-terrain units (Wet polygons (n = 4), Drained polygons (n = 4), Dried polygons (n = 2) and Mesic polygon rims (n = 4)) near thermo-erosion gullies, Bylot Island, Nunavut. The following plant families were found in the samples: *Cyperaceae* (*i.e. Carex aquatilis*, *Eriophorum angustifolium*, *Eriophorum scheuchzeri*), *Juncaceae* (*i.e. Luzula arctica*, *Luzula confusa*) and *Poaceae* (*Anthoxanthum arcticum*, *Arctagrostis latifolia*, *Dupontia fisheri*, *Festuca brachyphylla*).

2.5 Discussion

The rapid development of gullies generated a quick rearrangement of the hydrography in the polygonal complex. Ice-wedge collapse at the edge of low-centered polygons altered plant communities' diversity and productivity.

2.5.1 Polygons classification

Vegetation characteristics were valuable indicators for the classification of the polygon degradation with a gradient from the wet vegetation of undisturbed polygon to emergence of mesic vegetation in disturbed polygon. However, the integration of abiotic

environmental variables improved this classification, which became more comprehensive and richer in information. The three eco-terrain units of polygons identified in the field demonstrate that the success of this classification was an important first step to support the proposed eco-terrain units and to investigate the consequences of thermo-erosion gullying on plant communities.

2.5.2 Wetlands degradation

2.5.2.1 Soil moisture

In 2010, the late snowmelt due to important snowfall during the winter contributed to maintain a relatively high humidity in June and rainfalls of mid-July was an important water input after four relatively dry weeks. A majority of Drained and Dried polygons had lower soil moisture compared to Wet polygons at the end of the summer 2010. Thus, the collapse of rims or the simple formation of breaches and small cracks connecting polygons to the gullies caused an important hydrological disturbance for the low-centered wetlands. Intact Wet polygons capture and store large quantities of water from the spring snow melt leading to prolonged saturation. Heavy rainfalls also contributed to high soil moisture despite periods of drought during the summer as documented in the literature. According to Roulet & Woo (1986) and Woo & Young (2006), the low-centered polygon wetlands provide surface storage for snowmelt water and are normally subject to important flooding in the spring. Subsequently, evaporation generally draws down the water table in the thawed active layer, but occasional heavy rain event may revive the water level and maintain prolonged saturation (Rovansek *et al.* 1996; Woo *et al.* 2008). Our results show that Drained and Dried polygons also respond to major rainfalls given the high specific retention of peaty soils to absorb water (Roulet & Woo 1986) but, polygons affected by ice-wedge collapses had clearly lower soil moisture content throughout the summer. These results suggest that snowmelt water and rain water are rapidly collected and drained by depressions caused by ice wedge collapses (Seppälä 1997; Woo & Young 2006).

2.5.2.2 Thaw front depth

As expected in the literature (Nelson *et al.* 1998), thaw front depth was well correlated with soil moisture. We found that within five years of drainage thaw front depth of polygon centers had decreased and then remained stable, similar to adjacent undisturbed mesic environments. We explain the differences of the thaw front depth between Wet polygons and those affected by gullying (*i.e.* Drained polygons and Dried polygons) by the drying of mosses that rapidly created a drained, porous and unsaturated layer of low thermal conductivity in the upper soil horizons. In fact, after drainage low-centered polygons are capped with a thin insulating layer of dry peat. Billings & Peterson (1980) made similar observations about the drying of mosses and the impact on the active layer when high-center polygons were quickly formed along thermokarst erosion.

The contrast between deeper thaw front depth in Wet polygons and shallower thaw front depth in drier eco-terrain units (Drained polygons, Dried polygons and Mesic environments) depends on lower albedo, heat reserve from standing water and relatively high thermal conductivity of saturated soils of wet sites (Nelson *et al.* 1997). In contrast, the ground surface and most parts of the frost table of the ridges of polygons are above the water level and the dry peat acts as a more effective insulator, resulting in shallower depths of thaw front (Minke *et al.* 2009). The active layer in high latitude confines the rooting zone of wetland plant communities while the permafrost below, usually rich in ground ice seals the soil pores and behaves like an impermeable substrate preventing downward percolation of water (Woo & Young 2006).

2.5.2.3 Plant communities' modification

Low soil moisture and thin thaw front depth following gully formation led to gradual modification of wetland plant communities towards the emergence of mesic environment plant communities. The long term transition from low-centered polygon wetlands to dry high-centered polygons is describe in periglacial geomorphology (*i.e.* Mackay 2000; French 2007) and its gradual consequences on Arctic vegetation were studied (*i.e.* Billings & Peterson 1980; Ellis *et al.* 2008). We documented that

drainage due to gully cause a similar modification of the plant communities but more rapidly. Similarly to Woo & Young (2006), we illustrated that water saturated conditions are essential for the integrity of wetland plant communities and sudden shifts in the flow pathway or a marked reduction in water supply can quickly alter vegetation assemblages. The mesic plant species usually restricted to the rims of the polygons colonized polygon centers after only five to 10 years of drainage. The associated increase in local biodiversity of the transition is due to the presence of plants from both environments during the transition. Although we cannot predict for how long this high diversity will be maintained in the low diversity arctic environment, it will likely decrease and converge to the situation observed on mesic environments.

2.5.2.4 Food resources for geese

Above-ground live biomass measured in early August (July 31th to August 3rd 2010) tended to decrease from wet to dry eco-terrain units yet there were no significant difference likely due to the small sampling size. Biomass in Wet polygons adjacent to gullies was 53% time lower than what Gauthier *et al.* (2010) measured in the most productive ungrazed wetlands of the Qarlikturvik Valley (62.8 ± 11.4 g/m^2). A difference of two weeks from the date of sampling between our study and that of Gauthier *et al.* (2010) may explain these differences in biomass. Nevertheless our eco-terrain units were all sampled at same date and provide a valid comparison across these units. We studied old polygons that have been undisturbed for long periods of time and are usually dominated by *Carex aquatilis* (Billings & Peterson 1980). Sites of Gauthier *et al.* (2010) are dominated by *Dupontia fisheri* and *Eriophorum scheuchzeri* that usually dominate young polygons (Billings & Peterson 1980). Above-ground live biomass measured in Mesic polygon rims correspond closely with results obtained in Qarlikturvik Valley in 2009 by Doiron, Gauthier & Lévesque (unpublished data).

Hydrophilic graminoid biomass decreased significantly with the degradation of polygons (*i.e.* Drained polygons and Dried polygons). The decrease of *Poaceae* family and *Carex aquatilis* biomass in polygons affected by ice-wedge collapse led to a decrease of food resources for Greater Snow Goose foraging who preferentially feed on wetland

graminoids (Manseau & Gauthier 1993). *Eriophorum scheuchzeri*, one of the preferred species for geese, was absent from degraded polygons. One of the four Dried polygons sampled for biomass had an extremely high abundance of *Eriophorum angustifolium*, a mesic habitat species. When that site was excluded from the calculations, the plant species composition of Dried polygons was similar to Mesic polygon rims with a low total graminoid biomass. Finally, food resources available in degraded polygons were similar to that of mesic environments. *Juncaceae*, which were absent in Wet polygons but present in Dried polygons, are frequently grazed in mesic environments (Duclos 2002).

2.6 Conclusion

This study presents evidence that gullying lead to a rapid degradation of low-centered polygon wetlands in the High Arctic through an important redistribution of surface water. The consequences are major for the northern wetland ecosystems, with shifts in plant communities and habitat quality for herbivores like geese. This important and fast change is apparently restricted to the polygons affected by ice-wedge collapse at the margins of the gullies but probably affects also a larger area in the long term through water channeling. Gullying processes lead to an accelerated transformation similar to the predictable development of low-centered to high-centered polygons which occurs over periods of centuries to millennia. A detailed evaluation of total areas affected or at risk of such habitat degradation is essential to quantify the impact of this process on the carrying capacity of Greater Snow Goose in the context of global change.

2.7 Acknowledgements

Authors wish to thank Parks Canada – Sirmilik National Park, Northern Studies Center (CEN) and Dr Gilles Gauthier (Laval University) for the access to the field camp during summers 2009 and 2010. We also tank Alexandre Guertin-Pasquier and Etienne Godin for their fieldwork support as well as Alexandre Moreau, Stephan Ouellet, Noémie Boulanger-Lapointe for their help with statistical analyses. This project was made possible by the excellent logistic contribution of Polar Continental Shelf Program (PCSP) as well as the financial support of the International Polar Year (IPY) program of the Government of Canada, Natural Sciences and Engineering Research Council of Canada (NSERC), Fonds québécois de la recherche sur la nature et les technologies (FQRNT), Northern Scientific Training Program (NSTP) of the Department of Indian Affairs and Northern Development, the network of centers of excellence of Canada ArcticNet, NSERC CREATE training program in northern environmental sciences (EnviroNorth) and Groupe de recherche en biologie végétale (GRBV) of the Université du Québec à Trois-Rivières.

2.8 References

ACIA (2005) *Arctic Climate Impact Assessment*. Cambridge University Press: New York, 1042 pp.

Allard M (1996) Geomorphological changes and permafrost dynamics: key factors in changing arctic ecosystems. An example from Bylot Island, Nunavut, Canada. *Geoscience Canada*, **23**, 205–212.

Billings WD, Peterson KM (1980) Vegetational change and ice-wedge polygons through the thaw-lake cycle in Arctic Alaska. *Arctic and Alpine Research*, **12**, 413–432.

Billings WD (1987) Carbon balance of Alaskan tundra and taiga ecosystems: past, present and future. *Quaternary Science Reviews*, **6**, 165–177.

Chen ZH, Chen WJ, Leblanc SG, *et al.* (2010) Digital Photograph Analysis for Measuring Percent Plant Cover in the Arctic. *Arctic*, **63**, 315–326.

Couture NJ, Pollard WH (2007) Modelling geomorphic response to climatic change. *Climatic Change*, **85**, 407–431.

Daubenmire R (1959) A canopy-coverage method of vegetationnal analysis. *Northwest Science*, **33**, 43–64.

Duclos I (2002) *Milieux mésiques et secs de l'Île Bylot, Nunavut (Canada): caractérisation et utilisation par la Grande Oie des Neiges*. MSc thesis, Université du Québec à Trois-Rivières, Trois-Rivières, 113 pp.

Ellis CJ, Rochefort L, Gauthier G, *et al.* (2008) Paleoecological evidence for transitions between contrasting landforms in a polygon-patterned High Arctic wetland. *Arctic Antarctic and Alpine Research*, **40**, 624–637.

Fortier D, Allard M (2004) Late Holocene syngenetic ice-wedge polygons development, Bylot Island, Canadian Arctic Archipelago. *Canadian Journal of Earth Sciences*, **41**, 997–1012.

Fortier D, Allard M, Pivot F (2006) A late-Holocene record of loess deposition in ice-wedge polygons reflecting wind activity and ground moisture conditions, Bylot Island, eastern Canadian Arctic. *The Holocene*, **16**, 635–646.

Fortier D, Allard M, Shur Y (2007) Observation of rapid drainage system development by thermal erosion of ice wedges on Bylot Island, Canadian Arctic Archipelago. *Permafrost and Periglacial Processes*, **18**, 229–243.

French HM (1974) Active thermokarst processes, Eastern Banks Island, Western Canadian Arctic. *Canadian Journal of Earth Sciences*, **11**, 785–794.

French HM (2007) *The Periglacial Environment, Third Edition*. John Wiley & Sons Ltd, 458 pp.

Gauthier G, Cadieux M-C, Lefebvre J, *et al.* (2009). Population study of Greater Snow Geese and its nesting habitat on Bylot Island, Nunavut, in 2009: A progress report, 31 pp.

Gauthier G, Cadieux M-C, Lefebvre J, *et al.* (2010). Population study of Greater Snow Geese and its nesting habitat on Bylot Island, Nunavut, in 2010: A progress report, 32 pp.

Gauthier G, Hughes RJ, Reed R, *et al.* (1995) Effect of grazing by greater snow geese on the production of graminoids at an arctic site (Bylot Island, NWT, Canada). *Journal of Ecology*, **83**, 653–664.

Gauthier G, Rocheford L, Reed A (1996) The exploitation of wetland ecosystems by herbivores on Bylot Island. *Geoscience Canada*, **23**, 253–259.

Godin E, Fortier D (2010) Geomorphology of thermo-erosion gullies – case study from Bylot Island, Nunavut, Canada. *In: Proceedings 6th Canadian Permafrost Conference and 63rd Canadian Geotechnical Conference, Calgary.*

Godin E, Fortier D (2012) Fine scale spatio-temporal monitoring of multiple thermo-erosion gullies development on Bylot Island, eastern canadian archipelago. *In: Proceedings Tenth International Conference on Permafrost (TICOP), Salekhard, Russia.*

Hill MO, Gauch HG (1980) Detrended correspondence analysis: an improved ordination technique. *Vegetatio*, **42**, 47–58.

Hinzman LD, Bettez ND, Bolton WR, *et al.* (2005) Evidence and implications of recent climate change in northern Alaska and other arctic regions. *Climatic Change*, **72**, 251–298.

Hughes RJ, Reed A, Gauthier G (1994) Space and habitat use by greater snow goose broods on Bylot Island, Northwest Territories. *Journal of Wildlife Management*, **58**, 536–545.

Ihaka R,Gentleman R (1996) R: a language for data analysis and graphics. *Journal of Computational and Graphical Statistics*, **5**, 299–314.

International Polar Year (2012) *Climate Change Impact on Canadian Arctic Tundra. Protocols for taking vertical photographs and field measurements of plant height for biomass and LAI estimation in Arctic tundra (for vegetation height < 0.5 m).* Website: http://ipytundra.ca/protocols (Accessed February 2012).

ITIS (2011) *Integrated Taxonomic Information System.* Government of Canada. Website: www.cbif.gc.ca/ (Accessed February 2012).

Klein DR, Bay C (1991) Diet selection by vertabrate herbivores in the High Arctic of Greenland. *Holarctic Ecology*, **14**, 152–155.

Lantz TC, Kokelj SV (2008) Increasing rates of retrogressive thaw slump activity in the Mackenzie Delta region, N.W.T., Canada. *Geophysical Research Letters*, **35**, 1–5.

Mackay JR (2000) Thermally induced movements in ice-wedge polygons, western Arctic coast: A long-term study. *Geographie Physique et Quaternaire*, **54**, 41–68.

Mainguy J, Gauthier G, Giroux J-F, *et al.* (2006a) Gosling growth and survival in relation to brood movements in greater snow geese (*Chen caerulescens atlantica*). *The Auk*, **123**, 1077–1089.

Mainguy J, Gauthier G, Giroux J-F, *et al.* (2006b) Habitat use and behaviour of greater snow geese during movements from nesting to brood-rearing areas. *Canadian Journal of Zoology*, **84**, 1096–1103.

Manseau M, Gauthier G (1993) Interactions between greater snow geese and their rearing habitat. *Ecology*, **74**, 2045–2055.

Masse H, Rochefort L, Gauthier G (2001) Carrying capacity of wetland habitats used by breeding greater snow geese. *The Journal of Wildlife Management*, **65**, 271–281.

Minke M, Donner D, Karpov NS, *et al.* (2007) Distribution, diversity, development and dynamics of polygon mires: examples from Northeast Yakutia (Siberia). *Peatlands International*, **1**, 36–40.

Minke M, Donner N, Karpov N, *et al.* (2009) Patterns in vegetation composition, surface height and thaw depth in polygon mires in the Yakutian Arctic (NE Siberia): a microtopographical characterisation of the active layer. *Permafrost and Periglacial Processes*, **20**, 357–368.

Nelson FE, Hinkel KM, Shiklomanov NI, *et al.* (1998) Active-layer thickness in north central Alaska: systematic sampling, scale, and spatial autocorrelation. *Journal of Geophysical Research*, **103**, 28963–28973.

Nelson FE, Shiklomanov NI, Mueller GR, *et al.* (1997) Estimating active-layer thickness over a large region: Kuparuk River Basin, Alaska, U.S.A. *Arctic and Alpine Research*, **29**, 367–378.

Rovansek RJ, Hinzman LD, Kane DL (1996) Hydrology of a tundra wetland complex on the Alaskan Arctic Coastal Plain, U.S.A. *Arctic and Alpine Research*, **28**, 311-317.

Seppälä M (1997) Piping causing thermokarst in permafrost, Ungava Peninsula, Quebec, Canada. *Geomorphology*, **20**, 313–319.

ter Braak CJF (1986) Canonical correspondence analysis: a new eigenvector technique for multivariate direct gradient analysis. *Ecology*, **67**, 1167–1179.

ter Braak, CJF, Smilauer P, (1998) *CANOCO Reference Manual and User's Guide to CANOCO for Windows: Software for Canonical Ordination (version 4)*. Microcomputer Power, Ithaca, New York, 352 pp.

Toniolo H, Kodial P, Hinzman LD, *et al.* (2009) Spatio-temporal evolution of a thermokarst in Interior Alaska. *Cold Regions Science and Technology*, **56**, 39–49.

Vardy SR, Warner BG, Turunen J, *et al.* (2000) Carbon accumulation in permafrost peatlands in the Northwest Territories and Nunavut, Canada. *The Holocene*, **10**, 273–280.

Vogiatzakis IN, Griffiths GH, Mannion AM (2003) Environmental factors and vegetation composition, Lefka Ori massif, Crete, S. Aegean. *Global Ecology & Biogeography*, **12**, 131–146.

Woo M-K, Kane DL, Carey SK, *et al.* (2008) Progress in permafrost hydrology in the new millennium. *Permafrost and Periglacial Processes*, **19**, 237–254.

Woo M-K, Young KL (2003) Hydrogeomorphology of patchy wetlands in the High Arctic, polar desert environment. *Wetlands*, **23**, 291–309.

Woo M-K, Young KL (2006) High Arctic wetlands: their occurrence, hydrological characteristics and sustainability. *Journal of Hydrology*, **320**, 432–450.

Yoshikawa K, Hinzman LD (2003) Shrinking thermokarst ponds and groundwater dynamics in discontinuous permafrost near Council, Alaska. *Permafrost and Periglacial Processes*, **14**, 151–160.

Zoltai SC, McCormick KJ, Scotter GW (1983) *A natural resource survey of Bylot Island and adjacent Baffin Island, Northwest Territories.* Parks Canada, Ottawa, Ontario, 176 pp.

CHAPITRE III

REMOTE SENSING ESTIMATE OF WETLAND DEGRADATION SURROUNDING THERMO-EROSION GULLIES, BYLOT ISLAND, NUNAVUT, CANADA

En attente de soumission

Authors:

Naïm Perreault[1,2], Esther Lévesque[1,2], Daniel Fortier[2,3], Denis Gratton[4]

[1] Département de Chimie-Biologie, Université du Québec à Trois-Rivières, Trois-Rivières, QC, G9A 5H7, Canada

[2] Centre d'études nordiques, Université Laval, Québec, QC, G1V 0A6, Canada
[3] Département de géographie, Université de Montréal, Montréal, QC, H2V 2B8, Canada
[4] Département des sciences humaines, Université du Québec à Trois-Rivières, Trois-Rivières, QC, G9A 5H7, Canada

Corresponding author: Esther Lévesque, tel. +1-819-376-5011 ext.3351, fax +1-819-376-5210, e-mail: esther.levesque@uqtr.ca

Keywords: Arctic wetlands, thermo-erosion gullying, wetland vegetation, ice-wedge polygons, remote sensing, NDVI, unsupervised classification.

3.1 Abstract

Thermo-erosion gullies have significant impacts on surrounding wetlands, which are used by geese and other nesting birds. New drainage systems generate partial or complete drying of polygon centers which promote the emergence of mesic plant species, usually restricted to the rims of polygons. Using a combination of ground-surveys and GeoEye-1 high spatial resolution satellite data, we assessed the area affected by gully formation to evaluate the impact on wetlands of the Qarlikturvik valley, Bylot Island. First, a normalized difference vegetation index (NDVI) image was generated from a GeoEye-1 image acquired on 2nd of September 2010. Second, a unsupervised classification was created and classes corresponding to low NDVI values surrounding the three studied gullies were used for calculation of the disrupted areas. Results show that areas affected by drainage near gullies represent 55 m^2 per meter of gullying. Those areas are restricted to the low-centered polygons affected by ice-wedge collapses located at the margin of the gullies. Results of NDVI analyses highlight the rapid response of arctic wetlands to the drainage by thermo-erosion gullying and show the short term consequences.

3.2 Introduction

Arctic often refers to arid and cold polar desert environment where the ground remains frozen during the long winters and thaw as well as vegetation growth are limited to about 3 months each year (Woo & Young 2006). However, wetlands with exceptionally rich and lush vegetation occur because the permafrost prevents infiltration of rain, snowmelt and flood water (Tarnocai & Zoltai 1988). These wetlands are typically characterised by polygonal patterned grounds (Minke *et al.* 2007; 2009) formed by frost cracking and development of ice-wedges, which are well described in the periglacial geomorphology literature (*e.g.* Mackay & Burn 2002; French 2007). Arctic wetland environments dominated by hydrophilic graminoids offer important habitats used as grazing grounds by herbivores such as Muskoxen (*Ovibos moschatus*; Klein & Bay 1991) and large populations of migratory birds (Gauthier *et al.* 1996). On Bylot Island, wetlands are the preferred habitat of Greater Snow Goose (*Chen caerulescens*

atlanticus) for brood-rearing and hydrophilic graminoids are consumed intensively (Hughes *et al.* 1994; Gauthier *et al.* 1995; Masse *et al.* 2001). Geese are the most abundant herbivore in this system from late May to early September (Gauthier *et al.* 1996; Gauthier *et al.* 2011) and grazing reduced standing crop in wetlands every summer (Gauthier *et al.* 1995; Gauthier *et al.* 2005).

Gully network formation from rapid thermo-erosion in ice-rich permafrost can generate ground subsidence causing hydrological and geomorphological modifications to arctic wetlands (Fortier *et al.* 2007; Godin & Fortier, en révision). The infiltration of snowmelt runoff water into open frost cracks initiates the geomorphological processes, giving a classical zig-zag shape that follows the pattern of ice-wedges bounding polygons (Fortier *et al.* 2007; Godin *et al.* 2010). Of course, new drainage systems also have significant ecological consequences at local scales. Changes on adjacent wetlands promote a rapid invasion of low-centered polygons by mesic plant species to the expanse of hydrophilic graminoids (chapitre II). Extent of disrupted areas is unknown and is essential for a complete understanding of thermo-erosion gullying impacts on wetlands.

Remote sensing allows the observation and analysis of biophysical characteristics of vegetation in a large spatial and spectral context (Tieszen *et al.* 1997). However, tundra environments pose challenges to the estimation of biophysical variables because landscapes are characterized by multiple scales of spatial heterogeneity (*i.e.* non-sorted circles, stripes, ice-wedge polygons) that frequently interrupt plant cover (Stow *et al.* 2004; Laidler *et al.* 2008). New generation of high-resolution imagery can help learning the patterns of vegetation and ecosystem processes (Atkinson *et al.* 2007). Originally developed by Rouse *et al.* (1973), NDVI provides an estimate of the overall healthy leaf cover of the land cover (Ray 1994) with the ratios of reflection difference between red and near-infrared bands. NDVI is one of the most commonly used vegetation indices derived from satellite images and correlates well with ground characteristics of arctic vegetation (Hope *et al.* 1993; Stow *et al.* 1993) because it is particularly sensitive to sparse vegetation densities (Jackson & Huete 1991; Raynolds *et al.* 2008). According to

Riedel *et al.* (2005) and Huemmrich *et al.* (2010), NDVI is useful for estimating the amount of above-ground green biomass.

The aim of this paper is to evaluate the area affected by gully formation using GeoEye-1 high spatial resolution satellite data and ground-truthing observations. Changes in vegetation (transition from wet to mesic communities) and environmental parameters (soil moisture and thaw front depth) were used to determine these areas.

3.3 Material and methods

3.3.1 Study area

The study was conducted in the Qarlikturvik valley (73° 09' N, 79° 57' W) on Bylot Island, Nunavut, Canada (Figure 3.1A). Approximately 15 km long by 5 km wide, the Qarlikturvik valley is bounded to the north and south by plateaus, to the west by the sea and to the east by two glaciers (Figure 3.1B). A pro-glacial braided river that flows from the glaciers toward the sea crosses the valley. Relatively flat terraces located on each side of the river are developed with the accretion of aeolian sands and silts and the concurrent deposition of peat (Fortier *et al.* 2004). Syngenetic ice-wedge polygons formed and aggraded since the Late Holocene resulted in extensive polygon-patterned ground (Allard 1996; Fortier *et al.* 2004) and numerous low-centered polygons, high-centered polygons, polygon ponds, and thaw lakes (Zoltai *et al.* 1983; Hughes *et al.* 1994). According to Hughes *et al.* (1994), pond/lake, wet meadow, and upland habitats covered respectively 9, 14, and 77% of the study area. Organic soils predominate and active layer reaches 0.4 - 0.5 m in peaty-silt deposit and a few decimetres deeper in coarser grained materials (Fortier *et al.* 2006).

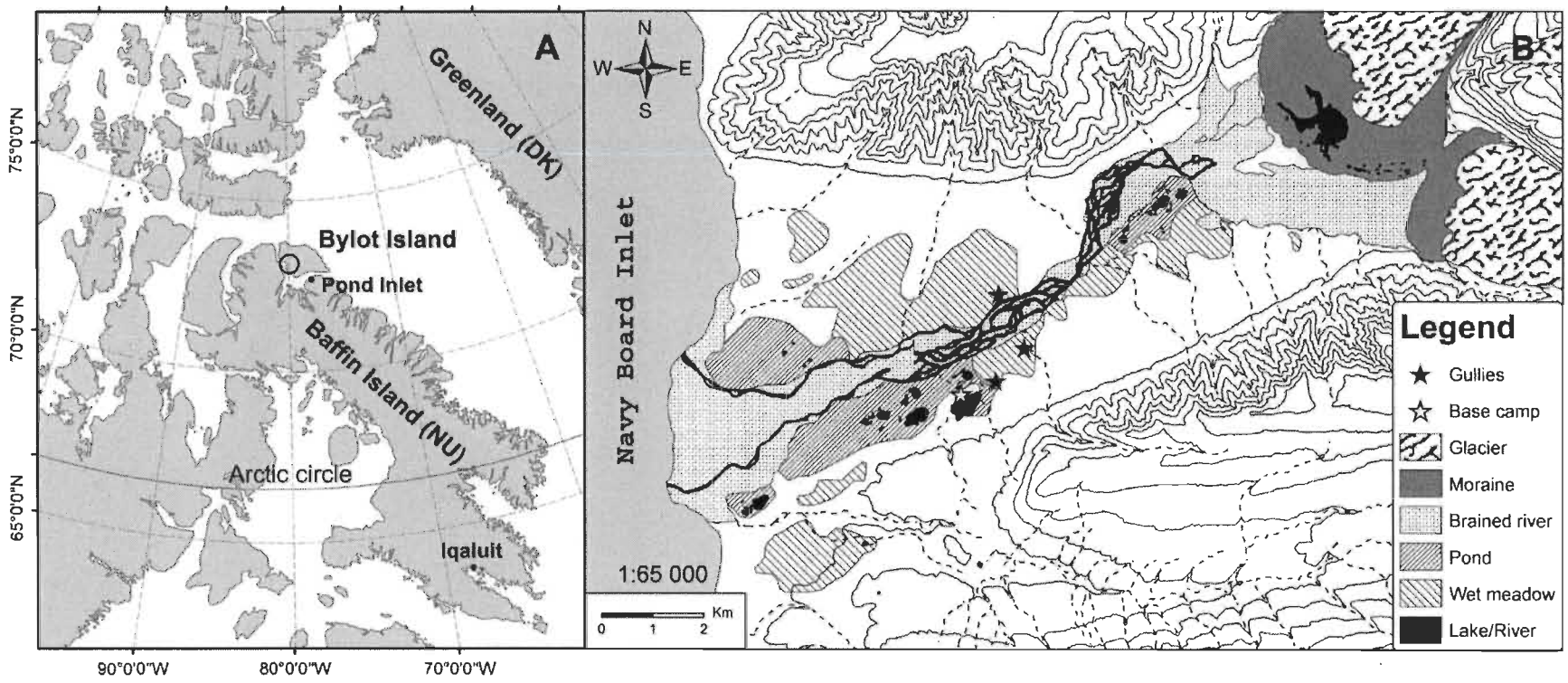

Figure 3.1 : Location of study area. (A) Bylot Island, Nunavut, Canada and the Qarlikturvik valley, south-western plain of Bylot Island (located by circle). (B) Qarlikturvik valley (based on Hughes *et al.* 1994) and the three thermo-erosion gullies studied (located by black stars).

In the Qarlikturvik valley, low-centered polygon typically range in size from 10 to 20 m in diameter (Gauthier *et al.* 1995) and are fed by snowmelt water from the surrounding hills. The vegetation in the center of polygons and near pools and lakes is dominated by sedges (*e.g. Carex aquatilis* var. *stans*, *Eriophorum scheuchzeri*), grasses (*e.g. Arctagrostis latifolia*, *Dupontia fischeri*, *Pleuropogon sabinei*) (Gauthier *et al.* 1996), and fen mosses (*e.g. Drepanocladus* spp., *Aulocomnium* spp.) (Ellis *et al.* 2008). On elevated polygonal rims, sloping terrain and hummocky tundra, the surface is better drained and covered by common mesic plant species including shrubs (*e.g. Salix* spp., *Vaccinium uliginosum* L.), forbs (*e.g. Cassiope tetragona* (L.) D. Don subsp. *tetragona*, *Oxytropis maydelliana* Trautv. subsp. *melanocephala* (Hook.) Porsild) and grasses (*e.g. Arctagrostis latifolia* R. Br. subsp. *latifolia*, *Alopecurus borealis* Trin., *Poa arctica* R. Br. s. lat., *Luzula confusa* Lindebl.; Zoltai *et al.* 1983).

3.3.2 Ground data collection

Field activities were conducted at peak season from July to early August 2009 and 2010. A total of 212 sampling sites located in low-centered polygon wetlands surrounding three thermo-erosion gullies provide a floristic inventory of wetlands surrounding new drainage systems (chapitre II). Sites were chosen using a stratified-random sampling along gullies (Gully A = 99 sampling sites, Gully B = 92 and Gully C = 21). Sampling sites were first classified into six eco-terrain units representing dominant vegetation types, physical characteristic and apparent soil moisture (Table 3.1). Plant species richness and cover were described using 0.7 m x 0.7 m quadrats. Central coordinates of every sampling site were collected for the center of the area considered ecologically similar with homogeneous vegetation and representative of the eco-terrain units using a GPS receiver (Garmin eTrex Venture HC) with an accuracy of about 4 - 5 m.

Table 3.1 : General description of the six eco-terrain units used on field observations, Bylot Island, Nunavut (chapitre II and annexe C).

Eco-terrain units (n)	Vascular plant species cover (%)	Green mosses cover (%)	Total green vegetation cover (%)	General description
Sediment zones (15)	10	6	16	Area partially or completely covered (mean cover of 80%) by fresh sediment deposition during the process of gullying.
Drained polygons (44)	25	27	52	Low-centered polygon recently affected by gullying (within 0 to 5 years), newly dried, covered by hydrophilic graminoids in poor condition and presence of rare mesic plant species.
Dried polygons (43)	20	21	41	Low-centered polygon affected by gullying (more than 5 years), covered by mesic plant species and rare hydrophilic graminoids.
Mesic polygon rims (35)	23	44	67	Edge between polygons characterize by hummocky tundra and covered by mesic plant species.
Mesic Zones (13)	19	61	80	Area characterizes by hummocky tundra and covered by mesic plant species.
Wet polygons (62)	28	62	90	Low-centered polygon non-affected by gullying, extremely wet site, covered by hydrophilic graminoids.

3.3.3 Satellite data analysis

Remote sensing analyses were conducted using GeoEye-1 high spatial resolution satellite data. The use of data such as cartography of gullies from Godin and Fortier (2012) and spatio-temporal evolution of Gully A from Godin & Fortier (en revision) were essential to the project. The program ITT's ENVI v4.8 was used for image pre-processing and processing whereas database development and spatial data analysis were performed with ESRI's ArcGIS v9.2. Method summary adopted in this study is illustrated in Figure 3.2.

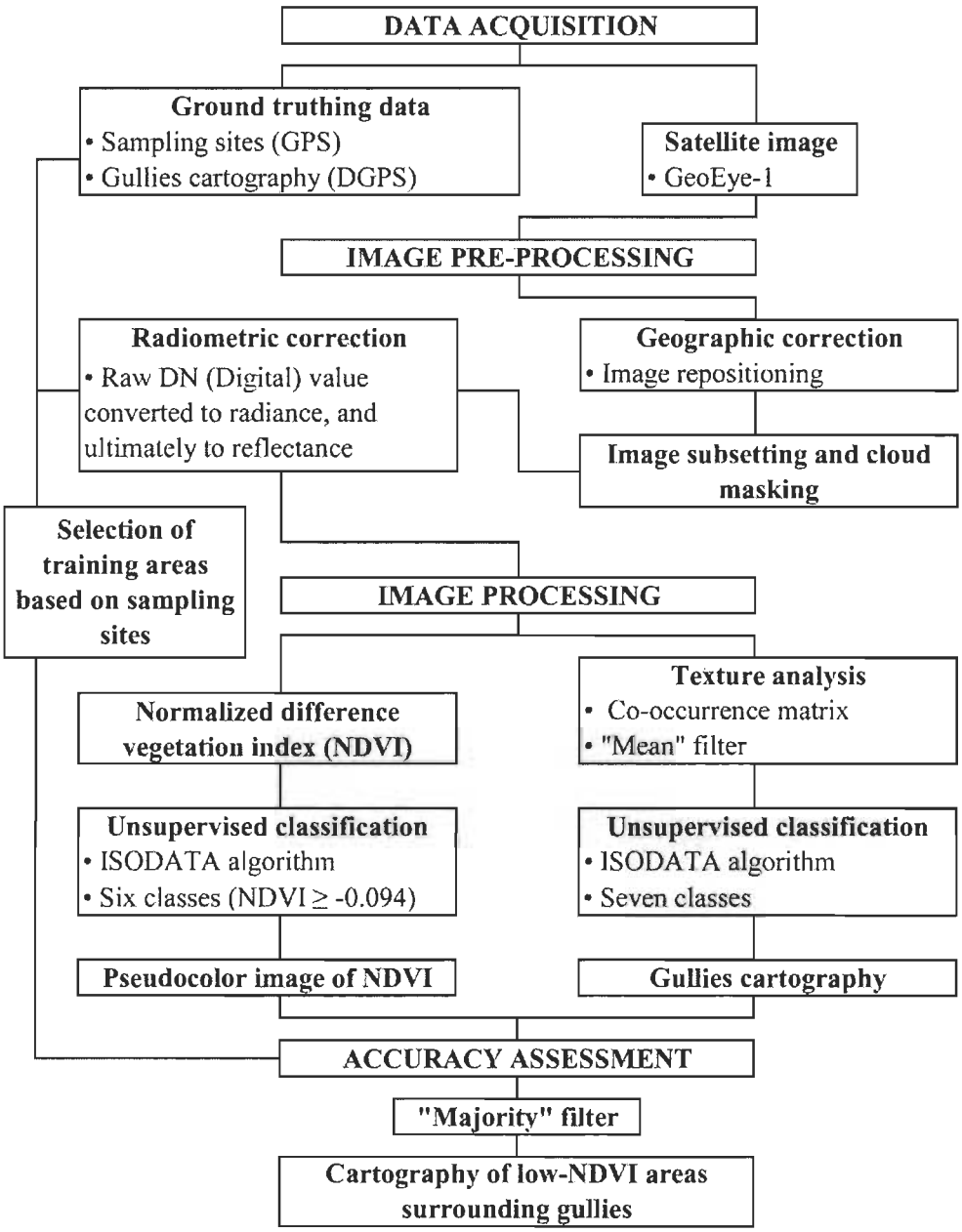

Figure 3.2 : Schematic diagram of the analysis approach.

3.3.3.1 Data pre-processing

The GeoEye-1 high spatial resolution satellite data used was acquired the September 2nd 2010 at 17h40 GMT and covered a total area of 14 km long by 19 km wide. GeoEye-1 standard bundle product consists of four spectral bands with a spatial resolution of 2 m and a 0.5 m high spatial resolution panchromatic band. The spectral ranges of these bands are 450-510 nm (blue), 510-580 nm (green), 655-690 nm (red),

780-920 nm (near-infrared) and 450-800 nm (panchromatic) (GeoEye, 2011). GeoEye-1 imagery was delivered Standard Geometrically Corrected in a geo-registered Universal Transverse Mercator (UTM, Zone 17 North) coordinates and WGS 84 datum with 11-bit radiometric resolution. Information about viewing and illumination geometry are available in Table 3.2 and a false color composite illustrating the general area using green, red and near-infrared original bands is available on Figure 3.3. Clouds covered approximately 5% of the scene.

Table 3.2 : GeoEye-1 viewing and illumination geometry of the scene acquired on September 2nd 2010 at 17h40 GMT, Bylot Island, Nunavut.

View Azimuth	View Elevation	Solar Azimuth Angle	Solar Elevation Angle
81.40 °	220.18 °	185.86 °	24.37 °

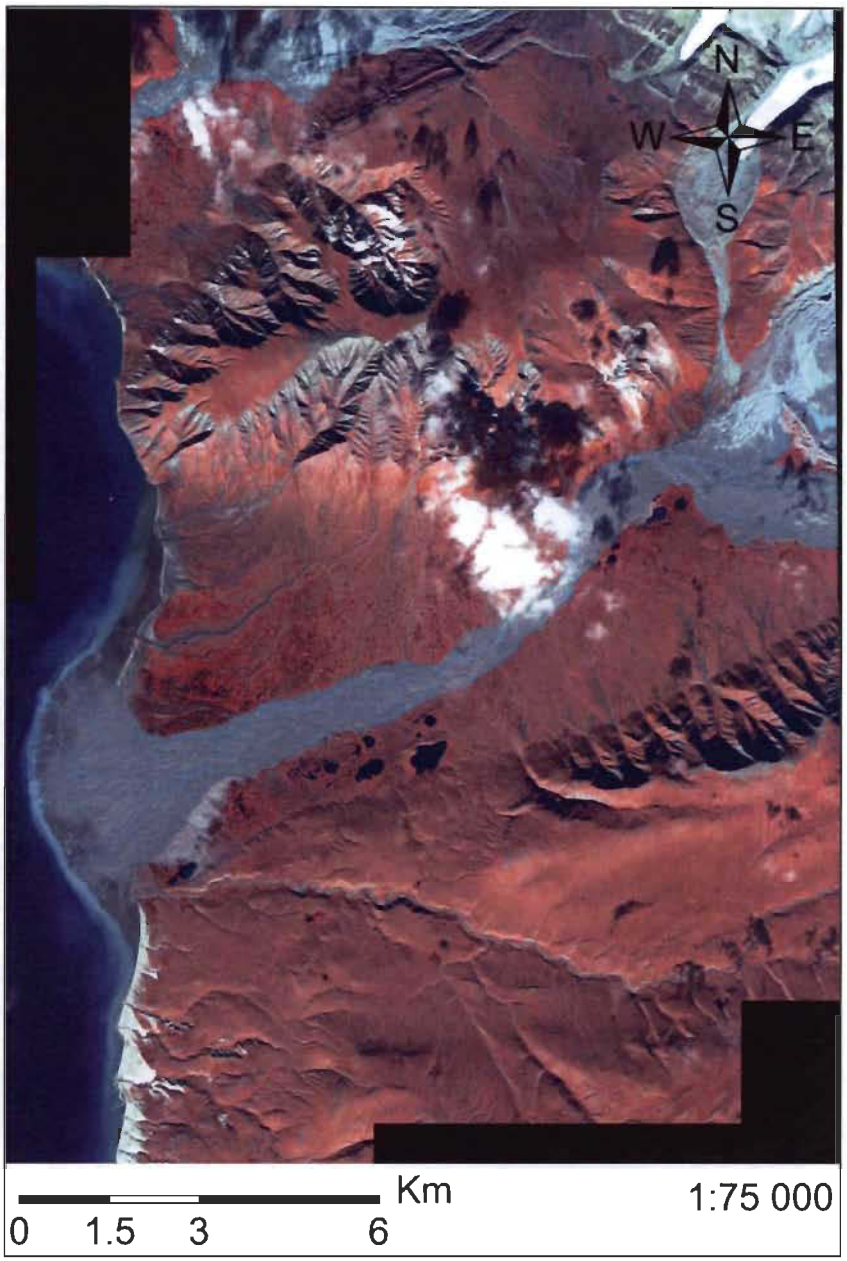

Figure 3.3 : False color (4-3-2) GeoEye-1 high spatial resolution satellite image of the Qarlikturvik valley, Bylot Island, Nunavut, acquired on September 2nd 2010 at 17h40 GMT.

The position of Gully A and Gully B recorded with a Trimble Differential Global Positioning System (DGPS; model Pathfinder Pro XRS with a TSC1 data collector) available through Godin and Fortier (2012) was used to apply a geographical correction to the scene to relocate the upper-left corner to 526299.75 E and 8130339.25 N. Details of DGPS differential correction are given in Godin and Fortier (2010). According to

Song *et al.* (2008), linear relationship between digital numbers (DN), radiance and reflectance units ensure that the raw DN units of the bands can directly be used for spatial analysis. However, as recommended for data comparison (Goward *et al.* 2003), uncalibrated DN units of all bands (blue, green, red, near-infrared and panchromatic bands) were converted to calibrated at-satellite radiance using provided "gain" and "offset" parameters (annexe D). A subset scene of the Quarlikturvik valley and clouds masking were done by digitizing boundaries manually to retain areas of interest for further processing.

A true color composite (blue, green and red bands) and a false colour composite (green, red and near-infrared bands) were fused with the panchromatic image to create 0.5 m standard pan-sharpened multispectral images to help the visual interpretation. Pan-sharpened image have the spectral characteristics of both inputs and the higher spatial resolution of the panchromatic band (Stow *et al.* 2004). Images were also enhanced using manual contrast stretching to improve quality and clarity. Gullies cartography and sampling site positions were then projected within the GeoEye-1 satellite image. To develop eco-terrain units NDVI values, visual interpretation and field characterisation (*i.e.* polygons size, form and adjacent environments) were used to select and draw corresponding training areas from the similar and homogeneous areas for which detailed vegetation descriptions and environmental characterisations were available (chapitre II). A minimum of 10 pixels (2 m * 2 m per pixel) were selected for each training area. Within six to nine pixels were selected for the six smaller sampling sites. Polygon rims were always excluded of selected training areas for the three polygon eco-terrain units. These reference areas were finally digitised as regions of interest (ROIs) in ENVI.

3.3.3.2 Vegetation index calculation

Red and near-infrared bands were converted into exoatmospheric reflectance (annexe D) to ultimately produce an NDVI image. Exoatmospheric reflectance allows comparison between sensors because it adjusts for direct solar irradiance (Goward *et al.* 2003). NDVI was then calculated following Equation 3.1 outlined by (Jackson & Huete 1991):

$$NDVI = (P_{nir} - P_{red})/(P_{nir} + P_{red}) \quad (3.1)$$

where,

NDVI = Normalized Difference Vegetation Index,

P_{nir} = Spectral reflectance in the near-infrared,

P_{red} = Spectral reflectance in the red.

NDVI provides a standardized method of comparing vegetation greenness and has a theoretical minimum of -1 and a maximum of 1. (Ray 1994). Vegetation is showed by an NDVI greater than 0 and the higher the NDVI value corresponding to the greater vegetation cover (Jackson & Huete 1991). Spectral reflectance in the near-infrared is where reflectance from the plant canopy is high and spectral reflectance in the red portion of the spectrum is where chlorophyll absorbs maximally (Raynolds *et al.* 2008; Raynolds & Walker 2009). Of course, NDVI was calculated to enhance discrimination between vegetation types and abundances and thereby aid the vegetation classification (Stow *et al.* 1993; Ray 1994). Eco-terrain unit NDVI values were obtained using pixels average of each training site as individual values.

3.3.3.3 Classification and accuracy assessment

An unsupervised classification of the NDVI dataset was performed using the Iterative Self-Organizing Data analysis technique (ISODATA; Tou *et al.* 1974). ISODATA clustering algorithm compares the radiometric value of each pixel with a predefined number of clusters (Manakos *et al.* 2000). Then, a standard confusion matrix was used to describe the relationship of class allocation relative to the ground reference data. Common measures such as overall accuracy and Kappa coefficient were calculated to evaluate classification accuracy (Congalton 1991; Smits *et al.* 1999; Foody 2002).

Overall accuracy is a value for the number of validation sampling sites that were classified correctly divided by the total number of validation sampling sites for all classes (Thomas *et al.* 2003). The Kappa coefficient (Equation 3.2) is a value for the difference between observed agreement of the classification and validation sites, showing the precision of the classification (Congalton & Green 2009).

$$K = \frac{P_o - P_c}{1 - P_c} \tag{3.2}$$

where,

K = Kappa coefficient,

P_o = the observed proportion of agreement,

P_c = the proportion of agreement that is expected to occur by chance.

A 3-pixel by 3-pixels majority filter was applied to the classified image to reduce the variability of spectral response and to make this more consistent with the ground truth. Then, the output image was spatially aggregated using spatial segmentation tool on NDVI classes. Spatial segmentation option was set to consider eight adjacent pixels for the connectivity and a minimum of 20 pixels must be contained per region. Finally, shapefiles were exported to the GIS and areas with low NDVI surrounding gullies were retained for calculation of the disrupted areas.

3.3.3.4 Texture analysis

Texture analysis was used to map subsidence areas of the gullyies. By using this method, we ensured that parts of gullies which are not mapped by the DGPS are properly included in the final map of affected areas. Texture analysis was also used as the Gully C was not mapped using the DGPS. The texture analysis was done by creating a grey-level co-occurrence matrix (GLCM) texture model (Haralick *et al.* 1973; Haralick 1979) using mean value of pixels on the panchromatic band. Windows size was set on 5-pixels by 5-pixels over the 0.5 m spatial resolution, which leads to an analysis of the texture patterns inside an area of 2.5 m by 2.5 m. A 7 classes ISODATA classification followed by a one pass of the majority filter to reduce the variability of spectral response

were performed. Classes corresponding to collapsed areas were spatially regrouped and used to map properly gullies at satellite data acquisition date. Sections of Gully A and B mapped in 2009 using a DGPS (Godin and Fortier, 2012) were used for ensure that gullies extent from texture analysis correspond.

3.3.3.5 Final affected areas mapping

Areas marked by a low NDVI corresponding to those of Sediment zones, Drained polygons and Dried polygons eco-terrain units along the three studied gullies were mapped and added to the gully cartography obtained from texture analysis. Visual interpretation of GeoEye-1 imagery was necessary to link low NDVI areas surrounding gullies in order to extract realistic final affected areas. The three studied gullies were then compared to other gullies found in the Qarlikturvik valley using field knowledge, DGPS data and unsupervised classification.

3.4 Results

3.4.1 Eco-terrain unit NDVI values

NDVI ranged from -0.73 to 0.74 for the processed scene (Figure 3.4). Based on the ground-survey, mean NDVI values extracted from sampling sites increased along eco-terrain units in the following sequence: Sediment zones, Drained polygons, Dried polygons, Mesic polygon rims, Mesic zones, and Wet polygons (Figure 3.5). The lowest NDVI mean value and the greatest variability were associated to the Sediment zones eco-terrain unit where the presence of bare ground varied greatly from 6% to 97.5%. Drained polygons and Dried polygons as well as Mesic polygon rims and Mesic zones, were not well contrasted, showing comparable NDVI values. Wet polygons, with the largest green moss carpet and vascular species cover, had the greatest NDVI values.

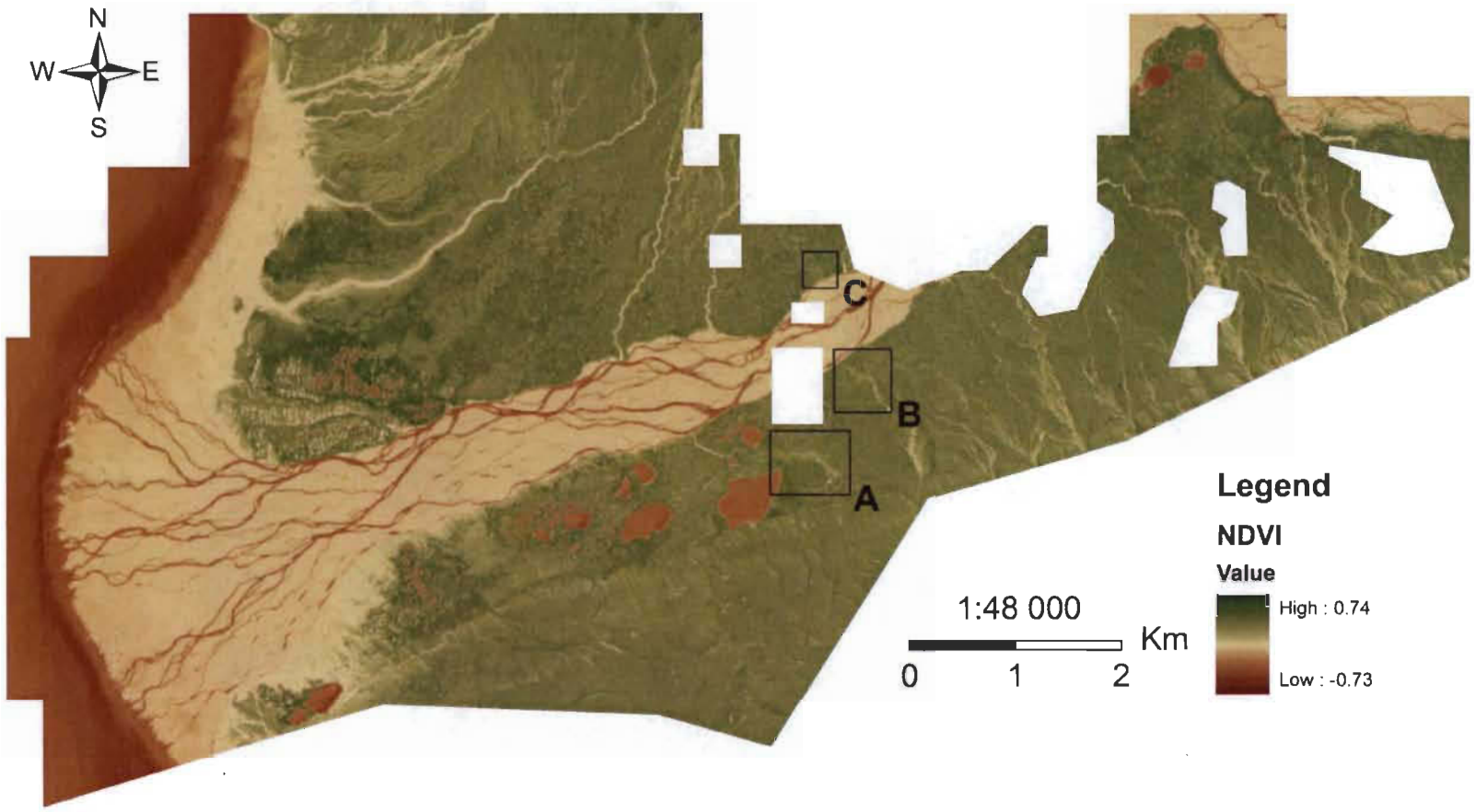

Figure 3.4 : Normalized difference vegetation index image of processing scene, Qarlikturvik valley, Bylot Island, Nunavut. Red areas represent regions of low NDVI (-0.73), while green areas indicate high NDVI (0.74). Gully A, B and C are located by rectangles.

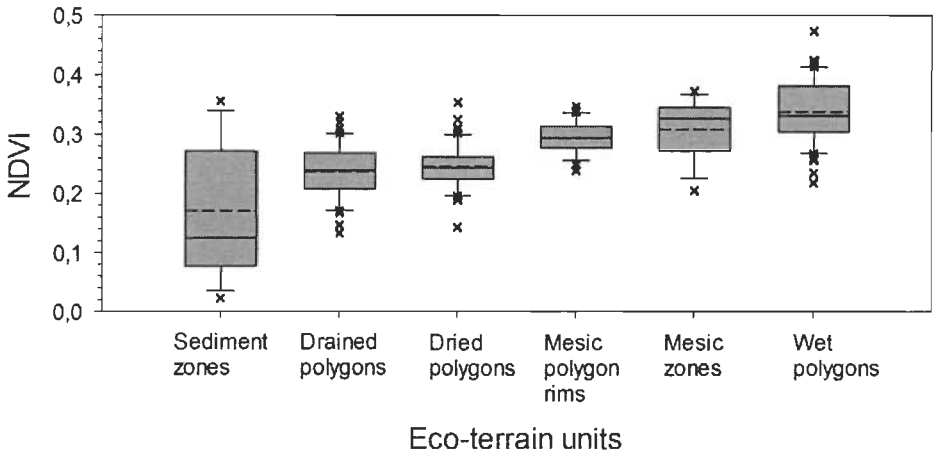

Figure 3.5 : NDVI values of eco-terrain units (Wet polygons, n = 62; Drained polygons, n = 44; Dried polygons, n = 43; Mesic zones, n = 13; Mesic polygon rims, n = 35; Sediment zones, n = 15), Bylot Island, Nunavut. 10^{th} percentiles, lower quartile, median, mean (dash), upper quartile and 90^{th} percentiles are shown.

3.4.2 Classification and accuracy assessment results

The final satellite-derived NDVI unsupervised classification was designed to provide six classes and mask water bodies (NDVI <-0.094) to remove a part of variance associated with non-vegetated surfaces. NDVI values between -0.094 and 0 were kept as they represent sediment areas found in and around gullies. Within the three first classes of the unsupervised classification (Figure 3.6), a portion of gray indicates an NDVI of -0.09 to 0.13 (Class 1), red indicates an NDVI of 0.13 to 0.22 (Class 2), and yellow indicates an NDVI of 0.22 to 0.27 (Class 3). Class 1 represents 31% of the classified image and was associated to non-vegetated areas like pro-glacial braided rivers and aeolian deposits. Pools were sometimes included in this class. Classes 2 and 3 represent 15% of the classified image and were mainly restricted to areas covered by very poor vegetation surrounding alluvial fans and drainage systems. Small patches corresponding to Class 3 were in rare cases found into polygonal grounds. Within the three last classes, a portion of light green indicates an NDVI of 0.27 to 0.32 (Class 4), bright green indicates an NDVI of 0.32 to 0.37 (Class 5), and dark green indicates an NDVI of 0.37 to 0.74 (Class 6). These classes represent 56% of the classified image and were associated to a gradient of wet and mesic environments found in polygonal patterned ground of the Qarlikturvik valley. An overall accuracy of 43.9% and a Kappa coefficient of 0.32 resulted when NDVI classes were directly linked to the six eco-terrain units (Table 3.3).

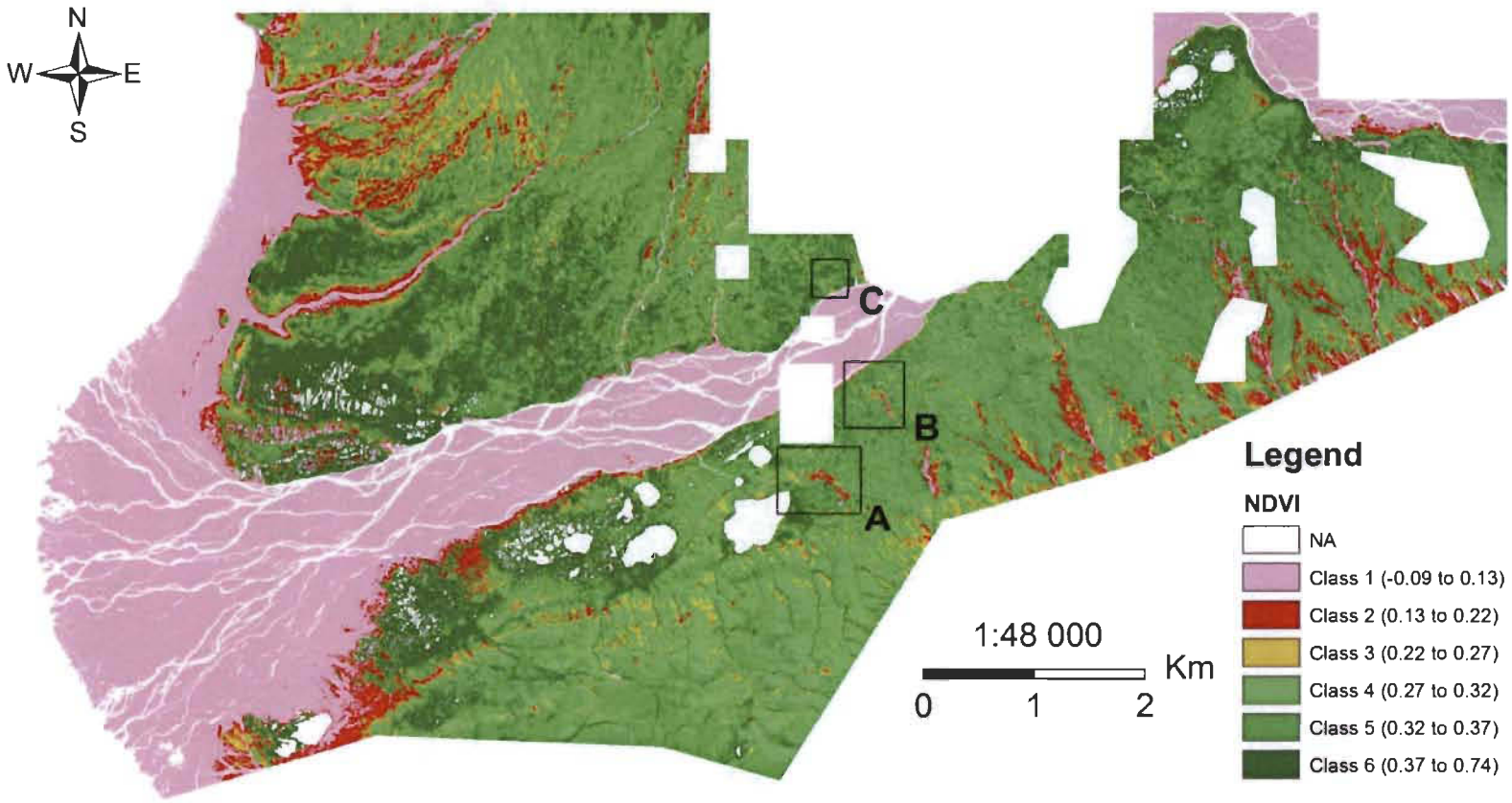

Figure 3.6 : Unsupervised classification of NDVI derived from GeoEye-1 imagery acquired the September 2nd 2010 at 17h40 GMT, Qarlikturvik valley, Bylot Island, Nunavut. Six classes were assigned using the ISODATA clustering algorithm by masking clouds and water bodies. Gully A, B and C are located by rectangles.

Table 3.3 : Confusion matrix based of 212 sampling sites used as ground-truthing observations, Bylot Island, Nunavut. Percent of sampling sites per eco-terrain units are showed.

Eco-Terrain units / **NDVI classes**	Sediment zones n = 15	Drained polygons n = 44	Dried polygons n = 43	Mesic polygon rims n = 35	Mesic zones n = 13	Wet polygons n = 62
Class 1 (-0.09 to 0.13)	**46.7**	0	0	0	0	0
Class 2 (0.13 to 0.22)	13.3	**40.9**	23.3	0	7.7	3.2
Class 3 (0.22 to 0.27)	20.0	38.6	**51.2**	17.1	15.4	6.5
Class 4 (0.27 to 0.32)	6.7	13.6	18.6	**57.1**	23.1	21.0
Class 5 (0.32 to 0.37)	6.7	6.8	4.7	25.7	**46.2**	37.1
Class 6 (0.37 to 0.74)	6.7	0	2.3	0	7.7	**32.3**
	Overall accuracy : 43.9%			Kappa coefficient : 0.32		

3.4.5 Affected areas

In the three case studied, unsupervised classification highlighted that wetland vegetation is affected by the new drainage systems (Figure 3.7; 3.8; 3.9). While Class 1 was particularly linked to collapsed areas and sediments deposited upstream of gullies, Classes 2 and 3 indicated different level of low green vegetation cover associated to Drained polygons and Dried polygons. Environments with high green vegetation cover classes (Class 4, 5 and 6) were usually found surrounding these low green vegetation cover areas. Thus, wet and mesic environments dominated at larger scale up to the boundary of affected areas. Drainage affected, including collapsed areas (based on the texture analysis) and low green vegetation cover areas, 60 344 m^2, 30 480 m^2 and 4 012 m^2 for Gully A, B and C, respectively (Table 3.4). These areas were located directly at the margin and were distributed throughout the length of studied gullies. They represent ratios of 72 m^2, 42 m^2 and 23 m^2 per meter of gullying for Gully A, B and C, respectively. The total ratio for the three case studies is 55 m^2 per meter of gullying.

No other gullies with as strong an impact on wetland vegetation comparable to Gully A and Gully B were found in low-centered polygons. However, two small gullies were identified 450 m west of Gully A. These active gullies affected 2 352 m^2 and 368 m^2 of a highly productive area. Prospection of drainage systems located in the mesic environments of the Qarlikturvik valley, revealed the presence of gullies yet adjacent areas did not have lower NDVI values. These gullies were generally not active and surrounded by vegetation having at least an NDVI index of 0.27 which does not differ from the general area. An active segment of an old drainage system was however found 275 m east of Gully B and low NDVI was detected on an area of 3 876 m^2. Drainage systems located in aeolian deposit areas were also explored using the produced NDVI image. Gullies were surrounded by non-vegetated environments corresponding to Class 1 of the classification.

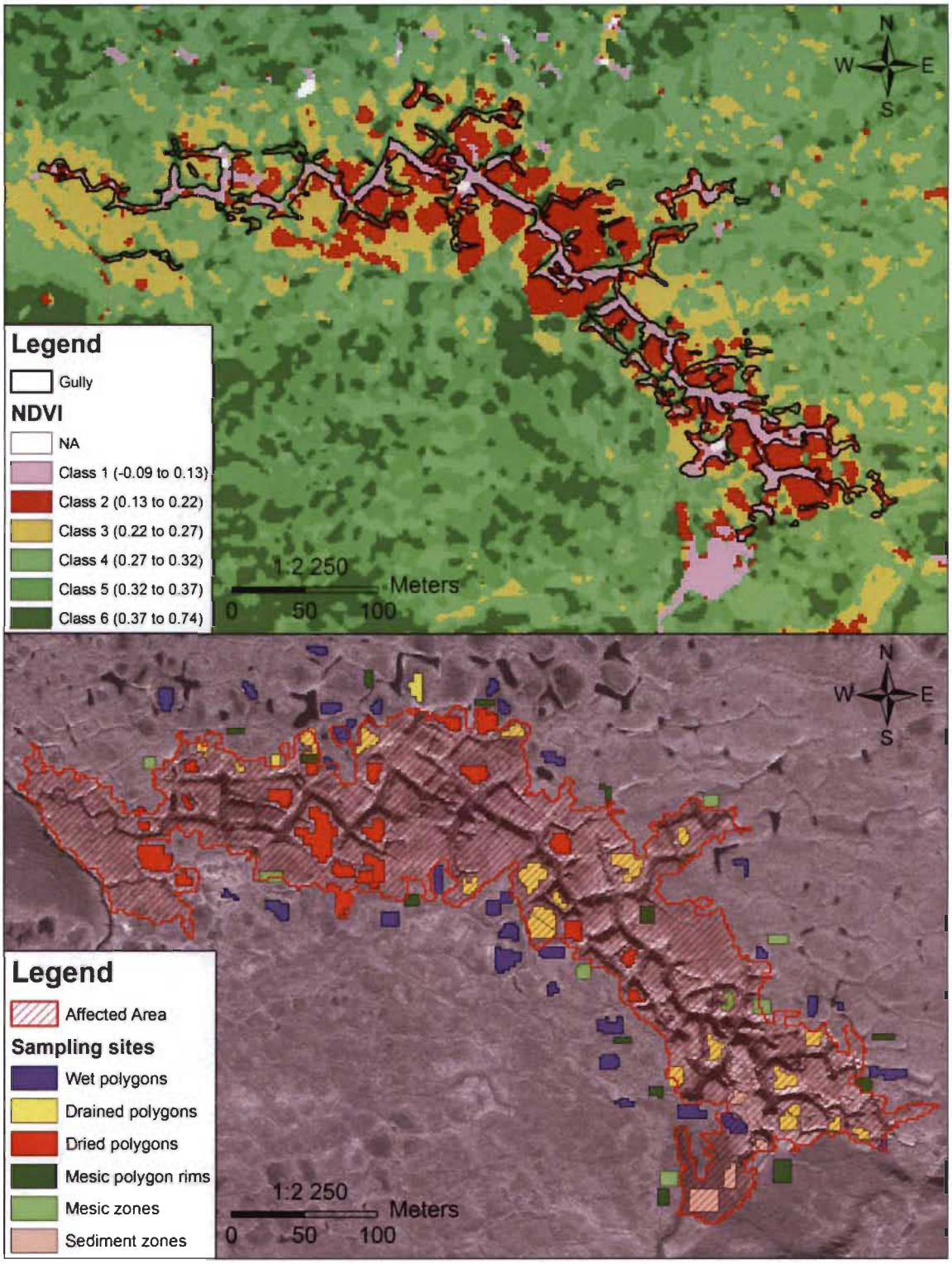

Figure 3.7 : Unsupervised classification of NDVI from GeoEye-1 imagery (top) and derived areas affected by gullying drainage (bottom), Gully A, Bylot Island, Nunavut.

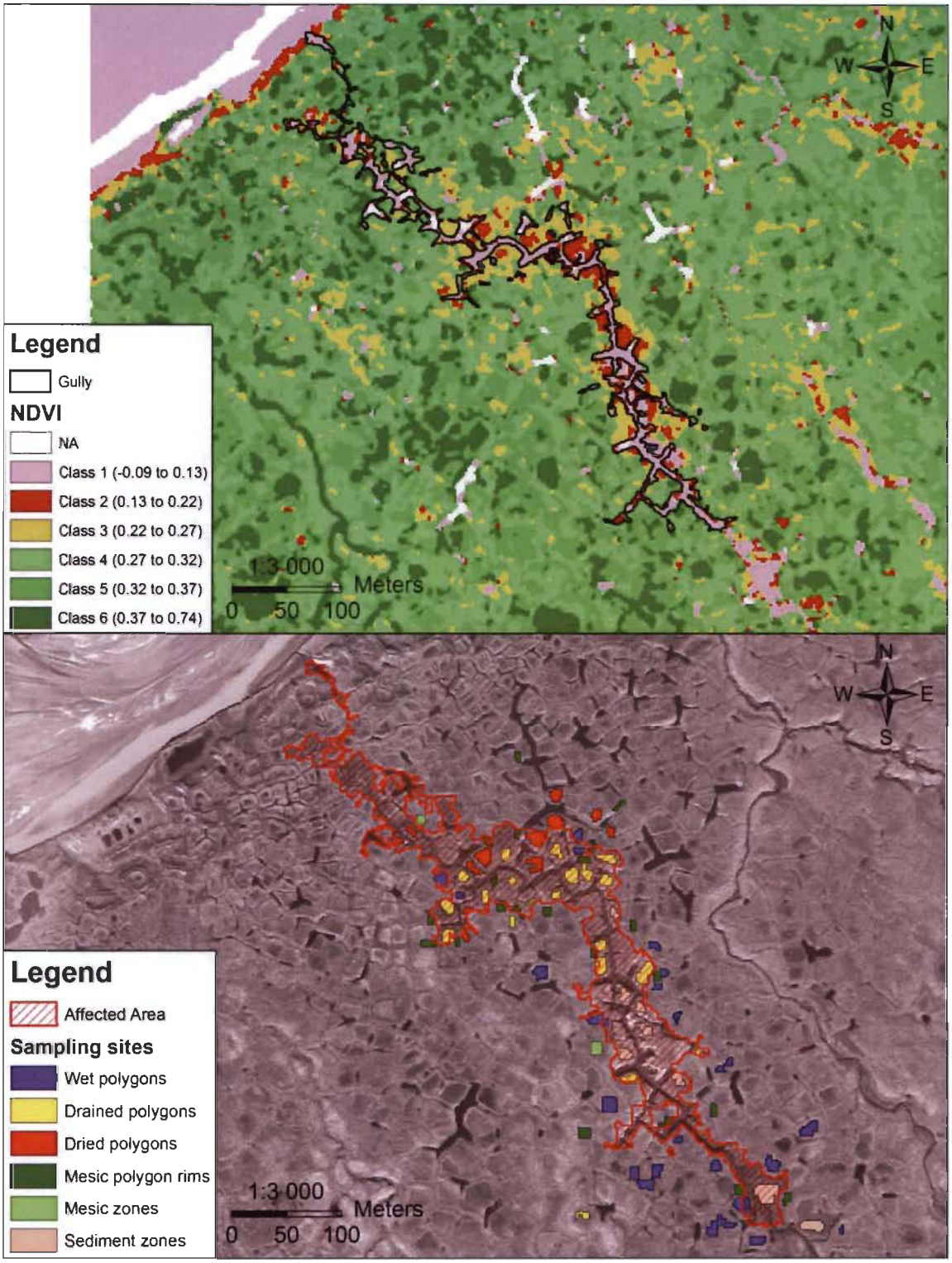

Figure 3.8 : Unsupervised classification of NDVI from GeoEye-1 imagery (top) and derived areas affected by gullying drainage (bottom), Gully B, Bylot Island, Nunavut.

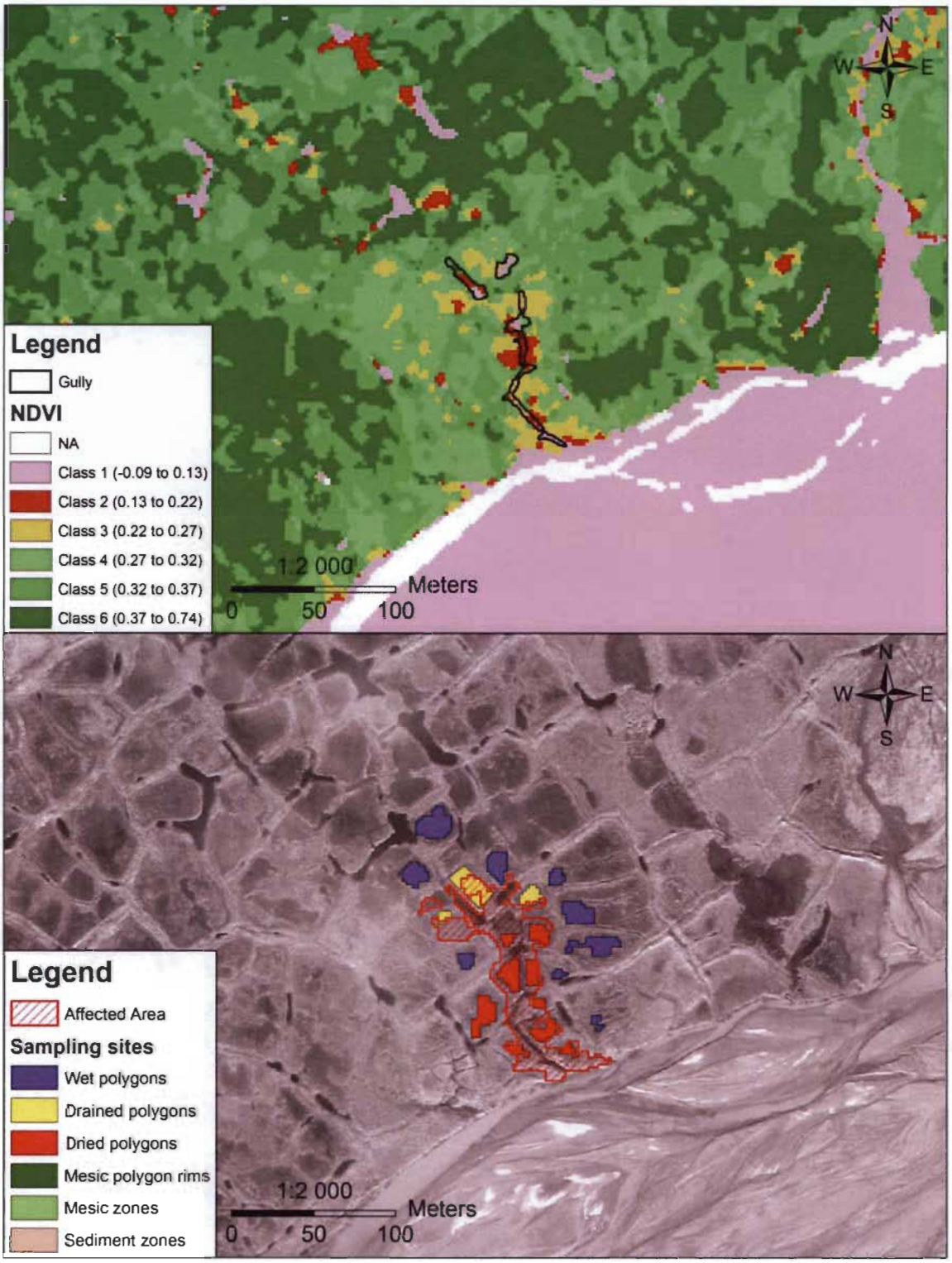

Figure 3.9 : Unsupervised classification of NDVI from GeoEye-1 imagery (top) and derived areas affected by gullying drainage (bottom), Gully C, Bylot Island, Nunavut.

Table 3.4 : Summary of affected areas according to gullies length, Bylot Island, Nunavut.

	Affected area (m^2)	Length of the main axis (m)	Ratio (m^2/m)
Gully A	60 344	835	72
Gully B	30 480	717	42
Gully C	4 012	180	23
Total	94 836	1 732	55

*Length of Gully A and Gully B are from Godin & Fortier (2012). Length of Gully C was measured using the measurement tool in ENVI.

3.5 Discussion

This study demonstrates the impact on vegetation of permafrost degradation along three thermo-erosion gullies located in low-centered polygon wetlands. An unsupervised classification on a NDVI image highlighted areas affected by gullying drainage with low NDVI values corresponding to a lower green vegetation cover. Areas with low NDVI were mostly confined to the edges of gullies where erosion modified drainage.

3.5.1 Accuracy of imagery analysis

Results of classification show a continuum in the NDVI values between the different eco-terrain units. Thus, wetlands and mesic environments are distinguished from disturbed eco-terrain units (Drained polygons, Dried polygons and Sediment zones) surrounding gullies. The ability to link eco-terrain units to classification classes was however limited from the high overlaps and relatively subtle differences in NDVI values between Drained polygons and Dried polygons as well as between Mesic zones and Mesic polygon rims. The presence of variable atmospheric scattering and absorption and cloud contamination in measurements are parameters that could influence our NDVI results (Goward *et al.* 2003). Nevertheless, we attribute part of misclassifications to the use of a satellite data acquired the September 2nd 2010. Season of growth had ended when the scene was acquired, limiting differences between low and high green vegetation cover eco-terrain units' values. According to Hope *et al.* (1993) and Stow *et al.* (1993), the most divergent signatures between tundra vegetation communities occur in late July during maximum greenness.

3.5.2 Case studies

According to our classification, low NDVI areas were found in low-centered polygons surrounding gullies (Figure 3.7). These areas were restricted to the edge of gullying illustrating the fact that ice-wedge collapse was a necessary condition for a radical decrease of the vegetation cover highlighted by a low NDVI index. The sudden shift in the water supply in these areas generate a decrease of moisture to an insufficient level for maintain wetland greenness. Drying of mosses contributes to a decrease of the NDVI of drained wetlands (Douma *et al.* 2007). According to Woo *et al.* (2006; 2008), snowmelt water released during a brief snowmelt period that lasts for 2–3 weeks in the Arctic is a reliable water supply and is crucial to the maintenance of wetlands. In this way, a partial degradation caused by the presence of breaches or cracks connecting to gullies as well as a general collapse of rims have major impact at snowmelt by directly affecting the duration and degree of wetland saturation. As also observed by Jorgenson *et al.* (2006), the degradation of ice wedges has reduced the integrity of polygons and has caused a redistribution of surface water from the adjacent tundra to the degraded trough network and broadened the ecological impacts.

Although thermo-erosion gullies were observed in the past (Billings & Peterson 1980), we are the first to evaluate the spatial consequences on polygon patterned wetlands. Overall, the three gullies are currently affecting 94 836 m^2 distributed along 1 740 m of gullying (Table 4.3). The variability between ratios of the three gullies (*i.e.* 72 m^2, 42 m^2 and 23 m^2 per meter of gullying) can be explained by variation in the number and the length of secondary axes of gullying, which was not considered. Indeed, Gully A differs from the two others by a significant number of secondary axes of gullying. At the opposite, the Gully C has no secondary axes and the lowest ratio of the three gullies. Variation in the size of polygons surrounding gullies can also explain in part this variability. By considering the total area of wetland characterized by permanent ponds (9%) and those forming graminoid meadows (14%) without standing water in the Qarlikturvik valley based on Hughes *et al.* (1994), the three studied gullies have disrupted within 10 years 0.6% of the most important habitat for geese. Thus, gully formation can represent an increase in cover of mesic environments at the expense of

wetlands at the scale of the Qarlikturvik valley. Drainage caused by thermo-erosion gullies is likely to affect larger areas than revealed by these results. Minor changes of hydrological conditions certainly induce more subtle changes in NDVI that are difficult to detect for wet polygons not located directly on the margins of gullies.

The spatio-temporal evolution of the Gully A has been closely monitored since its formation in 1999 until today (Fortier *et al.* 2007; Godin & Fortier 2010; Godin & Fortier 2012). Our results show disturbed areas with low NDVI throughout collapsed areas along this gully, showing that vegetation was quickly affected near the head of the gully and that the oldest sectors (11 years old) are still easily identified. Thus, oldest sectors are not yet covered by green vegetation equal to the baseline level of wetlands and mesic environments.

3.5.3 Other cases

Gullies located in mesic environments were usually surrounded by high cover green vegetation. Vegetation was well established and hydrological changes relatively small which do not prevent growth of tolerant mesic plant species. In addition, in most cases these disturbances were old and stabilized. For drainage systems located in aeolian deposit areas, no direct impact on vegetation were observed because vegetation cover was limited by the constant addition of new sediments. However, these systems can contribute to drain pools located upstream. These pools are usually surrounded by wetlands used by geese.

3.6 Conclusions

Our study assesses areas disrupted by thermo-erosion gullies in adjacent wetlands. The approach used has showed the strong potential of high-resolution imagery for identifying these areas by integrating a combination of ecological ground survey and remote sensing techniques. Results showed the consequence in short term of thermo-erosion gullying on arctic wetland vegetation. Using NDVI we can conclude that: (1) green vegetation cover decreases at a local scale, showing rapid response of arctic wetlands to the drainage by

thermo-erosion gullying; (2) in affected wetland areas, mesic vegetations establishment takes several years. The method was robust and can be used in large and/or inaccessible areas. Transitions from wetlands to mesic environments new equilibrium probably occur at a larger scale surrounding gullies but those more subtle changes can not be documented without long term comparisons.

3.7 Acknowledgments

Special thanks to Parks Canada – Sirmilik National Park, Northern Studies Center (CEN) and Dr Gilles Gauthier (Laval University) for access to the field camp in 2009 and 2010. We are grateful to Alexandre Guertin-Pasquier and Etienne Godin for their assistance in the field. Logistical support was provided by Polar Continental Shelf Program (PCSP).We acknowledge the financial support received from the International Polar Year (IPY) program of the Government of Canada, Natural Sciences and Engineering Research Council of Canada (NSERC), Fonds québécois de la recherche sur la nature et les technologies (FQRNT), Northern Scientific Training Program (NSTP) of the Department of Indian Affairs and Northern Development, the network of centers of excellence of Canada ArcticNet, NSERC CREATE training program in northern environmental sciences (EnviroNorth) and Groupe de recherche en biologie végétale (GRBV) of the Université du Québec à Trois-Rivières.

3.8 References

Allard M (1996) Geomorphological changes and permafrost dynamics: key factors in changing arctic ecosystems. An example from Bylot Island, Nunavut, Canada. *Geoscience Canada*, **23**, 205–212.

Atkinson DM, Treitz P (2007) Ecological classifications derived from spectral and vegetation data for Cape Bounty, Melville Island. *In: Proceedings of the First International Circumpolar Conference on Geospatial Sciences and Applications.* IPY GeoNorth 2007, 20–24 August, Yellowknife, Northwest Territories.

Billings WD, Peterson KM (1980) Vegetational change and ice-wedge polygons through the thaw-lake cycle in Arctic Alaska. *Arctic and Alpine Research*, **12**, 413–432.

Congalton RG (1991) A review of assessing the accuracy of classifications of remotely sensed data. *Remote Sensing Environment*, **37**, 354–6.

Congalton RG, Green K (2009) *Assessing the accuracy of remotely sensed data: principles and practices, 2nd edition*. CRC Press, Taylor & Francis Group, 183 pp.

Douma JC, Van Wijk MT, Lang SI, *et al.* (2007) The contribution of mosses to the carbon and water exchange of arctic ecosystems: quantification and relationships with system properties. *Plant, Cell and Environment*, **30**, 1205–1215.

Ellis CJ, Rochefort L, Gauthier G, *et al.* (2008) Paleoecological evidence for transitions between contrasting landforms in a polygon-patterned High Arctic wetland. *Arctic Antarctic and Alpine Research*, **40**, 624–637.

Foody GM (2002) Status of land cover classification accuracy assessment. *Remote Sensing of Environment*, **80**, 185–201.

Fortier D, Allard M (2004) Late Holocene syngenetic ice-wedge polygons development, Bylot Island, Canadian Arctic Archipelago. *Canadian Journal of Earth Sciences*, **41**, 997–1012.

Fortier D, Allard M, Pivot F (2006) A late-Holocene record of loess deposition in ice-wedge polygons reflecting wind activity and ground moisture conditions, Bylot Island, eastern Canadian Arctic. *The Holocene*, **16**, 635–646.

Fortier D, Allard M, Shur Y (2007) Observation of rapid drainage system development by thermal erosion of ice wedges on Bylot Island, Canadian Arctic Archipelago. *Permafrost and Periglacial Processes*, **18**, 229–243.

French HM (2007) *The Periglacial Environment, Third Edition*. John Wiley & Sons Ltd, 458 pp.

Gauthier G, Berteaux D, Bety J, *et al.* (2011) The tundra food web of Bylot Island in a changing climate and the role of exchanges between ecosystems. *Ecoscience*, **18**, 223–235.

Gauthier G, Giroux J-F, Reed A, *et al.* (2005) Interactions between land use, habitat use, and population increase in greater snow geese: what are the consequences for natural wetlands? *Global Change Biology*, **11**, 856–868.

Gauthier G, Hughes RJ, Reed R, *et al.* (1995) Effect of grazing by greater snow geese on the production of graminoids at an arctic site (Bylot Island, NWT, Canada). *Journal of Ecology*, **83**, 653–664.

Gauthier G, Rocheford L, Reed A (1996) The exploitation of wetland ecosystems by herbivores on Bylot Island. *Geoscience Canada*, **23**, 253–259.

GeoEye (2012) *High resolution imagery, earth imagery and geospatial services*. Website: http://geoeye.com/CorpSite/products/imagerysources/Default.aspx#geoeye1 (Accessed February 2012).

Godin E, Fortier D (2010) Geomorphology of thermo-erosion gullies – case study from Bylot Island, Nunavut, Canada. *In: Proceedings 6th Canadian Permafrost Conference and 63rd Canadian Geotechnical Conference, Calgary.*

Godin E, Fortier D (en révision) Geomorphology and spatio-temporal characterization of a thermo-erosion gully in the valley of glacier C-79, Bylot Island, Nunavut, Canada. *Canadian Journal of Earth Sciences*.

Godin E, Fortier D (2012) Fine scale spatio-temporal monitoring of multiple thermo-erosion gullies development on Bylot Island, eastern canadian archipelago. *In: Proceedings Tenth International Conference on Permafrost (TICOP), Salekhard, Russia.*

Goward SN, Davis PE, Fleming D, *et al.* (2003) Empirical comparison of Landsat 7 and IKONOS multispectral measurements for selected Earth Observation System (EOS) validation sites. *Remote Sensing of Environment*, **88**, 80–99.

Haralick RM (1979) Statistical and structural approaches to texture. *In: Proceedings of the IEEE*, **67**, 786–804.

Haralick RM, Shanmugam K, Dinstein I (1973) Textural features for image classification. *IEEE Transactions on Systems, Man, and Cybernetics*, **3**, 610–621.

Hope AS, Kimball JS, Stow DA (1993) The relationship between tussock tundra spectral reflectance proprieties and biomass and vegetation composition. *International Journal of Remote Sensing*, **14**, 1861–1874.

Hughes RJ, Reed A, Gauthier G (1994) Space and habitat use by greater snow goose broods on Bylot Island, Northwest Territories. *Journal of Wildlife Management*, **58**, 536–545.

Huemmrich KF, Gamon JA, Tweedie CE, *et al.* (2010) Remote sensing of tundra gross ecosystem productivity and light use efficiency under varying temperature and moisture conditions. *Remote Sensing of Environment*, **114**, 481–489.

Jackson RD, Huete AR (1991) Interpreting vegetation indices. *Preventive Veterinary Medicine*, **11**, 185–200.

Jorgenson MT, Shur YL, Pullman ER (2006) Abrupt increase in permafrost degradation in Arctic Alaska. *Geophysical Research Letters*, **33**, L02503, doi: 02510.01029/02005GL024960.

Klein DR, Bay C (1991) Diet selection by vertabrate herbivores in the High Arctic of Greenland. *Holarctic Ecology*, **14**, 152–155.

Laidler GJ, Treitz P (2003) Biophysical remote sensing of arctic environments. *Progress in Physical Geography*, **27**, 44–68.

Laidler GJ, Treitz P, Atkinson D (2008) Remote sensing of Arctic vegetation: relations between the NDVI, spatial resolution and vegetation cover on Boothia Peninsula, Nunavut. *Arctic*, **61**, 1–13.

LPSO (1998) *Landsat-7 science data user's handbook.* Landsat Project Science Office, Greenbelt, Maryland, 186 pp.

Mackay JR, Burn CR (2002) The first 20 years (1978-1979 to 1998-1999) of ice-wedge growth at the Illisarvik experimental drained lake site, western Arctic coast, Canada. *Canadian Journal of Earth Sciences*, **39**, 95–111.

Manakos I, Schneider T, Ammer U (2000) A comparison between the ISODATA and the eCognition classification methods on basis of field data. *IAPRS 2000*, **33**, 133–139.

Masse H (1998) *Estimation de la capacité de support des différents écosystèmes humides utilisés par la grande oie des neiges nichant à l'Île Bylot (Nunavut, Canada)*. Mémoire de maîtrise, Université Laval, Québec, 98 pp.

Masse H, Rochefort L, Gauthier G (2001) Carrying capacity of wetland habitats used by breeding greater snow geese. *The Journal of Wildlife Management*, **65**, 271–281.

Minke M, Donner D, Karpov NS, *et al.* (2007) Distribution, diversity, development and dynamics of polygon mires: examples from Northeast Yakutia (Siberia). *Peatlands International*, **1**, 36–40.

Minke M, Donner N, Karpov N, *et al.* (2009) Patterns in vegetation composition, surface height and thaw depth in polygon mires in the Yakutian Arctic (NE Siberia): a microtopographical characterisation of the active layer. *Permafrost and Periglacial Processes*, **20**, 357–368.

Ray (1994) *A FAQ on vegetation in remote sensing*. California Institute of Technology. Pasadena, California, USA, 18 pp.

Raynolds MK, Comiso JC, Walker DA, *et al.* (2008) Relationship between satellite-derived land surface temperatures, arctic vegetation types, and NDVI. *Remote Sensing of Environment*, **112**, 1884–1894.

Raynolds MK, Walker DA (2009) Effects of deglaciation on circumpolar distribution of arctic vegetation. *Canadian Journal of Remote Sensing*, **35**, 118–129.

Riedel SM, Epstein HE, Walker DA (2005) Biotic controls over spectral reflectance of arctic tundra vegetation. *International Journal of Remote Sensing*, **26**, 2391–2405.

Rouse JW, Haas RH, Schell JA, *et al.* (1973) Monitoring vegetation systems in the Great Plains with ERTS. *Third ERTS Symposium*, NASA SP-351 **1**, 309–317.

Song C, Dickinson MB (2008) Extracting forest canopy structure from spatial information of high resolution optical imagery: tree crown size versus leaf area index. *International Journal of Remote Sensing*, **29**, 5605–5622.

Soudani K, Francois C, le Maire G, *et al.* (2006) Comparative analysis of IKONOS, SPOT, and ETM+ data for leaf area index estimation in temperate coniferous and deciduous forest stands. *Remote Sensing of Environment*, **102**, 161–175.

Smits PC, Dellepiane SG, Schowengerdt RA (1999) Quality assessment of image classification algorithms for land-cover mapping: a review and a proposal for a cost-based approach. *International Journal of Remote Sensing*, **20**, 1461–1486.

Stow DA, Burn BH, Hope AS (1993) Spectral, spatial, and temporal characteristics on Arctic tundra reflectance. *International journal of remote sensing*, **14**, 2445–2462.

Stow DA, Hope A, McGuire D, *et al.* (2004) Remote sensing of vegetation and land-cover change in Arctic tundra ecosystems. *Remote Sensing of Environment*, **89**, 281–308.

Tieszen LL, Reed BC, Bliss NB, *et al.* (1997) NDVI, C_3 and C_4 production, and distributions in Great Plains grassland land cover classes. *Ecological Applications*, **7**, 59–78.

Thomas V, Treitz P, Jelinski D, *et al.* (2003) Image classification of a northern peatland complex using spectral and plant community data. *Remote Sensing of Environment*, **84**, 83–99.

Tou JT, Gonzalez RC (1974) *Pattern Recognition Principles*. Addison-Wesley Publishing Company, Reading, Massachusetts, 377 pp.

Woo M-K, Kane DL, Carey SK, *et al.* (2008) Progress in permafrost hydrology in the new millennium. *Permafrost and Periglacial Processes*, **19**, 237–254.

Woo M-K, Young KL (2006) High Arctic wetlands: their occurrence, hydrological characteristics and sustainability. *Journal of Hydrology*, **320**, 432–450.

Zoltai SC, McCormick KJ, Scotter GW (1983) *A natural resource survey of Bylot Island and adjacent Baffin Island, Northwest Territories*. Parks Canada, Ottawa, Canada, 176 pp.

ANNEXE A

USE OF VERTICAL PHOTOGRAPHS FOR ASSESSING PLANT SPECIES COVER

Objective

1. Determine if the use of vertical digital photography can be used to estimate efficiently arctic plant cover.
2. Compare the accuracy and repeatability of plant cover assessments obtained from visual estimates made in the laboratory with traditional plant cover field sampling completed in the Arctic.

Methods

A first plot of 70 cm * 70 cm in size was positioned at the center of 182 sampling sites selected during summer 2009. Cover of 59 vascular plant species was visually assessed as a vertical projection onto the ground of all above-ground parts of the individual plant using a modified scale of Daubenmire's (1959) classification (Table 2.1). Lichens, green mosses, dry mosses, bare ground, cryptogamic crust, geese feces, grubbing, litter, mushrooms, nostocs, standing dead and sanding water covers were also assessed in the same way. Then, a vertical photograph was taken from approx. 1.3 m above the quadrats. To reduce distortion, quadrats were positioned in the center of the photograph according to Chen *et al.* (2010) and "Climate Change Impacts on Canadian Arctic Tundra Ecosystems: Interdisciplinary and Multi-scale Assessments (CiCAT)" protocols from International Polar Year (2012). Two other random plots of same size (70 cm * 70 cm) were positioned into representative and homogenous area of the sampling site. Only vertical photographs were taken for these two plots.

Cover of vascular plant species and other taxa were determined on vertical photographs using a computer in the lab. The 7 cm superimposed grid integrates to the quadrat frame

and the use of zoom, brightness and contrast tools of the program Photoshop v7.0 helped the analysis of digital photography. Comparison between field sampling and corresponding vertical photograph plots was performed through the common dataset to assess the level of correspondence between the two methods. Data were analysed by linear regression with the program R v2.15.0.

Results and discussion

The comparison between the vegetation cover evaluation in the field and from vertical photographs reveals that the correlation varied from very good for certain species such as *Salix arctica* ($r^2 = 0.94$) and *Carex aquatilis* ($r^2 = 0.91$) and weaker for others species such as *Dupontia fisheri* ($r^2 = 0.71$) and *Eriophorum sheuchzeri* ($r^2 = 0.52$; Figure A.1). The strength of the relation depended of the level of difficulty in visual identification for each plant species and their abundance (Table A.1). For example, *Dupontia fisheri* and *Eriophorum sheuchzeri* have delicate foliage more difficult to see and to evaluate than the larger and more abundant *Carex aquatilis* and *Salix arctica*. However, by evaluating a large number of quadrats, the mean value obtained was comparable (Table A.2). Taking pictures coupled with a field sampling of a subset of the quadrats can increase the area sampled Chen *et al.* (2010), and provides documentation that supports the comparison over time. The use of a combination of field sampling and vertical photography allowed to sample more plots during the 2009 and 2010 field seasons.

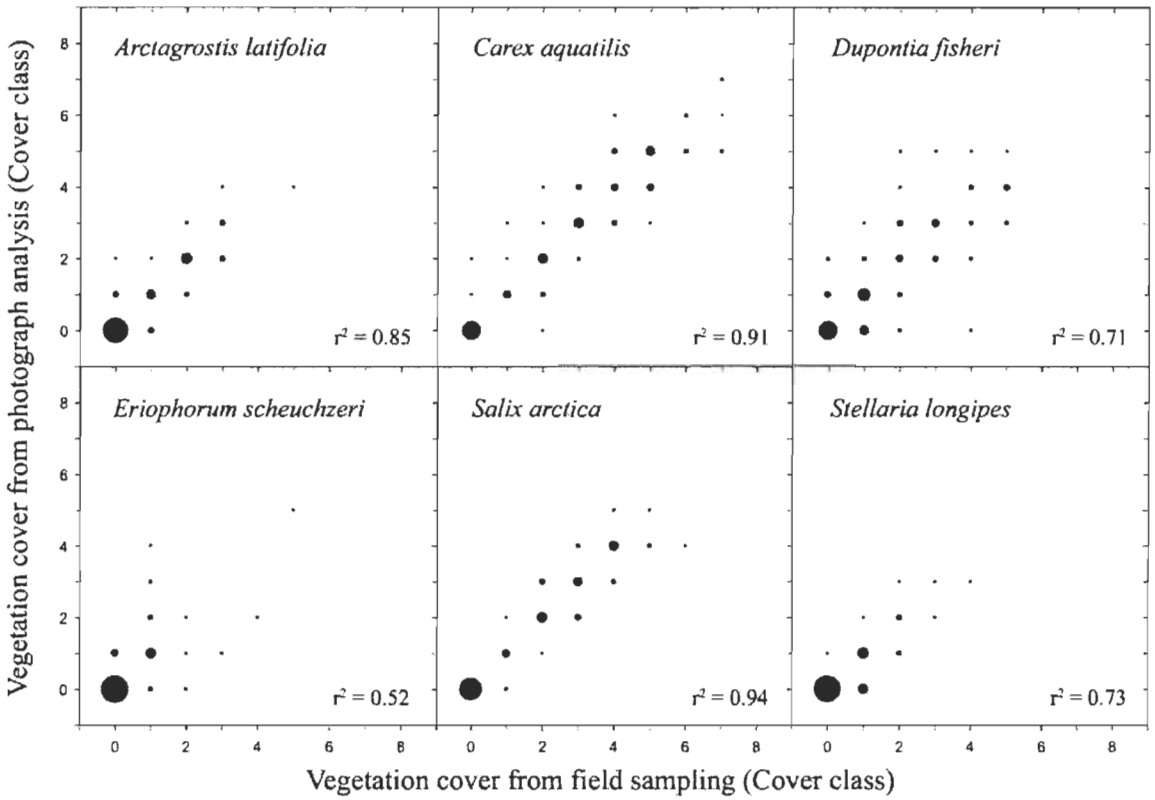

Figure A.1 : Bubble plots showing comparison of results from field sampling and vertical photograph analysis for six common plant species based on the same 182 plots selected during summer 2009, Bylot Island, Nunavut. Larger symbols indicate higher number of points and regression results (r^2) are included.

Table A.1 : Comparison of results from field sampling and vertical photograph analysis based on the same 182 plots selected during summer 2009, Bylot Island, Nunavut. Occurrence of each species in 182 plots, percentage of data with a 1:1 correlation including zero, percentage error of a single class including zero, Pearson's correlation (r) and regression (r^2) are showed for each taxa.

Taxa	Occurrence	1:1 correlation (%)	Error of a single class (%)	Pearson's correlation (r)	Regression (r^2)
Vascular plant species					
Asteraceae					
Tephroseris palustris	9	98.9	1.1	0.98	0.96
Brassicaceae					
Cardamine bellidifolia	11	97.3	2.8	0.69	0.48
Cardamine nymanii	23	91.2	8.8	0.50	0.25
Draba cinerea	2	98.9	1.1	NA	NA
Draba corymbosa	7	96.2	3.9	NA	NA
Draba lactea	17	90.7	9.3	NA	NA
Draba sp.	10	94.5	5.5	NA	NA
Eutrema edwardsii	6	97.8	2.2	0.49	0.24
Caryophyllaceae					
Cerastium alpinum	9	97.3	2.8	0.82	0.68
Minuartia rubella	3	98.9	1.1	0.49	0.24
Silene uralensis	1	100.0	0.0	1.00	1.00
Stellaria longipes	54	85.7	14.3	0.85	0.73
Cyperaceae					
Carex aquatilis	119	74.7	20.9	0.96	0.91
Carex marina	1	99.5	0.6	NA	NA
Eriophorum angustifolium	4	97.8	2.2	0.01	0.00
Eriophorum scheuchzeri	43	86.8	9.3	0.72	0.52
Equisetaceae					
Equisetum arvense	5	97.8	2.2	0.44	0.20

Taxa (continued)	Occurrence	1:1 correlation (%)	Error of a single class (%)	Pearson's correlation (r)	Regression (r^2)
Ericaceae					
Cassiope tetragona	1	99.5	0.6	1.00	1.00
Fabaceae					
Astragalus alpinus	5	99.5	0.6	0.98	0.96
Juncaceae					
Juncus biglumis	1	99.5	0.6	NA	NA
Luzula arctica	49	91.2	8.2	0.87	0.76
Luzula confusa	61	85.2	14.3	0.90	0.81
Papaveraceae					
Papaver sp.	2	100.0	0.0	1.00	1.00
Poaceae					
Alopecurus borealis	7	97.3	2.8	0.88	0.77
Anthoxanthum arcticum	20	89.6	7.1	0.53	0.28
Arctagrostis latifolia	64	86.3	13.2	0.92	0.85
Deschampsia brevifolia	1	99.5	0.0	NA	NA
Dupontia fisheri	118	63.2	29.1	0.84	0.71
Festuca brachyphylla	12	95.1	4.4	0.66	0.43
Phippsia algida	1	99.5	0.6	NA	NA
Pleuropogon sabinei	1	99.5	0.0	NA	NA
Poa arctica	24	89.0	11.0	0.54	0.29
Polygonaceae					
Bistorta vivipara	3	99.5	0.6	0.81	0.66
Oxyria digyna	1	99.5	0.6	NA	NA
Ranunculaceae					
Ranunculus hyperboreus	2	99.5	0.0	0.71	0.50
Ranunculus nivalis	1	99.5	0.6	NA	NA

Taxa (continued)	Occurrence	1:1 correlation (%)	Error of a single class (%)	Pearson's correlation (r)	Regression (r^2)
Rosaceae					
Dryas integrifolia	3	99.5	0.6	0.96	0.93
Salicaceae					
Salix arctica	87	84.6	14.8	0.97	0.94
Salix herbacea	6	99.5	0.6	0.96	0.92
Salix reticulata	24	94.0	5.5	0.93	0.86
Saxifragaceae					
Chrysosplenium tetrandrum	12	96.7	3.3	0.84	0.70
Micranthes foliolosa	28	91.2	8.8	0.70	0.50
Micranthes hieraciifolia	4	98.4	1.7	0.50	0.25
Saxifraga cernua	24	92.3	7.7	0.63	0.39
Saxifraga cespitosa	1	100.0	0.0	NA	NA
Saxifraga hirculus	21	95.1	5.0	0.81	0.66
Saxifraga oppositifolia	6	97.8	2.2	0.93	0.86
Scrophulariaceae					
Pedicularis sudetica	51	94.0	5.5	0.92	0.85
Lichen	81	83.0	14.8	0.92	0.85
Cladina sp.	4	98.4	1.7	0.57	0.32
Stereocaulon sp.	42	90.7	9.3	0.94	0.89
Peltigera sp	64	89.0	10.4	0.92	0.86
Green mosses	170	63.7	30.8	0.93	0.86
Aulacomnium sp.	105	64.8	27.5	0.92	0.84
Drepanochladus sp.	82	67.0	8.8	0.75	0.57
Pleurozium sp.	34	89.6	6.0	0.69	0.48
Polytricum sp.	114	68.7	24.7	0.82	0.67

Taxa (continued)	Occurrence	1:1 correlation (%)	Error of a single class (%)	Pearson's correlation (r)	Regression (r^2)
Dicranum sp.	76	73.1	14.3	0.60	0.36
Sphagnum sp.	6	97.3	2.8	0.67	0.44
Dry mosses	79	70.3	13.2	0.84	0.70
Aulacomnium sp.	8	95.6	1.7	0.01	0.00
Drepanochladus sp.	40	82.4	3.9	0.73	0.54
Pleurozium sp.	1	99.5	0.0	NA	NA
Polytricum sp.	3	98.4	0.6	0.01	0.00
Sphagnum sp.	2	99.5	0.6	0.95	0.90
Others					
Cryptogamic crust	62	83.0	12.6	0.91	0.83
Dicotyledon sp.	9	95.6	3.9	0.28	0.08
Nostoc sp.	2	99.5	0.6	0.71	0.50
Mushroom sp.	46	89.6	10.4	0.71	0.50
Environmental variables					
Bare ground	39	87.4	7.7	0.95	0.91
Geese feces	136	84.1	15.9	0.66	0.43
Grubbing	63	78.6	15.9	0.71	0.50
Litter	160	58.2	32.4	0.74	0.55
Standing dead	156	29.68	51.1	0.42	0.18
Standing water	14	95.6	3.9	0.97	0.95

Table A.2 : Comparison of results from field sampling (F) and vertical photograph analysis (P) based on the same 182 plots selected during summer 2009, Bylot Island, Nunavut. Results from a combination of the two methods (C) are given. Species specific mean of vegetation cover were added to provide a cover percentage per family (tr = cover < 0.01%; * = cover < 0.1%; <1 = cover < 1%).

Eco-terrain units	Wet polygons n = 52			Drained polygons n = 39			Dried polygons n = 32			Mesic zones n = 13			Mesic polygon rims n = 31			Sediment zones n = 15		
Taxa	F	P	C	F	P	C	F	P	C	F	P	C	F	P	C	F	P	C
Plant families																		
Asteraceae	tr	tr	tr	*	*	*	*	*	*	-	-	-	tr	tr	tr	4	4	3
Brassicaceae	*	*	*	<1	*	*	<1	<1	<1	<1	*	*	<1	<1	*	<1	*	*
Caryophyllaceae	*	tr	tr	<1	<1	<1	2	2	1	<1	<1	*	<1	<1	<1	<1	*	<1
Cyperaceae	22	19	18	21	20	20	10	8	8	2	2	3	<1	<1	<1	<1	2	1
Equisetaceae	*	tr	*	-	-	*	tr	tr	*	*	tr	*	tr	tr	tr	*	*	*
Ericaceae	-	-	-	-	-	-	tr	tr	tr	<1	*	*	tr	tr	tr	-	-	-
Fabaceae	tr	tr	tr	tr	tr	tr	*	<1	*	tr	tr	tr	<1	<1	<1	-	-	-
Juncaceae	*	*	*	<1	*	<1	3	3	3	2	2	2	3	3	4	tr	tr	tr
Onagraceae	tr	tr	tr	-	-	-	-	-	-	-	-	-	-	-	-	-	-	-
Papaveracea	-	-	-	-	-	-	*	*	tr	-	-	-	*	*	tr	tr	tr	tr
Poaceae	11	9	9	5	4	5	3	3	3	2	2	3	5	4	4	8	5	5
Polygonaceae	-	-	-	*	tr	tr	tr	*	*	-	-	-	*	*	*	tr	tr	tr
Pyrolaceae	-	-	-	-	-	-	-	-	tr	-	-	-	-	-	-	-	-	-
Ranunculaceae	-	-	-	-	-	-	-	*	tr	-	-	-	tr	tr	tr	<1	<1	<1
Rosaceae	-	-	-	-	-	-	tr	tr	*	tr	tr	*	<1	<1	<1	-	-	-
Salicaceae	1	1	1	1	1	1	4	3	3	11	9	11	18	15	15	<1	<1	<1
Saxifragaceae	<1	*	*	<1	<1	<1	2	1	2	<1	*	*	*	*	*	*	<1	*
Scrophulariaceae	1	<1	<1	<1	<1	<1	<1	<1	<1	*	tr	*	tr	tr	tr	<1	<1	*
Total	35	30	30	28	27	26	24	21	22	18	16	19	29	24	24	14	11	10

Eco-terrain units	Wet polygons n = 52			Drained polygons n = 39			Dried polygons n = 32			Mesic zones n = 13			Mesic polygon rims n = 31			Sediment zones n = 15		
Taxa (continued)	F	P	C	F	P	C	F	P	C	F	P	C	F	P	C	F	P	C
Lichen																		
Cladina sp.	-	-	-	-	-	-	tr	tr	*	*	*	*	*	*	<1	-	-	-
Stereocaulon sp.	tr	tr	tr	tr	*	*	<1	<1	<1	3	3	2	4	4	4	-	-	-
Peltigera sp.	*	*	*	*	*	*	<1	<1	<1	3	3	3	3	3	4	-	-	-
Total	<1	*	*	<1	*	*	2	1	2	6	5	5	10	7	9	-	-	-
Green mosses																		
Aulacomnium sp.	9	8	8	2	4	3	<1	<1	1	43	54	51	16	24	27	*	<1	<1
Drepanochladus sp.	28	40	39	16	25	22	<1	4	7	-	-	-	-	-	-	-	-	-
Pleurozium sp.	-	-	-	tr	tr	tr	*	*	*	2	<1	1	2	3	2	tr	tr	tr
Polytricum sp.	7	5	4	2	<1	1	7	7	7	<1	<1	<1	1	1	2	tr	tr	tr
Dicranum sp.	<1	1	1	2	<1	<1	3	2	2	1	3	2	3	4	3	4	5	5
Sphagnum sp.	*	*	<1	*	tr	tr	*	tr	tr	-	-	*	tr	tr	<1	-	-	-
Total	64	63	63	30	32	28	19	21	23	60	65	61	36	45	43	5	6	6
Dry mosses																		
Aulacomnium sp.	-	*	*	-	-	-	-	-	-	<1	<1	<1	-	1	1	-	-	-
Drepanochladus sp.	-	3	3	18	26	28	7	10	12	-	-	-	-	-	-	-	-	<1
Pleurozium sp.	-	-	-	-	-	-	-	<1	<1	-	-	-	-	-	-	-	-	-
Polytricum sp.	-	*	*	-	*	*	<1	tr	*	-	-	*	-	-	<1	-	-	-
Dicranum sp.	-	-	-	-	-	-	-	-	-	-	-	-	-	-	*	-	-	-
Sphagnum sp.	-	-	-	<1	<1	*	tr	*	tr	-	-	-	-	-	-	-	-	-
Total	tr	3	4	22	28	29	16	18	19	<1	1	1	<1	3	2	1	1	2

Eco-terrain units	Wet polygons n = 52			Drained polygons n = 39			Dried polygons n = 32			Mesic zones n = 13			Mesic polygon rims n = 31			Sediment zones n = 15		
Taxa (continued)	F	P	C	F	P	C	F	P	C	F	P	C	F	P	C	F	P	C
Others																		
Cryptogamic crust	-	-	tr	*	*	*	13	16	15	3	3	2	8	7	9	<1	*	*
Dicotyledon sp.	tr	tr	tr	*	tr	tr	tr	tr	tr	-	-	-	-	-	*	<1	<1	<1
Nostoc sp.	*	tr	*	-	-	*	-	-	-	-	-	-	-	-	-	-	-	-
Mushroom sp.	*	*	*	<1	<1	<1	<1	<1	<1	tr	tr	*	*	*	*	*	tr	tr
Environmental variables																		
Bare ground	1	*	*	5	5	5	<1	2	1	<1	*	<1	<1	1	1	74	82	80
Geese feces	<1	<1	<1	<1	<1	<1	<1	<1	<1	<1	<1	<1	<1	<1	<1	<1	<1	<1
Grubbing	1	<1	<1	2	2	3	<1	1	2	<1	<1	<1	-	-	-	-	-	-
Litter	2	1	2	3	2	3	5	4	4	6	5	6	8	7	7	<1	<1	<1
Standing dead	<1	2	2	<1	4	4	<1	3	3	<1	2	3	<1	1	1	<1	<1	1
Standing water	6	6	5	-	-	-	-	-	-	tr	tr	tr	-	-	-	<1	*	<1

ANNEXE B

COMPLETE NAME OF VASCULAR PLANT SPECIES INVENTORIED DURING FIELD SEASONS 2009 AND 2010 IN THE QARLIKTURVIK VALLEY, BYLOT ISLAND, NUNAVUT

Species name are from the integrated taxonomic information system (ITIS 2011). A total of 60 vascular taxa were recognized.

Asteraceae
Erigeron uniflorus var. *eriocephalus* (J.Vahl) Boivin
Taraxacum cf. *hyparcticum* Dahlst.
Tephroseris palustris (L.) Reichenbach
Brassicaceae
Cardamine bellidifolia L.
Cardamine nymanii Gand.
Draba cinerea Adams
Draba corymbosa R. Br.
Draba glabella Pursh
Draba lactea Adams
Draba nivalis Lilj.
Draba sp.*
Eutrema edwardsii R. Br.
Caryophyllaceae
Cerastium alpinum L. s. lat.
Minuartia rubella (Wahlenb.) Hiern.
Silene involucrata ssp. *involucrate* (Cham. & Schlecht.) Bocquet
Silene uralensis ssp. *uralensis* (Rupr.) Bocquet
Stellaria longipes ssp. *longipes* Goldie
Cyperaceae
Carex aquatilis var. *minor* Boott
Carex marina Dewey
Eriophorum angustifolium cf. ssp. *angustifolium* Honck.
Eriophorum scheuchzeri Hoppe s. lat./*russeolum* ssp. *Leiocarpum*
Equisetaceae
Equisetum arvense L. s. lat.
Ericaceae
Cassiope tetragona var. *tetragona* (L.) D. Don
Fabaceae
Astragalus alpinus var. *alpinus* L.
Oxytropis maydelliana ssp. *melanocephala* (Hook.) A.E. Porsild
Juncaceae
Juncus biglumis L.
Luzula arctica Blytt
Luzula confusa Lindebl.
Onagraceae
Epilobium arcticum Sam.
Papaveracea
Papaver sp. **
Poaceae
Alopecurus borealis Trin.
Anthoxanthum arcticum Veldkamp
Arctagrostis latifolia ssp. *latifolia* (R. Br.) Griseb.
Deschampsia brevifolia R. Br.
Dupontia fisheri R. Br.
Festuca brachyphylla ssp. *brachyphylla* Schult. & Schult. f.
Phippsia algida (Sol.) R. Br.
Pleuropogon sabinei R. Br.
Poa arctica R. Br. s. lat.
Polygonaceae
Bistorta vivipara (L.) Delarbre
Oxyria digyna (L.) Hill
Pyrolaceae
Pyrola grandiflora Radius
Ranunculaceae
Ranunculus hyperboreus Rottb.
Ranunculus nivalis L.
Rosaceae
Dryas integrifolia ssp. *integrifolia* M. Vahl

***Rosaceae* (continued)**
Potentilla hyparctica ssp. *hyparctica* Malte
Salicaceae
Salix arctica Pall.
Salix herbacea L.
Salix reticulata L.
Salix richardsonii Hook.
Saxifragaceae
Chrysosplenium tetrandrum (Lund) Th. Fries
Micranthes foliolosa (R. Br.) Gornall
Micranthes hieraciifolia (Waldst. & Kit.) Haworth
Micranthes nivalis (L.) Small
Saxifraga cernua L.
Saxifraga cespitosa L.
Saxifraga hirculus L.
Saxifraga oppositifolia L.
Scrophulariaceae
Pedicularis langsdorffii ssp. *arctica* (R. Br.) Pennell
Pedicularis sudetica ssp. *albolabiata* Hult.

* *Draba* sp. was not counted as a distinct species because it is probably one of the five species already mentioned.
** Papaver sp. includes *P. Dahlianum, P. Cornwalissense, P. Lapponicum* ssp. *occidentale).*

ANNEXE C

COVER (%) AND FREQUENCY (%) OF TAXA IDENTIFIED IN THE SIX ECO-TERRAIN UNITS DURING FIELD SEASONS 2009 AND 2010, BYLOT ISLAND, NUNAVUT

A combination of vertical photograph analysis and field visual evaluation was used to evaluate cover (tr = cover < 0.01 %; * = cover < 0.1%; <1 = cover < 1%) and frequency of taxa.

Eco-terrain units	Wet polygons n = 62		Drained polygons n = 44		Dried polygons n = 43		Mesic zones n = 13		Mesic polygon rims n = 35		Sediment zones n = 15	
Taxa	C	F	C	F	C	F	C	F	C	F	C	F
Vascular plant species												
Asteraceae												
Erigeron uniflorus		-		-	tr	(7)		-	tr	(3)		-
Taraxacum cf. *hyparcticum*		-		-	tr	(2)		-		-		-
Tephroseris palustris	tr	(3)	*	(14)	*	(9)		-		-	3	(80)
Brassicaceae												
Cardamine bellidifolia	tr	(3)	tr	(7)	*	(26)	*	(23)	*	(29)	tr	(20)
Cardamine nymanii	tr	(15)	*	(30)	*	(28)	tr	(8)	tr	(9)	*	(27)
Draba cinerea		-		-	tr	(12)		-		-	tr	(7)
Draba corymbosa		-	tr	(2)	tr	(16)	tr	(15)	tr	(23)	tr	(13)
Draba glabella	tr	(2)		-		-		-		-	tr	(7)
Draba lactea	tr	(3)	tr	(16)	*	(72)	tr	(69)	*	(69)	tr	(7)
Draba nivalis		-		-	tr	(5)		-	tr	(3)		-
Draba sp.		-	tr	(5)	<1	(49)	*	(8)	*	(17)		-
Eutrema edwardsii	tr	(2)	tr	(11)	*	(26)	tr	(31)	tr	(40)	tr	(7)

Eco-terrain units	Wet polygons n = 62		Drained polygons n = 44		Dried polygons n = 43		Mesic zones n = 13		Mesic polygon rims n = 35		Sediment zones n = 15	
Taxa (continued)	C	F	C	F	C	F	C	F	C	F	C	F
Caryophyllaceae												
Cerastium alpinum	tr	(5)	tr	(20)	<1	(53)	*	(38)	*	(46)	tr	(20)
Minuartia rubella	-		tr	(5)	*	(12)	tr	(8)	*	(11)	-	
Silene involucrata	tr	(2)	tr	(2)	tr	(7)	-		tr	(6)	-	
Silene uralensis	tr	(11)	tr	(20)	*	(40)	tr	(15)	tr	(6)	-	
Stellaria longipes	tr	(11)	*	(59)	<1	(84)	*	(85)	<1	(91)	<1	(33)
Cyperaceae												
Carex aquatilis	15	(100)	18	(95)	6	(88)	3	(77)	<1	(37)	<1	(47)
Carex marina	-		tr	(2)	-		-		-		-	
Eriophorum angustifolium	<1	(39)	<1	(27)	<1	(33)	-		-		tr	(20)
Eriophorum scheuchzeri	2	(87)	<1	(64)	tr	(21)	*	(15)	tr	(3)	<1	(60)
Equisetaceae												
Equisetum arvense	*	(5)	*	(2)	*	(12)	*	(8)	tr	(6)	*	(13)
Ericaceae												
Cassiope tetragona	-		-		tr	(9)	*	(15)	tr	(20)	-	
Fabaceae												
Astragalus alpinus	-		tr	(2)	<1	(23)	tr	(15)	<1	(43)	-	
Oxytropis maydelliana	tr	(2)	-		tr	(2)	-		tr	(9)	-	
Juncaceae												
Juncus biglumis	-		tr	(2)	-		-		tr	(3)	tr	(7)
Luzula arctica	tr	(13)	*	(41)	<1	(95)	<1	(92)	1	(97)	-	
Luzula confusa	*	(10)	<1	(34)	3	(95)	1	(100)	3	(97)	-	
Onagraceae												
Epilobium arcticum	tr	(2)	-		-		-		-		-	
Papaveraceae												
Papaver sp.	-		-		tr	(2)	-		tr	(11)	tr	(20)

Eco-terrain units	Wet polygons n = 62		Drained polygons n = 44		Dried polygons n = 43		Mesic zones n = 13		Mesic polygon rims n = 35		Sediment zones n = 15	
Taxa (continued)	C	F	C	F	C	F	C	F	C	F	C	F
Poaceae												
Alopecurus borealis	<1	(16)	tr	(9)	tr	(14)	tr	(69)	tr	(63)	*	(27)
Anthoxanthum arcticum	<1	(71)	*	(43)	tr	(14)	tr	(8)	tr	(3)	tr	(7)
Arctagrostis latifolia	<1	(45)	*	(32)	<1	(37)	3	(100)	3	(97)	<1	(80)
Deschampsia brevifolia		-		-	tr	(2)		-		-		-
Dupontia fisheri	7	(94)	5	(95)	2	(74)	<1	(46)	*	(6)	4	(100)
Festuca brachyphylla	tr	(3)	*	(32)	<1	(79)	tr	(46)	*	(51)	tr	(7)
Phippsia algida		-		-	*	(5)		-		-	tr	(27)
Pleuropogon sabinei	tr	(5)	tr	(7)		-		-	tr	(3)	*	(47)
Poa arctica	tr	(34)	*	(45)	<1	(77)	tr	(92)	<1	(94)	tr	(47)
Polygonaceae												
Bistorta vivipara	tr	(2)	tr	(2)	tr	(14)		-	*	(37)	tr	(7)
Oxyria digyna		-		-	tr	(14)		-		-		-
Pyrolaceae												
Pyrola grandiflora		-		-	tr	(2)		-		-		-
Ranunculaceae												
Ranunculus hyperboreus		-		-		-		-		-	<1	(53)
Ranunculus nivalis		-		-	tr	(2)		-	tr	(3)		-
Rosaceae												
Dryas integrifolia		-		-	tr	(16)	*	(54)	*	(51)		-
Potentilla hyparctica		-		-	*	(7)		-	tr	(6)		-
Salicaceae												
Salix arctica	1	(52)	<1	(55)	3	(98)	9	(100)	13	(100)	<1	(87)
Salix herbacea		-		-	*	(14)	<1	(15)	*	(37)		-
Salix reticulata	tr	(2)	tr	(9)	<1	(60)	2	(85)	1	(83)	tr	(13)
Salix richardsonii	tr	(8)	tr	(5)	tr	(23)	tr	(23)	tr	(11)		-

Eco-terrain units	Wet polygons n = 62		Drained polygons n = 44		Dried polygons n = 43		Mesic zones n = 13		Mesic polygon rims n = 35		Sediment zones n = 15	
Taxa (continued)	C	F	C	F	C	F	C	F	C	F	C	F
Saxifragaceae												
Chrysosplenium tetrandrum	tr	(5)	<1	(34)	*	(35)		-		-		-
Micranthes foliolosa	*	(19)	*	(43)	<1	(77)	tr	(15)	tr	(6)		-
Micranthes hieraciifolia	tr	(3)		-	*	(16)	*	(46)	tr	(37)		-
Micranthes nivalis		-		-	*	(19)		-	tr	(3)		-
Saxifraga cernua	tr	(21)	*	(48)	<1	(72)	*	(31)	tr	(34)	*	(13)
Saxifraga cespitosa		-		-	tr	(9)	tr	(23)	tr	(20)		-
Saxifraga hirculus	*	(29)	*	(55)	<1	(70)	tr	(69)	tr	(34)	tr	(7)
Saxifraga oppositifolia		-		-	<1	(37)	*	(15)	tr	(29)		-
Scrophulariaceae												
Pedicularis langsdorffii	tr	(2)		-	tr	(2)	tr	(15)	tr	(3)		-
Pedicularis sudetica	<1	(94)	<1	(75)	*	(47)	*	(31)	tr	(9)	*	(20)
Total	28		25		20		19		23		10	
Lichen												
Cladina sp.		-		-	*	(26)	*	(46)	*	(57)		-
Stereocaulon sp.	tr	(3)	*	(16)	<1	(67)	2	(85)	3	(94)		-
Peltigera sp	*	(31)	*	(39)	<1	(74)	3	(100)	4	(100)		-
Total	*		*		2		5		8			-
Green mosses												
Aulacomnium sp.	8	(82)	3	(70)	1	(86)	51	(100)	27	(100)	<1	(33)
Drepanochladus sp.	40	(92)	21	(73)	5	(33)		-	-			-
Pleurozium sp.		-	tr	(2)	*	(5)	1	(85)	1	(66)	tr	(7)
Polytricum sp.	4	(84)	1	(77)	6	(98)	<1	(77)	2	(100)	tr	(7)
Dicranum sp.	1	(26)	<1	(30)	4	(93)	2	(77)	3	(89)	5	(20)
Sphagnum sp.	<1	(23)	tr	(14)	tr	(14)	*	(8)	<1	(11)		-

Eco-terrain units	Wet polygons n = 62		Drained polygons n = 44		Dried polygons n = 43		Mesic zones n = 13		Mesic polygon rims n = 35		Sediment zones n = 15	
Taxa (continued)	C	F	C	F	C	F	C	F	C	F	C	F
Total	62		27		21		61		44		6	
Dry mosses												
Aulacomnium sp.	*	(2)	<1	(2)	<1	(9)	<1	(54)	<1	(23)	-	
Drepanochladus sp.	2	(10)	29	(70)	17	(47)	-		-		<1	(7)
Pleurozium sp.	-		<1	(2)	<1	(2)	-		-		-	
Polytricum sp.	*	(2)	*	(5)	1	(21)	*	(8)	*	(11)	-	
Dicranum sp.	-		-		-		-		*	(6)	-	
Sphagnum sp.	-		*	(5)	tr	(7)	-		-		-	
Total	3		32		25		1		3		2	
Others												
Cryptogamic crust	tr	(2)	*	(5)	15	(79)	2	(69)	8	(97)	*	(20)
Dicotyledon sp.	tr	(2)	tr	(5)	tr	(2)	-		*	(3)	*	(53)
Nostoc sp.	*	(10)	*	(5)	-		-		-		-	
Mushroom sp.	*	(47)	<1	(73)	<1	(74)	*	(62)	*	(80)	tr	(20)
Environmental variables												
Bare ground	*	(2)	5	(14)	1	(28)	<1	(15)	<1	(40)	80	(100)
Geese feces	<1	(94)	<1	(100)	<1	(100)	<1	(100)	<1	(100)	<1	(73)
Grubbing	1	(69)	3	(64)	2	(53)	<1	(31)	tr	(3)	-	
Litter	1	(90)	2	(95)	3	(95)	6	(100)	6	(100)	<1	(40)
Standing dead	2	(97)	4	(98)	2	(91)	3	(100)	1	(100)	1	(53)
Standing water	8	(40)	-		-		tr	(8)	-		<1	(13)

ANNEXE D

RADIOMETRIC CALIBRATION

The application of radiometric calibrations allows converting raw digital numbers (DN) into at-sensor radiance, a comparable physical unit (Soudani *et al.* 2006). At-sensor radiance is also necessary for the calculation of the exoatmospheric reflectance. To achieve this, it is necessary to apply the calibration factors determined at the time of image acquisition. These parameters, expressed in terms of "gain" and "offset" found in image headers (Table D.1), were used to convert the digital value measured by the sensor radiometric value (Soudani *et al.* 2006). Radiance (L) was calculated using the following relationship (Equation D.1) (Goward *et al.* 2003):

$$L_\lambda = \text{gain} * \text{DN} + \text{offset} \qquad \text{(D.1)}$$

where,

L_λ = Sensor-measured spectral radiance ($W/m^2/sr/\mu m$),

gain = Change in radiance as a function of digital number,

DN = Digital number,

offset = The DN value where zero radiance is detected.

It is difficult to compare spectral radiance because they vary as a function of both ground conditions and solar illumination conditions (Goward *et al.* 2003). Exoatmospheric reflectance is more easily compared between sensors than at-sensor radiance by normalizing for solar irradiance (Goward *et al.* 2003). The conversion to exoatmospheric reflectance is also necessary for the calculation of NDVI index. Reflectance (ρ_p) was calculated using the following formula (Equation D.2) (GeoEye unpublished data; LPSO 1998):

$$\rho_{p\lambda} = \frac{\pi L_\lambda d^2}{ESUN_\lambda \cos(\theta_s)} \quad (D.2)$$

where,

$\rho_{p\lambda}$ = Unitless exoatmospheric reflectance,

L_λ = Radiance for spectral band λ at the sensor's aperture ($W/m^2/\mu m/sr$),

d = Earth-Sun distance in astronomical units from Table D.2,

$ESUN_\lambda$ = Mean solar exoatmospheric irradiances from Table D.3 ($W/m^2/\mu m$),

θ_s = Solar zenith angle (90° - *Solar Elevation Angle*).

Table D.1 : "Gain" and "offset" of bands found in image headers on the high-resolution GeoEye-1 imagery acquired the September 2nd 2010 at 17h40 GMT.

Bands	GAIN	OFFSET
Blue	.014865	.000
Green	.017183	.000
Red	.016194	.000
Near-infrared	.009593	.000
Panchromatic	.017786	.000

Table D.2 : Earth-sun distance in astronomical units.

Julian Day	**Distance**	**J. Day**	**Dist.**	**J. Day**	**Dist.**	**J. Day**	**Dist.**	**J. Day**	**Dist.**
1	0.9832	74	0.9945	152	1.0140	227	1.0128	305	0.9925
15	0.9836	91	0.9993	166	1.0158	242	1.0092	319	0.9892
32	0.9853	106	1.0033	182	1.0167	258	1.0057	335	0.9860
46	0.9878	121	1.0076	196	1.0165	274	1.0011	349	0.9843
60	0.9909	135	1.0109	213	1.0149	288	0.9972	365	0.9833

*From GeoEye (unpublished data).

Table D.3 : GeoEye-1 band dependant parameters.

GeoEye-1 Band (λ)	Bandwidth (nm)	$Esun_\lambda$ ($W/m^2/\mu m$)
Panchromatic	307.437	1616.61
Blue	58.354	1959.82
Green	64.614	1852.92
Red	31.632	1504.98
Near IR	101.189	1038.76

*From GeoEye (unpublished data).

ANNEXE E

TWINSPAN CLUSTER ANALYSIS OF THE 212 SAMPLING SITES ON BYLOT ISLAND, NUNAVUT

Vascular plant species (n = 59), lichens, green mosses, dry mosses, cryptogamic crust, nostocs and mushrooms covers were used as species. Eigenvalues and indicator species for each division are included. Twinspan for windows (wintwins), v2.3 was used.

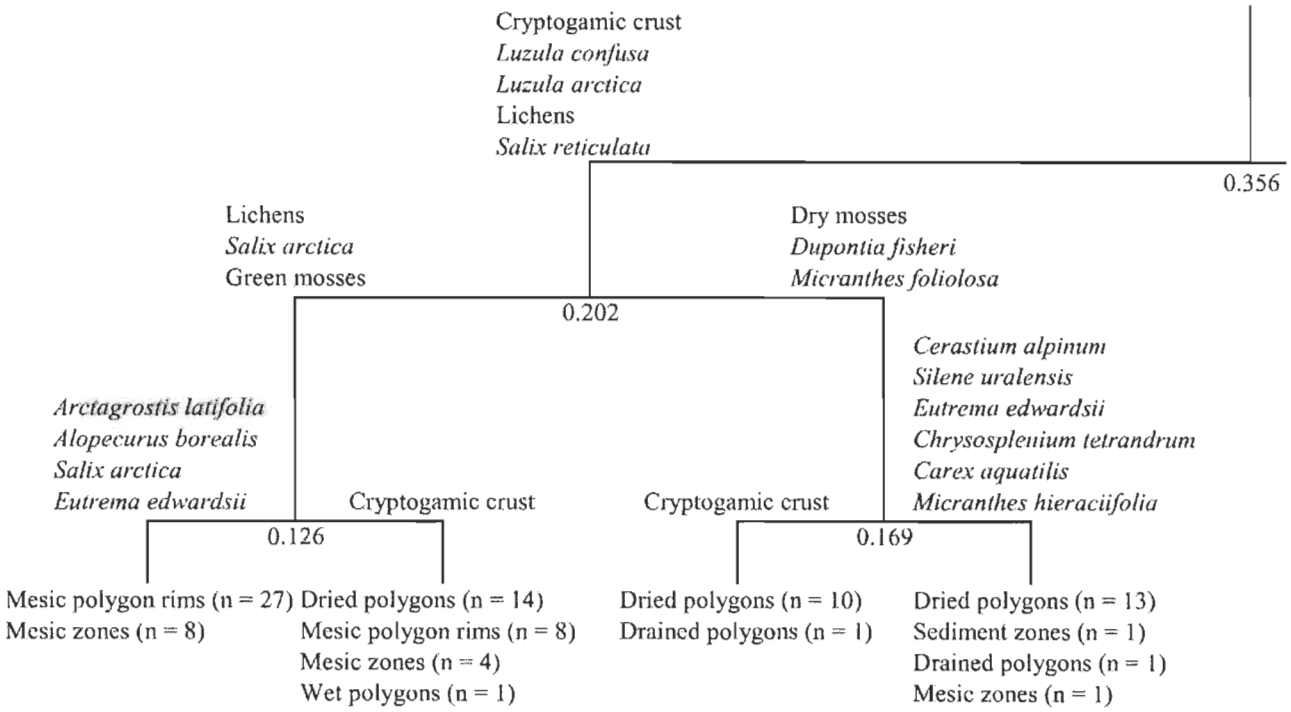

ANNEXE E (CONTINUED)

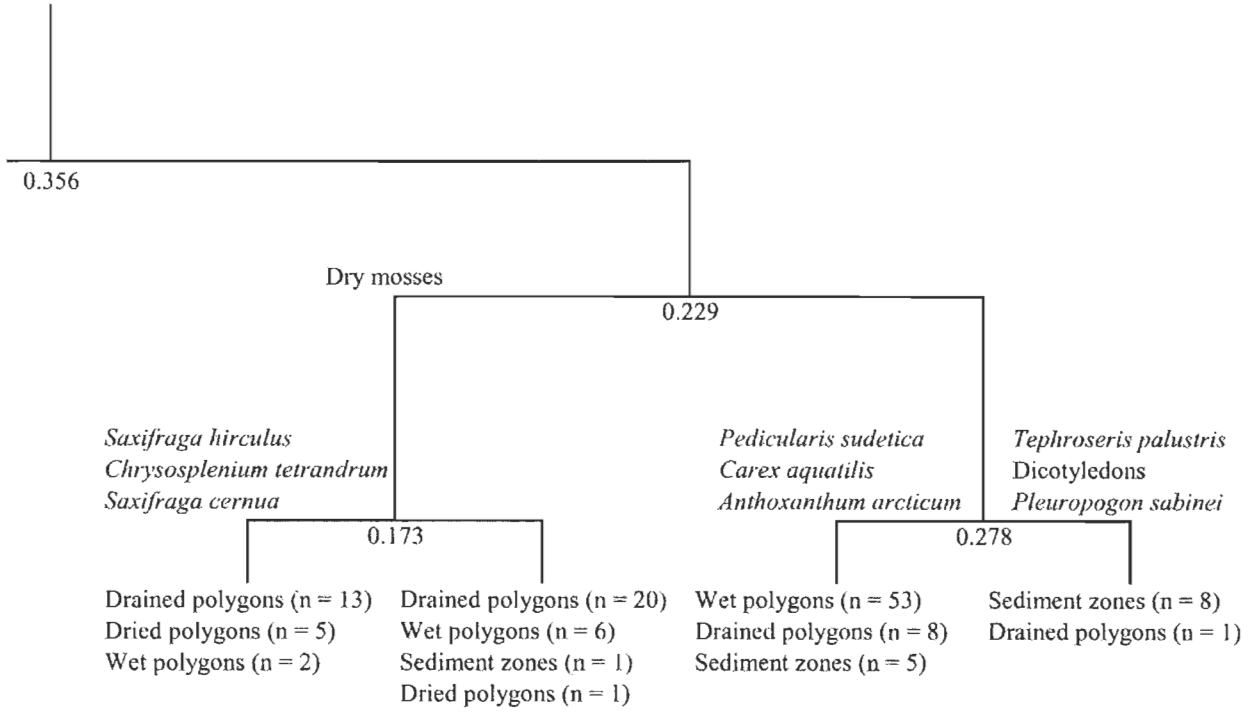

ANNEXE F

DESCRIPTION OF THE FOUR CONTINUOUS MONITORING STATIONS

Four continuous monitoring stations were positioned at the beginning of summer 2010 (June 25th) and recovered at the end of the season (July 31th). Stations S1 and S2 were located near Gully A and stations S3 and S4 were located near Gully B (Table F.1). Soil moisture and temperature were monitored and graminoids biomass was sampled in five plots adjacent to each station.

At each of the four stations, in order to document the soil moisture (top 10 cm) evolution throughout the summer of eco-terrain units, an Em5b datalogger (Decagon Devices) was positioned with five ECH_2O EC-5 moisture sensors (Decagon Devices). Moisture sensors were deployed at a distance of 1-2 meters from the edge of polygons and inserted vertically in the ground. As it was not possible to reach all eco-terrain unit types for every station (constrained by cable length of 5 meters), some types were duplicated when sensors were available for a total of 20 plots (4 Wet polygons, 4 Drained polygons, 2 Dried polygons and 4 Mesic polygon rims).

A series of IButton (IButton Devices) with a precision of 0.5 °C were deployed near soil moisture sensors to document soil temperatures evolution. Near each ECH_2O EC-5 moisture sensor, the first IButton was set near the ground surface (top 2 cm) and the second IButton was set deeper (top 10 cm). Data series started on June 25th and ended on July 30th with a resolution of one recording per hour.

For the 20 plots, an exclosure of 1 m * 1 m was positioned above soil moisture and temperature sensors. They were made of chicken wire 30 cm high in late June, before the arrival of the geese to prevent grazing on the vegetation (Figures F.1 to F.4). Plant biomass was sampled inside the exlosures (chapitre II).

Table F.1 : Metadata summary of the four continuous monitoring stations set up for summer 2010, Bylot Island, Nunavut.

Station	Location (WGS 84, UTM 17N)	Sampling site	Eco-terrain unit	Soil moisture (Volumetric water content; %)		Soil temperature (C°)	
				Data logger	Sensors	IButton (top 10 cm)	IButton (top 2 cm)
S1 (Gully A) Figure F.1	533829.204E, 8118468.764N	331	Drained polygon	6711	1	3; 43	4; B33
		332	Mesic polygon rim		2	5; B22	6; B9
		333*	Dried polygon		3	7; B35	8; B62
		333*	Dried polygon		4	9; A6	10; B63
		573	Wet polygon		5	1; 41	2; 42
S2 (Gully A) Figure F.2	533943.854E, 8118507.300N	637*	Wet polygon	6712	1	11; B53	12; B1
		637*	Wet polygon		2	13; B84	14; B55
		334	Mesic polygon rim		3	15; B3	16; B17
		335*	Dried polygon		4	17; B70	18; B40
		335*	Dried polygon		5	19; B49	20; A3
S3 (Gully B) Figure F.3	534504.862E, 8119064.304N	682	Drained polygon	6713	1	21; B37	22; B10
		337*	Drained polygon		2	23; A10	24; A8
		337*	Drained polygon		3	25; B60	26; A4
		336*	Mesic polygon rim		4	27; B89	28; B92
		336*	Mesic polygon rim		5	29; A9	30; B36
S4 (Gully B) Figure F.4	534564.384E, 8119056.426N	669	Wet polygon	6710	1	31; B69	32
		338*	Wet polygon		2	33	34
		338*	Wet polygon		3	35	36
		339	Mesic polygon rim		4	37	38
		670	Drained polygon		5	39	40

* Duplication of the sampling site.

Figure F.1 : S1 station near Gully A, Bylot Island, Nunavut (photograph taken in July 2010).

Figure F.2 : S2 station near Gully A, Bylot Island, Nunavut (photograph taken in July 2010).

Figure F.3 : S3 station near Gully B, Bylot Island, Nunavut (photograph taken in July 2010).

Figure F.4 : S4 station near Gully B, Bylot Island, Nunavut (photograph taken in July 2010).

ANNEXE G

PUNCTUAL POINT MEASUREMENTS OF SOIL MOISTURE (TOP 10 CM) USING AN ECH$_2$O EC-5 MOISTURE SENSOR RECORDED DURING SUMMER 2010, BYLOT ISLAND, NUNAVUT. SPECIFIC MEAN OF VOLUMETRIC WATER CONTENT (VWC; %) WERE ADDED TO PROVIDE RESULTS PER DATE.

Where N = number of site in this eco-terrain unit category, n = number of sites measured per date,
VWC = Mean volumetric water content, SE = Standard error.

Eco-terrain units	Wet polygons N = 62			Drained polygons N = 44			Dried polygons N = 43			Mesic zones N = 13			Mesic polygon rims N = 35			Sediment zones N = 15		
Date	n	VWC	SE	n	VWC	SE	n	VWC	SE	n	VWC	SE	n	VWC	SE	n	VWC	SE
2010-07-05	23	42.6	2.0	19	23.2	1.6	12	22.2	2.5	5	15.8	3.5	21	18.5	1.6	7	34.2	5.4
2010-07-06	30	31.2	2.4	22	20.2	1.9	22	21.9	1.1	8	19.5	4.5	10	23.1	3.4	4	37.0	3.5
2010-07-08	4	32.5	6.3	4	13.5	8.2	2	28.2	2.2	-	-	-	4	NA	3.7	-	-	-
2010-07-09	19	39.9	2.4	9	15.4	4.7	1	16.4	-	3	24.3	1.4	8	15.9	1.4	9	28.6	3.7
2010-07-11	4	26.8	1.8	11	20.3	2.9	11	20.1	3.2	1	14.3	-	10	19.6	1.7	-	-	-
2010-07-16	23	49.1	1.5	19	30.0	1.7	12	28.9	2.0	5	23.1	4.9	22	25.5	1.7	11	33.0	3.2
2010-07-18	12	50.2	1.1	8	36.8	2.9	15	35.2	2.0	2	23.8	3.6	3	27.9	6.0	-	-	-
2010-07-19	9	49.8	1.0	3	42.3	4.2	9	29.0	1.4	-	-	-	-	-	-	-	-	-
2010-07-23	7	43.8	6.2	4	28.6	7.2	3	26.0	2.0	1	27.1	-	2	17.8	1.4	1	40.4	-
2010-07-24	30	48.9	1.7	22	31.1	2.3	22	33.8	1.9	8	28.9	3.7	13	23.9	3.0	4	43.8	1.3
2010-07-26	23	52.1	0.7	19	32.9	2.3	12	29.4	1.7	5	21.7	4.7	22	29.0	2.0	11	30.1	4.0
2010-07-30	53	48.5	1.2	41	30.8	1.4	34	31.3	1.2	13	25.1	2.9	35	29.2	1.7	15	33.8	3.4